

ScholarWorks@GSU

Mechanistic Enzymology of Flavin-dependent Catalysis in Bacterial D-Arginine Dehydrogenase and Choline Oxidase

Authors	Gannavaram, Swathi
Citation	Gannavaram, Swathi. (2014). "Mechanistic Enzymology of Flavin-dependent Catalysis in Bacterial D-Arginine Dehydrogenase and Choline Oxidase". Georgia State University. https://doi.org/5671683
DOI	https://doi.org/10.57709/5671683
Download date	2026-05-08 11:14:47
Link to Item	https://hdl.handle.net/20.500.14694/2847

MECHANISTIC ENZYMOLOGY OF FLAVIN-DEPENDENT CATALYSIS IN BACTERIAL D-ARGININE DEHYDROGENASE AND CHOLINE OXIDASE

by

SWATHI GANNAVARAM

Under the Direction of Giovanni Gadda

ABSTRACT

D-Arginine dehydrogenase (DADH) catalyzes the oxidation of D-arginine to imino arginine using FAD as the cofactor. The enzyme is part of a recently discovered two-enzyme complex from *Pseudomonas aeruginosa* involved in arginine utilization. Function of the enzyme within the organism is unknown. Work on this enzyme has been undertaken to understand the structure as well as its reaction mechanism so as to eventually assign a function to the enzyme within the physiological context. In the reductive half-reaction $2 e^-$ and $1 H^+$ are transferred from the amino acid substrate to FAD cofactor. In the oxidative half-reaction the reducing equivalents from the FAD cofactor are passed to an electron acceptor that is yet to be discovered. The enzyme has been established to have no reactivity with O_2 . Choline oxidase (CHO) from *Arthrobacter globiformis* is a well characterized member of Glucose-Methanol-Choline Superfamily

that reacts with molecular O₂. It catalyzes the oxidation of choline to glycine betaine mediated by betaine aldehyde intermediate using FAD as the cofactor and O₂ as the oxidant to regenerate oxidized FAD for further reaction. Glycine betaine, the product of the reaction is an important osmolyte that regulates nutrients for plants under stressful conditions. Therefore it is of commercial interest to genetically engineer crops that do not typically possess competent pathways for glycine betaine synthesis.

In this dissertation molecular details concerning the reductive half-reaction of DADH and oxidative half-reaction of CHO have been studied using a combination of steady state kinetics, rapid kinetics, pH, multiple substrates, mutagenesis, substrate deuterium and solvent isotope effects, viscosity effects or computational approaches.

In DADH, the oxidation of amino acid substrate by FAD has been shown to most likely proceed via hydride transfer mechanism in the reductive half-reaction with Glu87, Tyr53, Tyr249 and His48 emerging as key players in substrate binding, catalysis or for up keeping the integrity of the FAD cofactor. In CHO, the oxidative half-reaction proceeds without stabilization of any reaction intermediates with H atom from reduced FAD and H⁺ from solvent or solvent exchangeable site occurring in the same kinetic step.

INDEX WORDS: D-Arginine dehydrogenase, Choline oxidase, FAD, Reductive half-reaction, Hydride transfer, Oxidative half-reaction, Molecular O₂

MECHANISTIC ENZYMOLOGY OF FLAVIN-DEPENDENT CATALYSIS IN BACTERIAL D-ARGININE DEHYDROGENASE AND CHOLINE OXIDASE

by

SWATHI GANNAVARAM

A Dissertation Submitted in Partial Fulfillment of the Requirements for the Degree of

Doctor of Philosophy

College of Arts and Sciences

Georgia State University

2014

Copyright by
Swathi Gannavaram
2014

MECHANISTIC ENZYMOLOGY OF FLAVIN-DEPENDENT CATALYSIS IN BACTERIAL D-ARGININE DEHYDROGENASE AND CHOLINE OXIDASE

by

SWATHI GANNAVARAM

Committee Chair: Giovanni Gadda

Committee: Dale E. Edmondson

Aimin Liu

Donald Hamelberg

Electronic Version Approved:

Office of Graduate Studies

College of Arts and Sciences

Georgia State University

August 2014

DEDICATION

I dedicate my dissertation work to my husband, Srikanth Pydimarry for being the major force, energy, catalyst and everything else in allowing me to pursue my doctorate dream while making the going comfortable and pleasant. I love you from the bottom of my heart and hope I made you proud.

I also dedicate this dissertation to the members my family. My parents Giri Prasad Gannavaram and Subrahmanyeswari Devi and my sister Vandana Gannavaram have always been unconditional in their love and support. I owe my success in the science field to my parents and grandparents all of whom have had a huge influence in my decision of choosing a career in the sciences. I hope I made them proud and can continue to rise up to their expectations. My heartfelt gratitude goes to Ms. Anandamma for having unwavering faith in me and my family. I am forever indebted to her.

Finally, I dedicate this work to all my extended family members. I am especially grateful to my parents-in-law Srinivas and Padma Pydimarry. They came into my life at a later part of my doctorate program but the love and support I have received from each one of them has been unmatched.

ACKNOWLEDGEMENTS

The five years of my life invested into becoming a doctor in philosophy and the path leading to it have been life changing. I would like to set the stage by earnestly thanking my guide and advisor in this adventure, Dr. Giovanni Gadda. His direction and discipline have been imperative in my growth as a scientist. I am especially thankful to him for going out of his way to work along with me on my weaknesses and turning them into my strongpoints. While conducting research in his laboratory, I have always enjoyed the sense of freedom to try different things and venture into territories unknown. He has always been there every time I was down or needed a nudge to try. The most important quality that he instilled in me is the ability to be critical of data, scientific or otherwise and ask questions, no holds barred. I am very glad and proud to say that through the training received from him and interactions with the past and present group members, I feel better prepared for the next step in my ongoing scientific journey.

I am especially grateful to my dissertation committee members, Drs. Dale Edmondson, Aimin Liu and Donald Hamelberg for not only keeping track of my research progress but for being generous with their time, holding valuable discussions and proposing ideas that were crucial for my research. I have met each one of them within and outside of committee meetings and it has been a pleasure on both counts. I imbibed a few helpful qualities from each one of them allowing for my own personal growth. Words cannot justify how thrilled and humbled I have been to have one of my role models, Dale Edmondson on board. I have always looked up to him and will continue to do so wherever I go. I want to thank Dale profusely for passing down his knowledge on an array of topics and for being such a fine gentleman. His scientific rigor and zest for science are unparalleled and I promise to strive for those qualities along my sojourn.

I met some of my best friends during these five years. Rizvan Uluisik was my very first student who I reluctantly accepted to train not because he was a beginner but because I was a novice myself. What a great learning experience that turned out into and I had happily trained six other students after him. Thank you Rizvan for being my guinea pig! On a more serious note, he has always stood by me and is a true friend for life. My best and stimulating scientific discussions always involve him and I look forward to having many more of those. Crystal Smitherman, the most boisterous and bubbly person that I have come across also happened to be one of my best lab mates and friend for life. We have together had a lot of memorable times in and out of the laboratory. Travelling to a scientific conference will not quite be the same without her. Through all the ups and downs of my stay in the Gadda group, I wouldn't replace any of the people that I had the opportunity of working with. I want to thank Dr. Elvira Romero for being a constant inspiration and always willing to listen to my ideas and holding discussions every time I approached her. Travelling in MARTA would have been painful if not for Daniel Ouedraogo and Dan Su. The on-train science discussions with them were some of the best. I want to extend my thanks to all the current members including Francesca Salvi, Jacob Ball and Quan Bui, the three of whom I had the opportunity of training. They have been the best bunch. My acknowledgements wouldn't be justified if I do not include some of the former lab members who played a major role in shaping my initial years in the lab. Dr. Hongling Yuan, Dr. Andrea Pennati, Dr. Kunchala Rungrisuriyachay (who trained me), Dr. Osbourne Quaye, Sandra Hagens, Dr. Kevin Francis and Dr. Steffan Finnegan have all left an impression on me. I have been lucky in terms of having Dr. Alexander Spring and Dr. Sarah Sirin as my collaborators. They were ever so friendly and willing to listen, both of which were crucial for me to have a strong working relationship. Financial support has been one of the main aspects in attending conferences and developing contacts and I cannot thank Molecular

Basis of Disease Area of Focus efficiently directed by Dr. Susanna Greer enough for all the great initiatives and opportunities that I was provided with. I want to give a huge shout out to all my friends including my dearest Akanksha Panwar and Dr. Pankaj Jain as well as my well-wishers who I knew from before or during the course of my Ph.D. at Georgia State University for letting me believe there is indeed light at the end of the tunnel.

TABLE OF CONTENTS

LIST OF TABLES	ix
LIST OF FIGURES	x
LIST OF SCHEMES	xiii
1 INTRODUCTION.....	1
1.1 Flavins	1
<i>1.1.1 Brief history.....</i>	<i>1</i>
<i>1.1.2 Chemistry.....</i>	<i>1</i>
<i>1.1.3 Modified natural flavins</i>	<i>3</i>
<i>1.1.4. Oxidative half-reaction.....</i>	<i>6</i>
1.2 Specific Goals	7
1.3 References	11
2 AMINO ACID DEHYDROGENATION BY FLAVOENZYMES.....	18
2.1 Significance of flavoenzymes.....	18
2.2 α-Amino acids.....	20
<i>2.2.1 Molecular chirality.....</i>	<i>20</i>
<i>2.2.2 Chiral homogeneity.....</i>	<i>21</i>
<i>2.2.3 D-Amino acids.....</i>	<i>21</i>

2.2.4	<i>Enzymes involved in α-amino acid metabolism</i>	22
2.3	Structural comparisons of D-amino acid oxidase, D-arginine dehydrogenase, L-amino acid oxidase and other related enzymes	25
2.3.1	<i>Key conserved catalytic residues</i>	26
2.3.2	<i>Structural similarities and dissimilarities in DAAO, DADH, LAAO</i>	28
2.4	Mechanism of amino acid dehydrogenation	30
2.5	Conclusion	35
2.6	References	35
3	pH AND KINETIC ISOTOPE EFFECTS OF D-ARGININE DEHYDROGENASE WITH MULTIPLE SUBSTRATES	41
3.1	Abbreviations	41
3.2	Highlights	41
3.3	Abstract	41
3.4	Introduction	42
3.5	Experimental Procedures	45
3.6	Results	48
3.7	Discussion	52
3.8	Acknowledgements	56
3.9	References	56

4 MECHANISTIC AND COMPUTATIONAL STUDIES ON THE REDUCTIVE HALF-REACTION OF TYROSINE TO PHENYLALANINE ACTIVE SITE VARIANTS OF D-ARGININE DEHYDROGENASE	59
4.1 Abbreviations	59
4.2 Abstract.....	59
4.3 Introduction.....	60
4.4 Experimental Procedures	63
4.5 Results	68
4.6 Discussion.....	76
4.7 Conclusions.....	80
4.8 Acknowledgements	81
4.9 References	81
5 BIOCHEMICAL AND STRUCTURAL CHARACTERIZATION OF GREEN FLAVIN FROM MUTANT VARIANT OF D-ARGININE DEHYDROGENASE	84
5.1 Abbreviations	84
5.2 Introduction.....	84
5.3 Experimental Procedures	89
5.4 Results	93
5.5 Discussion.....	107
5.6 Conclusion	112

5.7 Acknowledgements	113
5.8 References	113
6 RELATIVE TIMING OF HYDROGEN AND PROTON TRANSFERS IN THE REACTION OF FLAVIN OXIDATION CATALYZED BY CHOLINE OXIDASE...	119
6.1 Abstract.....	119
6.2 Introduction.....	119
6.3 Experimental Procedures.....	122
6.4 Results and Discussion.....	125
6.5 References	133
7 GENERAL DISCUSSION AND CONCLUSIONS	138
7.1 References	142
8 RESCUING OF THE HYDRIDE TRANSFER REACTION IN THE GLU312ASP VARIANT OF CHOLINE OXIDASE BY A SUBSTRATE ANALOGUE.....	146
8.1 Abstract.....	146
8.2 Introduction.....	147
8.3 Experimental Procedures.....	149
8.4 Results	152
8.5 Discussion.....	157

8.6 Acknowledgements160

8.7 References160

LIST OF TABLES

Table 1.1 Nobel prize winners in the field of flavins.....	1
Table 2.1 Selected enzymes processing amino acids.....	23
Table 3.1 pH Effects on k_{cat}/K_m and k_{cat} of PaDADH.	49
Table 3.2 pH Effects on Kinetic Isotope Effects with D-Leucine.	51
Table 4.1 Apparent Steady-State Kinetic Parameters for wild-type, Y53F, and Y249F PaDADH.	69
Table 4.2 pH Dependence of k_{red} and K_d in wild type, Y53F, and Y249F PaDADH.	73
Table 4.3 KIEs on k_{red} in the Y53F and Y249F enzymes ^a	74
Table 5.1 Enzymes with 6 OH flavins.	88
Table 6.1 Deuterium kinetic isotope effects on the second-order rate constant for flavin oxidation during steady-state turnover of choline oxidase.	128
Table 8.1 Reductive Half-Reaction with Choline and 3-HPTA as Substrate for Choline Oxidase Wild-type and Glu312Asp Variant.	154

LIST OF FIGURES

Figure 1.1 Representation of isoalloxazine ring system and the type of interactions with active site residues (modified from ref 4).....	2
Figure 1.2 Site of covalent linkage (indicated by arrows) on the isoalloxazine ring by active site residues in flavoproteins	4
Figure 1.3 Non-covalent substitutions on isoalloxazine ring of flavin. Modified from Figure 5.3 in chapter 5.....	5
Figure 1.4 General reaction scheme of the two-enzyme complex involved in D- to L-arginine racemization in <i>Pseudomonas aeruginosa</i> (Modified from Chapter 4, Scheme 4.1).....	9
Figure 2.1 Structural illustration of riboflavin, FMN, FAD and (iso)alloxazine ring. Modified from Chapter 5	18
Figure 2.2 Active site of pkDAAO (PDB code:1KIF).....	26
Figure 2.3 Interaction of iminoarginine (IAR) with Glu87 and Thr50 in paDADH (PDB code: 3NYE).....	27
Figure 2.4 Conserved Tyr residues in pkDAAO (blue) and paDADH (purple).....	30
Figure 3.1 Interactions of iminoarginine with active site residues of PaDADH.	44
Figure 3.2 pH-profiles of k_{cat} (A) and k_{cat}/K_m (B) with D-arginine (●) and D-lysine (○).	49
Figure 3.3 pH-profiles of k_{cat} (A) and k_{cat}/K_m (B) with D-methionine (●) and D-leucine (○).	50
Figure 3.4 Kinetic isotope effects on k_{red} at pH 8.5 with D-leucine (black) and D-leucine _{d10} in (red).....	52
Figure 4.1 The active site of PaDADH in complex with iminoarginine at 1.3 Å resolution (PDB: 3NYE).....	63

Figure 4.2 Illustration of the QM region in (a) open, substrate free, and (b) closed, substrate bound configurations.	66
Figure 4.3 UV-Visible absorption spectra of the Y53F (blue), Y249F (green), and wild-type <i>Pa</i> DADH (black) in 20 mM Tris-Cl, 10% glycerol, pH 8.7 and 22 °C.....	69
Figure 4.4 Reductive half-reactions for the Y53F and Y249F enzymes with D-leucine.....	70
Figure 4.5 Effects of pH on k_{red} and k_{rev} of the Y53F (top panel) and Y249F enzymes (bottom panel) with D-leucine.....	72
Figure 4.6 Effects of pH on $^{app}K_d$ of the Y53F and Y249F enzymes with D-leucine.....	72
Figure 4.7 Electrophilicity of the substrate binding sites close to the flavin C4a and N5 atoms in wild-type, Y53F and Y249F <i>Pa</i> DADH.	75
Figure 5.1 UV-Visible absorbance spectrum of green and yellow fractions.	94
Figure 5.2 UV-Visible absorbance spectrum of chromophores obtained from HPLC	96
Figure 5.3 1H NMR of bottom = FAD, middle = synthesized 6-OH FAD, top = HPLC purified 6-OH FAD.	98
Figure 5.4 A) HSQC spectra of aromatic regions of synthesized 6-OH (left) and FAD (right). B) slices from TOCSY spectra showing coupling between position 9 of the (iso)alloxazine ring and the adjacent methyl protons (left synthesized, right HPLC purified). C) HSQC spectrum of 6-OH FAD methyl protons.....	99
Figure 5.5 Negative ion ESI mass spectrum of the modified flavin isolated from DADH-Y249F enzyme.	100
Figure 5.6 pH titration of 6-OH FAD extracted from DADH-Y249F.....	102
Figure 5.7 Biochemical reactivity of DADH-Y249F bound FAD and 6-OH FAD.....	104

Figure 5.8 Illustration of DADH active sites of the optimized DADH models: (a) wild type, (b) Y249F, (c) wild type – 6OH-FAD, and (d) Y249F – FAD-6OH.	106
Figure 5.9 Illustration of the characterized active site cavities of the optimized DADH models: (a) wild type, (b) Y249F, (c) wild type – 6OH-FAD, and (d) Y249F – FAD-6OH.	107
Figure 5.10 Thermodynamics of key hydration sites around C6 carbon for DADH variants: (a) wild type, (b) Y249F, (c) wild type – 6OH-FAD, and (d) Y249F – FAD-6OH.	108
Figure 5.11 Van der Waals sphere representation of (a) unmodified flavin and (b) C6-hydroxylated flavin.	112
Figure 6.1 pD and viscosity contributions to solvent effects on $k_{\text{cat}}/K_{\text{ox}}$	127
Figure 6.2 Time-resolved absorbance spectroscopy of the oxidation of reduced choline oxidase with O ₂	131
Figure 8.1 The interaction between the carboxylate on residue 312 of choline oxidase and the trimethylammonium moiety of the activated substrate.	149
Figure 8.2 Reductive half-reaction of the Glu312Asp enzyme with 3-HPTA Stopped-flow traces were obtained at 450 nm upon mixing anaerobically the enzyme and substrate under pseudo first-order conditions at pH 10.0 and 25 °C.	155
Figure 8.3 pH-dependence of the steady-state kinetic parameters for wild-type choline oxidase (empty circles) with choline and Glu312Asp enzyme (solid circles) with 3-HPTA as substrate.	156

LIST OF SCHEMES

Scheme 1.1 Illustration of redox states of flavin cofactor. Note that the flavin has been shown to exist in the neutral form in this scheme while it can additionally exist in anionic form as well (Modified from ref 4).....	3
Scheme 1.2 Simplified illustration of the overall reaction scheme of flavin-dependent catalysis..	3
Scheme 1.3 Simplified reaction of reduced flavin (singlet) and O ₂ (triplet state) leading to flavin oxidation (modified from ref 6)	7
Scheme 2.1 Illustration of redox states of flavin cofactor. Note that the flavin has been shown to exist in the neutral form in this scheme while it can additionally exist in anionic form as well ...	19
Scheme 2.2 Illustration of the site of dehydrogenation in α -amino acids by flavoenzymes	20
Scheme 2.3 General scheme of reactions catalyzed by (a.) DAAO, (b.) LAAO and (c.) DADH	24
Scheme 2.4 Schematic representation of carbanion mechanism (a-b-c), hydride transfer (d-e) and polar nucleophilic attack (f-g-h) as catalyzed by amino acid oxidases and dehydrogenases. Scheme borrowed from Chapter 4	33
Scheme 3.1 Oxidation of D-Arginine by PaDADH.	43
Scheme 3.2 Reductive Half-reaction of PaDADH.	43
Scheme 3.3 Oxidative Half-reaction of PaDADH.	43
Scheme 4.1 Schematic illustration of D- to L-arginine racemization in <i>P. aeruginosa</i> and possible fates of L-arginine.....	61
Scheme 4.2 Possible mechanisms for CN bond oxidation by PaDADH: carbanion (a-b-c), hydride transfer (d-e) and polar nucleophilic attack (f-g-h).	62
Scheme 4.3 The reductive half-reaction catalyzed by the Y53F enzyme with D-leucine ^a	79
Scheme 5.1 Chemical structure of flavins	85

Scheme 5.2 Some modifications of the (iso)alloxazine moiety resulting in long wavelength absorbance and green coloration.....	85
Scheme 5.3 General reaction mechanism of PaDADH.....	87
Scheme 6.1 Possible routes for flavin oxidation in flavoproteins.....	121
Scheme 6.2 Reductive and oxidative half-reactions by choline oxidase with 1,2-[² H ₄]-choline as substrate; note that the timing for the cleavages of the various bonds is not addressed here.	122

1 INTRODUCTION

1.1 Flavins

1.1.1 *Brief history*

Flavins are yellow chromophores that have been first isolated from Cow's milk and reported more than a century ago by an English scientist by the name A. Winter Blyth. Research on flavins flourished during the early 19th century when it was identified to be a part of the vitamin B complex. Richard Kuhn and Paul Karrer independently determined and confirmed the structure and named it riboflavin based on its color and chemical structure. During his ground breaking work on cellular respiration, Otto Warburg extracted a flavoprotein from yeast that oxidizes NADPH using molecular oxygen in the course of its reaction. Hugo Theorell, a Swedish biochemist discovered that the flavin cofactor of the flavoprotein isolated by Warburg is not riboflavin but has an additional phosphate group which later came to be known as flavin mononucleotide (FMN). Hans Krebs discovered a second flavoprotein that is involved in D-amino acid metabolism called D-amino acid oxidase while Warburg and Christian showed that the cofactor in use is not riboflavin or FMN. Alexander Todd and his coworkers were responsible for the chemical synthesis of FAD as a proof of structure to the one isolated from DAAO.¹ The popularity for the flavin field stems from the fact that six Nobel prizes have been awarded in the research related either directly or indirectly to flavin chemistry (**Table 1.1**).

Table 1.1 Nobel prize winners in the field of flavins

Scientists	Year
Otto Warburg	1931
Paul Karrer	1937
Richard Kuhn	1938
Hans Krebs	1953
Hugo Theorell	1955
Alexander Todd	1957

1.1.2 *Chemistry*

Flavins are multifunctional and the structure that allows such versatility is the three membered-ring system: 7,8-dimethyl-isoalloxazine which is formed by the fusion of xylene, pyrazine and pyrimidine

rings¹⁻³ (**Figure 1.1**). The hydrophobicity of xylene ring makes important hydrophobic interactions in the enzyme active site offering stability while the electron deficient pyrimidine ring allows electron transfer chemistry that the flavins are known for.³ Flavins occur in multiple redox states and associated colors: oxidized (yellow) and reduced (colorless) are the two extremes while intermediary species is the semiquinoid (blue and red) form.^{1, 3-5} The semiquinoid and fully reduced forms can further exist as anionic or neutral depending on their protonation states (**Scheme 1.1**).^{1, 3, 4} Each redox state of flavin chromophore also has unique spectral property⁵, a feature that is well exploited in the characterization of flavoproteins. Because of their redox nature, flavoproteins bring about catalysis via two half reactions, namely, the reductive half reaction where the flavin cofactor accepts reducing equivalents from first substrate followed by the oxidative half-reaction where the reducing equivalents from the flavin are passed to second substrate which is molecular oxygen (O₂) in many cases.^{1, 3, 6} The classification of the reductive and oxidative half-reactions is with respect to flavins (**Scheme 1.2**). Although they constitute one catalytic cycle, the reductive and oxidative half-reactions operate independent to one another. While a lot of work has been focused on the mechanism of the transfer of reducing equivalents onto the flavin^{7, 8}, much less is known on the mode of transfer of reducing equivalents from flavin to the second substrate and more specifically O₂ mainly because of the chemical properties associated with it.^{1, 6, 9, 10}

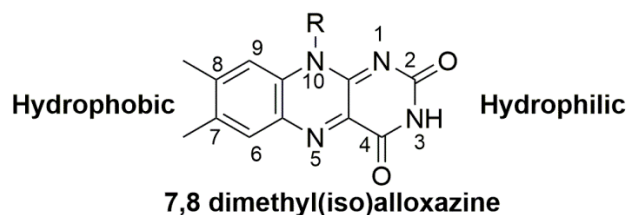
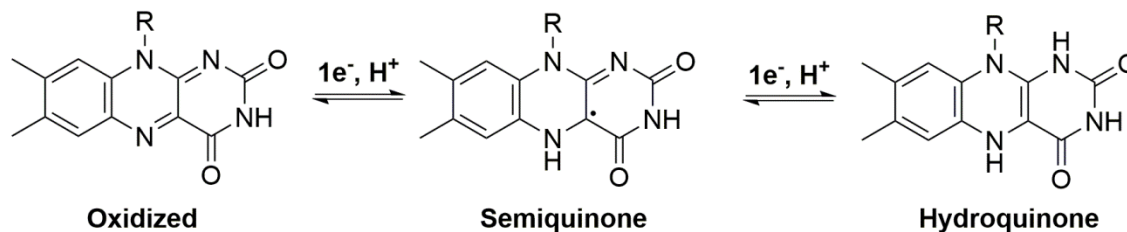
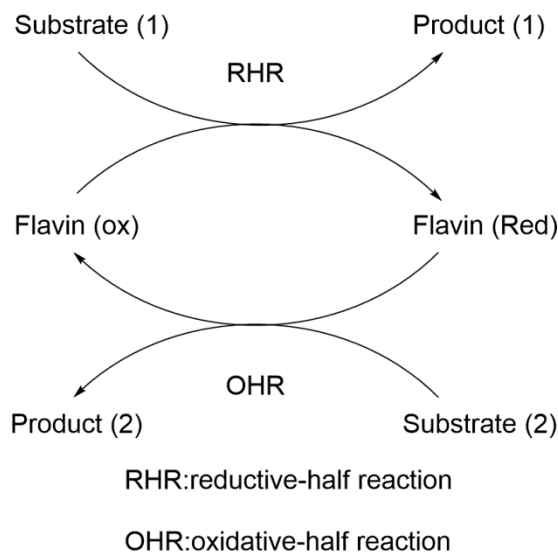


Figure 1.1 Representation of isoalloxazine ring system and the type of interactions with active site residues (modified from ref 4)



Scheme 1.1 Illustration of redox states of flavin cofactor. Note that the flavin has been shown to exist in the neutral form in this scheme while it can additionally exist in anionic form as well (Modified from ref 4).



Scheme 1.2 Simplified illustration of the overall reaction scheme of flavin-dependent catalysis

1.1.3 Modified natural flavins

Although riboflavin, FMN and FAD are the most commonly occurring forms of flavins in biology, there are many accounts of modifications on these cofactors that result in their derivatives with slightly or greatly altered spectral and/or chemical properties.² These are found either naturally or have been artificially synthesized as probes to gain further knowledge on flavin chemistry.^{4, 11} Natural modifications of flavins can be divided into at least two categories:

i.) covalently bound FMN and FAD are attached to proteins via modifications at C6 atom or 8 α -methyl group of the isoalloxazine ring system (**Figure 1.2**).^{2, 12} First covalently linked flavoprotein was reported to exist by Singer and coworkers in succinate dehydrogenase in 1950.^{2, 13} The covalent bond was

between an active site histidine $N(3)$ and 8α -methyl group of FAD.¹³ Subsequent studies showed the existence of other linkages like histidine ($N(1)$), S-cysteinyl or O-tyrosyl at the 8α -position and S-cysteinyl at C6 of the isoalloxazine.^{2, 12} The process of covalent bond formation is referred to as flavinylation. In 2005, bicovalently linked flavins have also been reported for the first time from the crystal structure of fungal glucooligosacchharide oxidase studies.¹⁴ BLASTP analysis showed that such linkages seem restricted to bacteria, fungus and plant kingdoms with no reports from archae and animal kingdoms.¹⁵ Furthermore enzymes from the *p*-cresolmethylhydroxylase (PCMH) superfamily in general seem to be predisposed to have mono or bicovalent flavin linkages, while monocovalent linkages are more common in proteins with NADP-Rossman, GMC (FAD-dependent enzymes) and TIM barrel (FMN-dependent enzymes) topologies. So far 43 proteins have been reported with flavin mono or bicovalent linkages.¹⁵

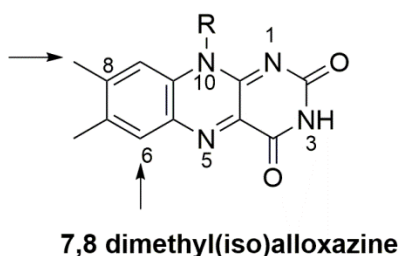
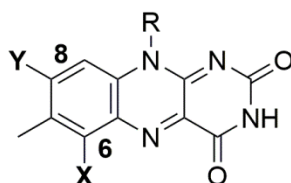


Figure 1.2 Site of covalent linkage (indicated by arrows) on the isoalloxazine ring by active site residues in flavoproteins

Several interpretations have been put forth to rationalize flavinylation process in flavoproteins. The midpoint redox potential has been shown to be greatly tuned allowing turnover of catalytically difficult substrates.¹⁶⁻¹⁸ Another feature of covalent linkages is the restriction of cofactor movement allowing higher enzyme to cofactor incorporation and better catalytic efficiency.¹⁹ Proper positioning of cofactor is key since studies on choline oxidase showed that for mutation of the His99 involved in covalent linkage to Asn not only caused for the loss of the linkage but also resulted in the lowering of kinetic parameters, k_{cat}/k_m and $k_{cat} \leq 30$ fold. Temperature dependence of the isotope effect on the rate constant for flavin reduction (k_{red}) suggested that the preorganization that is required for the transfer of hydride ion from the

alcohol substrate to the N(5) of flavin is affected because of the loss of flavinylation.²⁰ These reports from different enzymes provide evidence that some enzymes may have evolved to optimize catalysis via covalently attached flavin cofactors. It has however not been established as to what conditions drive flavinylation in these enzymes and if there may be any general properties guiding such a process.



X = OH; Y = H

Y = OH, NH₂; X = H

Figure 1.3 Non-covalent substitutions on isoalloxazine ring of flavin. Modified from Figure 5.3 in Chapter 5

ii.) O- or N-substitutions at 6th and 8th position of isoalloxazine

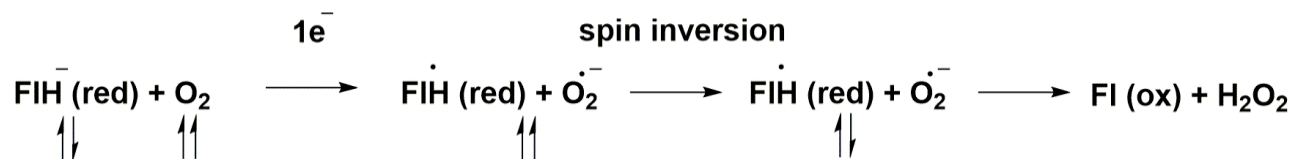
Like covalent linkages, the 6th and 8th positions are susceptible to substitution reactions by the -NH₂ and -OH functional groups (**Figure 1.3**).² These substitutions do not however result in covalent linkage to the protein. Modifications of flavin by -OH functional group have first been isolated in 1970: 6 and 8-hydroxy FAD from electron transferring flavoprotein and 6-hydroxy FMN from pig kidney glycolate oxidase.^{21, 22} Additional examples include 8-hydroxy-5-deazaflavin detected in extracts of methylotrophic bacteria with distinct chemical properties compared to riboflavins and its analogues;² antibiotic 8-aminoriboflavins termed “roseoflavins” synthesized by a species of *Streptomyces*.^{2, 23} Furthermore 6-hydroxy FAD and FMN have been reported in numerous bacteria, invertebrates and even humans.²⁴⁻²⁹ These unusual flavins have distinct spectral properties^{11, 21} and are present in combination with the naturally occurring flavin cofactor and hence are not found in stoichiometric amounts in the proteins.

They have also been shown not to have the same catalytic competence as the unmodified flavin cofactors.^{21, 24, 26-28} Little is known about their origin and biological importance. Notwithstanding, they have been synthesized artificially along with several other unnatural flavins as probes to further knowledge on flavin mediated chemistry in flavoproteins.¹¹

1.1.4. Oxidative half-reaction

Reduced flavin formed during the reductive half-reaction can react with various secondary substrates that act as oxidants in the oxidative half reaction. Molecular oxygen is a prime example of oxidants that the flavoproteins can react with. The reaction has also received considerable interest since molecular oxygen is unreactive toward most biological molecules because of its diradical nature in the ground state.^{6, 30} As a result it needs to be activated for reaction.^{6, 30} In solution, the reaction between reduced flavin in singlet state and molecular oxygen in its triplet ground state is very slow because of the spin difference linked to the two species (**Scheme 1.3**).^{6, 30} The same reaction catalyzed in the active site of a flavoprotein achieves a boost of several orders of magnitude or may be lowered significantly than in solution.⁶ This clearly indicated that flavoproteins have differential reactivity for molecular oxygen and based on this property, there are four proposed classes of flavoproteins:⁶

1. Dehydrogenases: They are defined by poor or no reactivity toward O₂. Poor reactivity can lead to the production of H₂O₂ and O₂^{•-} as products.
2. Transferases: They react poorly with O₂, resulting in the formation of neutral flavin semiquinone radical and O₂^{•-}.
3. Oxidases: They are known to react swiftly with molecular oxygen and are characterized by the production of H₂O₂ and fully oxidized flavin.
4. Monooxygenases: As the name suggests, only one oxygen atom proceeds to reduction as H₂O while the second atom is inserted into the reaction product. They are also known for rapid reaction with O₂.



Scheme 1.3 Simplified reaction of reduced flavin (singlet) and O₂ (triplet state) leading to flavin oxidation (modified from ref 6)

In the oxidative half-reaction, reaction of free reduced flavin with O₂ has been shown to proceed via the formation of C4a-hydroperoxide. It has therefore been proposed that when flavoproteins react with molecular O₂, flavin-derived intermediates possibly form along the reaction pathway. Monooxygenases is the only class of flavoenzymes that have experimental evidence demonstrating the involvement of detectable flavin-based C4a-(hydro)peroxide intermediates in the reaction pathway of reduced flavin with O₂.^{6, 10} For oxidases however, there does not seem to be a defined path like monooxygenases when it comes to the reaction with O₂ with the exceptions of pyranose 2-oxidase^{31, 32} and a mutant of NADH oxidase³³. Flavin-dependent dehydrogenases on the other hand react more readily with other oxidants like NAD(P)⁺, cytochrome, quinone etc so as to regenerate the reduced flavin during the oxidative half reaction. As seen here, molecular O₂ is not a requisite for the oxidation of the reduced flavoproteins. Therefore, this quality of flavoproteins allows them to carry out redox reactions in aerobic as well as anaerobic organisms.

1.2 Specific Goals

Reaction profile of flavoproteins divided into the reductive and oxidative half reactions gives rise to multiple mechanistic possibilities for each half reaction. Although catalytic mechanisms are well understood for some classes or families of enzymes,^{7, 8} mechanistic details for several others are still nascent.⁷ For instance, while the reductive half-reaction most likely involves the transfer of hydride ion from the substrate to the flavin in alcohol and α-hydroxy acid oxidizing enzymes,⁷ a clear winner hasn't emerged in group of enzymes oxidizing amino acids except in D-amino acid oxidase mainly because

structural and mechanistic data are lacking in enzymes carrying out similar reactions.⁷ Additionally, oxidative half-reaction of monooxygenases progress with the formation of C4a-(hydro)peroxy flavin^{6, 34} in the reaction with O₂ but the science behind oxygen reactivity of flavin-dependent oxidases is still at an elementary stage.^{6, 9, 10} While several new aspects on the chemistry of natural unmodified flavins (FMN and FAD) are still surfacing, knowledge on the biological significance and origin of naturally occurring substituted flavins is fragmentary. Specifically, many cases of detection of C6 modification of the isoalloxazine ring by a hydroxyl group have been recurrent with the first case of detection reported approximately half a century ago.²¹

The overall goal of this dissertation is to expound several aspects of flavin-chemistry: roles in amino acid oxidation; insights into the 6-hydroxy substitution on the cofactor; and their reactivity with molecular oxygen using bacterial D-arginine dehydrogenase (DADH) and choline oxidase (CHO) as model systems.

A novel two-enzyme pathway involved in the metabolism of L-arginine was discovered recently in *Pseudomonas aeruginosa* wherein D-arginine is converted to L-arginine by catabolic D-arginine dehydrogenase (PaDADH) and anabolic L-arginine dehydrogenase (PaDADH) (**Figure 1.4**).³⁵ PLP-dependent and independent racemases are generally involved in D and L racemization.³⁶ Therefore, the discovery of the two-enzyme complex is of interest to understand the various ways of racemization of amino acids. PaDADH, the first enzyme in the complex is FAD-dependent and catalyzes the oxidation of not only D-arginine but most D-amino acids to their corresponding imino acids.³⁷⁻³⁹ The imino acids are proposed to be deaminated non-enzymatically to α -keto acids in the presence of water with the release of ammonia (**Figure 1.4**).³⁸ Ammonia has been suggested to play a role in pH homeostasis in biofilms which is a key survival tactic of many pathogenic bacteria.^{40, 41} Therefore ammonia generated from the breakdown of D-amino acids by PaDADH may contribute to pseudomonads' virulence and pathogenicity. Previous structural and kinetic work on the enzyme showed that the enzyme binds and oxidizes cationic substrates the best followed by zwitterionic/hydrophobic substrates but not anionic substrates and glycine.^{37, 38, 42} Multiple binding modes have been reported which are substrate dependent.³⁷ Furthermore, the catalytic mechanism of amino acid oxidation for which multiple mechanistic possibilities can be envisioned due to the

versatile nature of FAD has been reported to proceed with the transfer of a “hydride equivalent” from substrate amino acid (D-Leu) to FAD.⁴² Although a flavin radical based mechanism has been ruled out, the results are still consistent with a carbanion, hydride ion transfer and polar nucleophilic attack mechanisms during amino acid oxidation.⁴² Furthermore, several key active site residues emerged from these studies with proposed roles in substrate specificity and catalysis.^{37, 42}

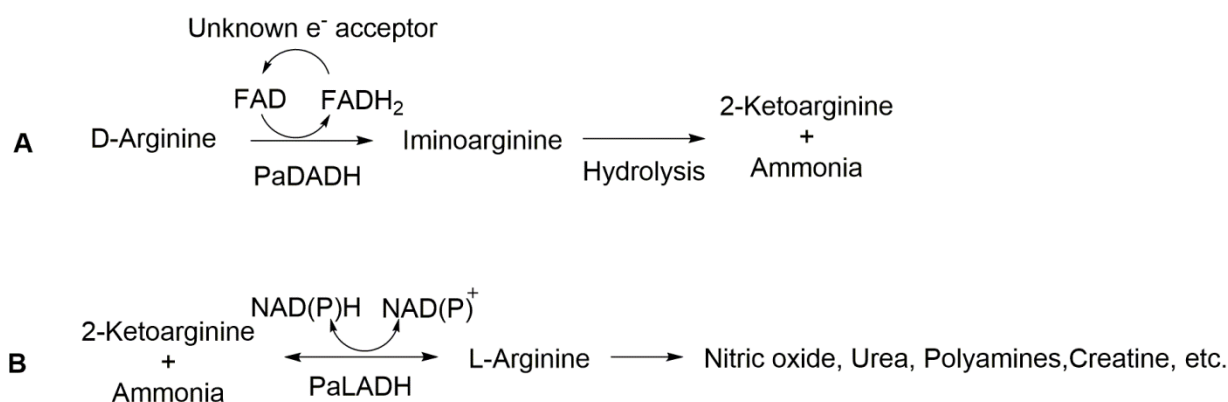


Figure 1.4 General reaction scheme of the two-enzyme complex involved in D- to L-arginine racemization in *Pseudomonas aeruginosa* (Modified from Chapter 4, Scheme 4.1)

Chapter 2 in this dissertation sets stage with a review on the general structural and common mechanistic pathways adopted by amino acid-processing enzymes. As reported in previous studies, PaDADH exhibits high specificity for cationic and neutral substrates. Chapter 3 aims to gain further insights concerning the preference for cationic and zwitterionic D-amino acids by PaDADH at the level of active site interactions using multiple substrates, pH effects and kinetic isotope effects on steady state and/or rapid reaction kinetics.

Tyr53 and Tyr249 are located < 4 Å from iminoarginine, the co-crystallized product in the crystal structure of PaDADH. The residues have been proposed to play crucial roles in substrate binding and oxidation in PaDADH and possibly affect the timing of the NH and CH bond cleavages that are obligatory for amino acid oxidation. Tyr53 and 249 have been manipulated mutagenically to Phe and the variant

enzymes were elucidated for effects on substrate binding, catalysis as well as in minimizing the catalytic possibilities adopted by PaDADH between carbanion, hydride ion and polar nucleophilic attack mechanisms using deuterium substrate and solvent isotope effects on rapid reaction kinetics and computational approaches using QM/MM methodologies. This work has been described in Chapter 4. Mutation of Tyr249 to Phe resulted in the variant enzyme incorporated with partially modified FAD cofactor. Chapter 5 in this dissertation addresses spectroscopic and spectrometric characterization of the modified FAD isolated from the Tyr249Phe mutant of PaDADH as 6 hydroxy FAD; furthermore computational approaches have been sought to answer fundamental questions associated with molecular properties and reactivity of 6-hydroxy FAD in PaDADH.

Choline oxidase (E.C.1.1.3.17), also known as choline: oxygen-1-oxidoreductase, catalyzes the conversion of choline and oxygen to glycine betaine (GB) and hydrogen peroxide in *Arthobacter globiformis*. It uses covalently bound FAD for the reaction. The reaction occurs in two steps with the transfer of $2e^-$ in each step via an aldehyde intermediate (betaine aldehyde). The reaction by choline oxidase has biotechnological relevance because the product of its reaction,⁴³ glycine betaine, is a well-known osmolyte.^{43, 44} It has been shown that in plants subjected to harsh environmental conditions like high salinity, low temperatures and drought, GB plays an important role in regulating the stress. It is synthesized naturally in some plant species like spinach and wheat and not in others like rice, tomato and maize. As such, introduction of GB biosynthetic pathway into these non-accumulators results in enhanced tolerance for environmental stresses. Therefore, introduction of bacterial *codA* gene that expresses choline oxidase to create transgenic plants is of economic significance.⁴⁴

Several mechanistic and structural studies on wild-type choline oxidase established the catalytic mechanism of choline oxidation to glycine betaine to proceed via hydride transfer mechanism with several active site residues like Ser101, Glu312, Asn510, His351, Val464, and His466 proposed to play key roles in substrate binding, positioning, activation, stabilization of transition state or reactivity with oxygen.⁴⁵⁻⁵⁴ Moreover, the positive charges residing on the betaine aldehyde intermediate and glycine betaine product

have been shown to be essential for reaction with molecular oxygen by reduced FAD in CHO.^{48, 55} Furthermore, crystal structure of choline oxidase showed that FAD was trapped in a C4a-peroxy adduct form in the absence of any bound ligand.⁵⁶ Experimental evidence for such flavin-derived intermediate has previously been shown only in pyranose-2 oxidase and a mutant of NADH oxidase.³¹⁻³³ Therefore, questions on the existence of C4a-peroxy flavin intermediate in choline oxidase as part of the reaction pathway or an artifact of exposure to the high frequency X-ray beam are still not fully established. Finally, Chapter 6 in this dissertation addresses the possible mechanism followed by choline oxidase in the reaction of reduced FAD with O₂ applying deuterium isotope effects on steady state kinetics and rapid-reaction kinetics using a stopped-flow spectrophotometer.

1.3 References

1. Massey, V. (2000) The chemical and biological versatility of riboflavin, *Biochemical Society transactions* 28, 283-296.
2. Ghisla, S., and Edmondson, D. E. (2001) Flavin Coenzymes, In *eLS*, John Wiley & Sons, Ltd.
3. Ghisla, S., and Massey, V. (1989) Mechanisms of flavoprotein-catalyzed reactions, *European journal of biochemistry / FEBS* 181, 1-17.
4. Ghisla, S., and Massey, V. (1986) New flavins for old: artificial flavins as active site probes of flavoproteins, *The Biochemical journal* 239, 1-12.
5. Massey, V., and Palmer, G. (1966) On the existence of spectrally distinct classes of flavoprotein semiquinones. A new method for the quantitative production of flavoprotein semiquinones, *Biochemistry* 5, 3181-3189.
6. Massey, V. (1994) Activation of molecular oxygen by flavins and flavoproteins, *The Journal of biological chemistry* 269, 22459-22462.
7. Fitzpatrick, P. F. (2001) Substrate dehydrogenation by flavoproteins, *Accounts of chemical research* 34, 299-307.

8. Fitzpatrick, P. F. (2010) Oxidation of amines by flavoproteins, *Archives of biochemistry and biophysics* 493, 13-25.
9. Chaiyen, P., Fraaije, M. W., and Mattevi, A. (2012) The enigmatic reaction of flavins with oxygen, *Trends in biochemical sciences* 37, 373-380.
10. Mattevi, A. (2006) To be or not to be an oxidase: challenging the oxygen reactivity of flavoenzymes, *Trends in biochemical sciences* 31, 276-283.
11. Ghisla, S., Massey, V., and Yagi, K. (1986) Preparation and some properties of 6-substituted flavins as active site probes for flavin enzymes, *Biochemistry* 25, 3282-3289.
12. Mewies, M., McIntire, W. S., and Scrutton, N. S. (1998) Covalent attachment of flavin adenine dinucleotide (FAD) and flavin mononucleotide (FMN) to enzymes: the current state of affairs, *Protein science : a publication of the Protein Society* 7, 7-20.
13. Singer, T. P., Kearney, E. B., and Massey, V. (1956) Observations on the flavin moiety of succinic dehydrogenase, *Archives of biochemistry and biophysics* 60, 255-257.
14. Huang, C. H., Lai, W. L., Lee, M. H., Chen, C. J., Vasella, A., Tsai, Y. C., and Liaw, S. H. (2005) Crystal structure of glucooligosaccharide oxidase from *Acremonium strictum*: a novel flavinylation of 6-S-cysteinyl, 8 α -N1-histidyl FAD, *The Journal of biological chemistry* 280, 38831-38838.
15. Hille, R., Miller, S., and Palfey, B. (2012) *Handbook of Flavoproteins, Volume 1 Oxidases, Dehydrogenases and Related Systems*.
16. Heuts, D. P., Winter, R. T., Damsma, G. E., Janssen, D. B., and Fraaije, M. W. (2008) The role of double covalent flavin binding in chito-oligosaccharide oxidase from *Fusarium graminearum*, *The Biochemical journal* 413, 175-183.
17. Huang, C. H., Winkler, A., Chen, C. L., Lai, W. L., Tsai, Y. C., Macheroux, P., and Liaw, S. H. (2008) Functional roles of the 6-S-cysteinyl, 8 α -N1-histidyl FAD in glucooligosaccharide oxidase from *Acremonium strictum*, *The Journal of biological chemistry* 283, 30990-30996.

18. Winkler, A., Kutchan, T. M., and Macheroux, P. (2007) 6-S-cysteinylation of bi-covalently attached FAD in berberine bridge enzyme tunes the redox potential for optimal activity, *The Journal of biological chemistry* 282, 24437-24443.
19. Heuts, D. P., Scrutton, N. S., McIntire, W. S., and Fraaije, M. W. (2009) What's in a covalent bond? On the role and formation of covalently bound flavin cofactors, *The FEBS journal* 276, 3405-3427.
20. Quaye, O., Cowins, S., and Gadda, G. (2009) Contribution of flavin covalent linkage with histidine 99 to the reaction catalyzed by choline oxidase, *The Journal of biological chemistry* 284, 16990-16997.
21. Mayhew, S. G., Whitfield, C. D., Ghisla, S., and Schuman-jörns, M. (1974) Identification and Properties of New Flavins in Electron-Transferring Flavoprotein from *Peptostreptococcus elsdenii* and Pig-Liver Glycolate Oxidase, *European Journal of Biochemistry* 44, 579-591.
22. Ghisla, S., and Mayhew, S. G. (1976) Identification and Properties of 8-Hydroxyflavin -Adenine Dinucleotide in Electron-Transferring Flavoprotein from *Peptostreptococcus elsdenii*, *European Journal of Biochemistry* 63, 373-390.
23. Pedrolli, D. B., Nakanishi, S., Barile, M., Mansurova, M., Carmona, E. C., Lux, A., Gartner, W., and Mack, M. (2011) The antibiotics roseoflavin and 8-demethyl-8-amino-riboflavin from *Streptomyces davawensis* are metabolized by human flavokinase and human FAD synthetase, *Biochemical pharmacology* 82, 1853-1859.
24. Huang, L., Scrutton, N. S., and Hille, R. (1996) Reaction of the C30A mutant of trimethylamine dehydrogenase with diethylmethylamine, *The Journal of biological chemistry* 271, 13401-13406.
25. Mewies, M., Basran, J., Packman, L. C., Hille, R., and Scrutton, N. S. (1997) Involvement of a flavin iminoquinone methide in the formation of 6-hydroxyflavin mononucleotide in trimethylamine dehydrogenase: a rationale for the existence of 8 α -methyl and C6-linked covalent flavoproteins, *Biochemistry* 36, 7162-7168.

26. Morpeth, F. F., and Jones, G. D. (1986) Resolution, purification and some properties of the multiple forms of cellobiose quinone dehydrogenase from the white-rot fungus *Sporotrichum pulverulentum*, *The Biochemical journal* 236, 221-226.
27. Negri, A., Massey, V., and Williams, C. H., Jr. (1987) D-aspartate oxidase from beef kidney. Purification and properties, *The Journal of biological chemistry* 262, 10026-10034.
28. Tedeschi, G., Negri, A., Cecilian, F., Ronchi, S., Vetere, A., D'Aniello, G., and D'Aniello, A. (1994) Properties of the flavoenzyme D-aspartate oxidase from *Octopus vulgaris*, *Biochimica et biophysica acta* 1207, 217-222.
29. Marshall, K. R., Gong, M., Wodke, L., Lamb, J. H., Jones, D. J., Farmer, P. B., Scrutton, N. S., and Munro, A. W. (2005) The human apoptosis-inducing protein AMID is an oxidoreductase with a modified flavin cofactor and DNA binding activity, *The Journal of biological chemistry* 280, 30735-30740.
30. Gadda, G. (2012) Oxygen activation in flavoprotein oxidases: the importance of being positive, *Biochemistry* 51, 2662-2669.
31. Sucharitakul, J., Wongnate, T., and Chaiyen, P. (2011) Hydrogen peroxide elimination from C4a-hydroperoxyflavin in a flavoprotein oxidase occurs through a single proton transfer from flavin N5 to a peroxide leaving group, *The Journal of biological chemistry* 286, 16900-16909.
32. Thotsaporn, K., Chenprakhon, P., Sucharitakul, J., Mattevi, A., and Chaiyen, P. (2011) Stabilization of C4a-hydroperoxyflavin in a two-component flavin-dependent monooxygenase is achieved through interactions at flavin N5 and C4a atoms, *The Journal of biological chemistry* 286, 28170-28180.
33. Mallett, T. C., and Claiborne, A. (1998) Oxygen reactivity of an NADH oxidase C42S mutant: evidence for a C(4a)-peroxyflavin intermediate and a rate-limiting conformational change, *Biochemistry* 37, 8790-8802.
34. Palfey, B. A., and McDonald, C. A. (2010) Control of catalysis in flavin-dependent monooxygenases, *Archives of biochemistry and biophysics* 493, 26-36.

35. Li, C., and Lu, C.-D. (2009) Arginine racemization by coupled catabolic and anabolic dehydrogenases, *Proceedings of the National Academy of Sciences* 106, 906-911.
36. Yoshimura, T., and Esak, N. (2003) Amino acid racemases: functions and mechanisms, *Journal of bioscience and bioengineering* 96, 103-109.
37. Fu, G., Yuan, H., Li, C., Lu, C. D., Gadda, G., and Weber, I. T. (2010) Conformational changes and substrate recognition in *Pseudomonas aeruginosa* D-arginine dehydrogenase, *Biochemistry* 49, 8535-8545.
38. Yuan, H., Fu, G., Brooks, P. T., Weber, I., and Gadda, G. (2010) Steady-state kinetic mechanism and reductive half-reaction of D-arginine dehydrogenase from *Pseudomonas aeruginosa*, *Biochemistry* 49, 9542-9550.
39. Li, C., and Lu, C. D. (2009) Arginine racemization by coupled catabolic and anabolic dehydrogenases, *Proceedings of the National Academy of Sciences of the United States of America* 106, 906-911.
40. Zhu, Y., Weiss, E. C., Otto, M., Fey, P. D., Smeltzer, M. S., and Somerville, G. A. (2007) *Staphylococcus aureus* biofilm metabolism and the influence of arginine on polysaccharide intercellular adhesin synthesis, biofilm formation, and pathogenesis, *Infection and immunity* 75, 4219-4226.
41. Beenken, K. E., Dunman, P. M., McAleese, F., Macapagal, D., Murphy, E., Projan, S. J., Blevins, J. S., and Smeltzer, M. S. (2004) Global gene expression in *Staphylococcus aureus* biofilms, *Journal of bacteriology* 186, 4665-4684.
42. Yuan, H., Xin, Y., Hamelberg, D., and Gadda, G. (2011) Insights on the mechanism of amine oxidation catalyzed by D-arginine dehydrogenase through pH and kinetic isotope effects, *Journal of the American Chemical Society* 133, 18957-18965.
43. Fan, F., Ghanem, M., and Gadda, G. (2004) Cloning, sequence analysis, and purification of choline oxidase from *Arthrobacter globiformis*: a bacterial enzyme involved in osmotic stress tolerance, *Archives of biochemistry and biophysics* 421, 149-158.

44. Ahmad, R., Kim, M. D., Back, K. H., Kim, H. S., Lee, H. S., Kwon, S. Y., Murata, N., Chung, W. I., and Kwak, S. S. (2008) Stress-induced expression of choline oxidase in potato plant chloroplasts confers enhanced tolerance to oxidative, salt, and drought stresses, *Plant cell reports* 27, 687-698.
45. Fan, F., and Gadda, G. (2005) On the catalytic mechanism of choline oxidase, *Journal of the American Chemical Society* 127, 2067-2074.
46. Fan, F., and Gadda, G. (2005) Oxygen- and temperature-dependent kinetic isotope effects in choline oxidase: correlating reversible hydride transfer with environmentally enhanced tunneling, *Journal of the American Chemical Society* 127, 17954-17961.
47. Fan, F., and Gadda, G. (2007) An internal equilibrium preorganizes the enzyme-substrate complex for hydride tunneling in choline oxidase, *Biochemistry* 46, 6402-6408.
48. Gadda, G., Fan, F., and Hoang, J. V. (2006) On the contribution of the positively charged headgroup of choline to substrate binding and catalysis in the reaction catalyzed by choline oxidase, *Archives of biochemistry and biophysics* 451, 182-187.
49. Quaye, O., Lountos, G. T., Fan, F., Orville, A. M., and Gadda, G. (2008) Role of Glu312 in binding and positioning of the substrate for the hydride transfer reaction in choline oxidase, *Biochemistry* 47, 243-256.
50. Ghanem, M., and Gadda, G. (2005) On the catalytic role of the conserved active site residue His466 of choline oxidase, *Biochemistry* 44, 893-904.
51. Rungsisuriyachai, K., and Gadda, G. (2008) On the role of histidine 351 in the reaction of alcohol oxidation catalyzed by choline oxidase, *Biochemistry* 47, 6762-6769.
52. Finnegan, S., Agniswamy, J., Weber, I. T., and Gadda, G. (2010) Role of valine 464 in the flavin oxidation reaction catalyzed by choline oxidase, *Biochemistry* 49, 2952-2961.
53. Finnegan, S., Yuan, H., Wang, Y. F., Orville, A. M., Weber, I. T., and Gadda, G. (2010) Structural and kinetic studies on the Ser101Ala variant of choline oxidase: catalysis by compromise, *Archives of biochemistry and biophysics* 501, 207-213.

54. Yuan, H., and Gadda, G. (2011) Importance of a serine proximal to the C(4a) and N(5) flavin atoms for hydride transfer in choline oxidase, *Biochemistry* 50, 770-779.
55. Fan, F., Germann, M. W., and Gadda, G. (2006) Mechanistic studies of choline oxidase with betaine aldehyde and its isosteric analogue 3,3-dimethylbutyraldehyde, *Biochemistry* 45, 1979-1986.
56. Orville, A. M., Lountos, G. T., Finnegan, S., Gadda, G., and Prabhakar, R. (2009) Crystallographic, spectroscopic, and computational analysis of a flavin C4a-oxygen adduct in choline oxidase, *Biochemistry* 48, 720-728.

2 AMINO ACID DEHYDROGENATION BY FLAVOENZYMES

2.1 Significance of flavoenzymes

Flavin mononucleotide (FMN) or flavin adenine dinucleotide (FAD) is generally referred to as flavin cofactor. The flavin cofactors are derivatives of vitamin B2 also referred to as riboflavin (**Figure 2.1**).^{1, 2} Enzymes using these cofactors catalyze a wide variety of biologically important chemical reactions.³ In fact up to 3% of all genes in prokaryotic and eukaryotic genomes are estimated to code for flavoenzymes.⁴ They are typically involved in redox catalysis and responsible for a plethora of reactions ranging from the complicated photo emission or repair of damaged DNA to simple dehydrogenation of alcohols, α -hydroxy acids and α -amino acids.^{3, 5, 6} Because of their ubiquitous nature, ease of characterization, spectral properties there is an overabundance of information on flavoenzymes making it one of the well-studied classes of enzymes.

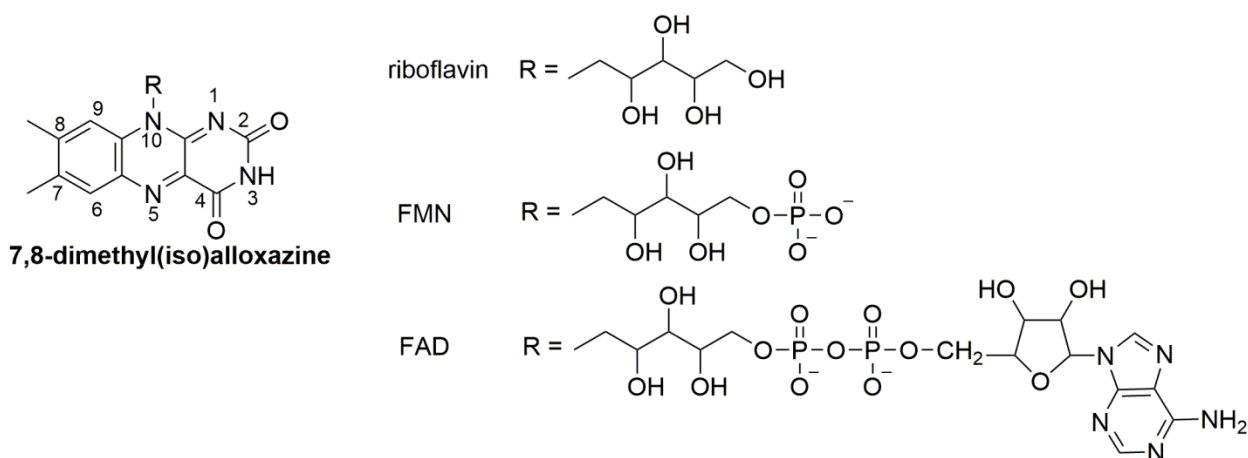
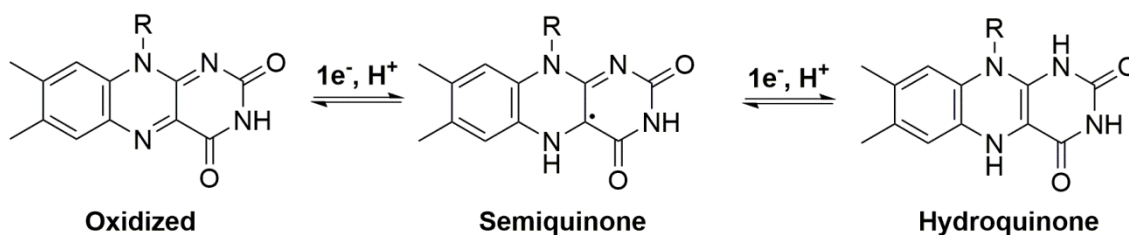


Figure 2.1 Structural illustration of riboflavin, FMN, FAD and (iso)alloxazine ring. Modified from Chapter 5

The reactive site of a flavin cofactor is the 7,8-dimethylisoalloxazine moiety (**Figure 2.1**) which can shuttle between an oxidized, one electron and two electron reduced forms (**Scheme 2.1**).^{1, 5, 6} For fully reduced state, the potential (E_m , pH 7) is approximately -200 mV. Interactions of the isoalloxazine moiety with protein active site influences the redox potential to be from anywhere between -495 mV to +80mV.⁶

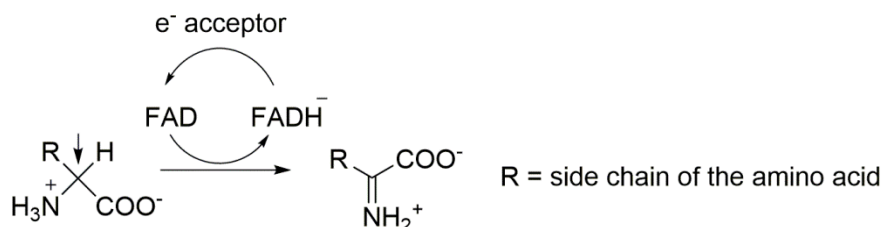
This is one of the important properties of flavin cofactors that confer chemical versatility on flavoenzymes. While isoalloxazine ring system engages in redox chemistry, its side chain (**Figure 2.1**) allows proper positioning and stability in the active site for optimal catalysis.⁶ The possibility of one electron or two electron transfers from substrates gives rise to multiple possibilities: transfer of a single electron, hydrogen atoms or a hydride ion.⁷ The electron deficient pyrimidine nucleus of the isoalloxazine ring system is susceptible to nucleophilic attacks either at the N(5) or C(4a) sites with the possibility of flavin-adduct formation during the course of catalysis.^{2, 6} Because of the various possibilities in the transfer of reducing equivalents from the substrate onto flavin, multitude of mechanistic possibilities can be envisioned for different classes of flavoenzymes.⁷⁻⁹ This review however will focus only on the dehydrogenation of α -amino acids (D/L) catalyzed by flavoenzymes.



Scheme 2.1 Illustration of redox states of flavin cofactor. Note that the flavin has been shown to exist in the neutral form in this scheme while it can additionally exist in anionic form as well

Flavoenzymes break down α -amino acids by oxidizing the bond between the α -carbon and the amine nitrogen (**Scheme 2.2**). Flavin dependent C-N bond oxidations involving amino acids or amines are found in key life processes like cell-signaling¹⁰ and regulatory processes¹¹, cell growth and death^{12, 13}, neurotransmission¹⁴⁻¹⁶, and metabolism¹⁷. As a result imbalance in the regulation or function of these enzymes can have detrimental effects.^{10, 12, 18, 19} Hence, knowledge on mechanistic details concerning amine oxidations in the flavin mediated reaction profile is important to understand the mode of action of the involved enzymes. As more information becomes available for a wide variety of enzymes, predictions can be made on the most common catalytic route adopted by topologically similar or dissimilar flavoenzymes, which

in turn allows prediction of the nature of the transition state in the reaction coordinate. A detailed understanding of high-energy transition states will play a crucial role in rational drug design for those flavoenzymes involved in specific health disorders or disease conditions.



Scheme 2.2 Illustration of the site of dehydrogenation in α -amino acids by flavoenzymes

2.2 α -Amino acids

2.2.1 Molecular chirality

The concept of molecular chirality was first discovered in 1848 by the French scientist, Louis Pasteur based on the crystal studies he undertook on sodium ammonium salt of *dextro*-tartaric acid and paratartaric acid.²⁰ At that time, he used dissymmetry (*dissymétrie*) or dissymmetric (*dissymétrique*) to describe handedness at the molecular level which later on became synonymous with the terms coined by Sir William Thomson (Lord Kelvin) namely, chiral and chirality.^{20, 21} Louis Pasteur is also credited with the discovery of enantioselectivity in biochemical processes with his work on fermentation of tartaric acid in the year 1857, a decade after his discovery of molecular handedness.^{20, 22} Enantioselectivity, which is the preference for one stereoisomer over the other, is an important concept in biology since most biochemical processes involve amino acids and sugars among others, which can exist as non-superposable mirror image forms i.e. D/L-forms in simple notation. The D/L notation is not to be confused with *d* (*dextro-rotary*)/*l* (*levo-rotary*) notation which represent rotation of plane polarized light in clockwise and counter-clockwise directions respectively by isomers. The D/L representation in amino acids in fact denotes the arrangement in space of the functional groups around the chiral α -carbon; either right-handed or left-

handed. D/L notation indicates the optical activity of glyceraldehyde isomers which are superposable with amino acid and carbohydrate enantiomers^{22, 23}

2.2.2 *Chiral homogeneity*

Although amino acids can exist in two-forms, only the L-forms participate in the ribosomal synthesis of proteins that are involved in various cellular processes.²² Furthermore, Stanley Miller in 1953 established that amino acids might possibly be present since primitive earth through his Miller-Urey experiments;²⁴ nonetheless, the selection of L-isomer in the primordial environment for the evolution of life still needs to be comprehended. While one theory proposes it's a matter of chance that the L-amino acids have been selected over D-amino acids,²⁵ another theory argues parity-violating energy differences between L and D-amino acids resulting in enantiomeric excess (ee) of one enantiomer over the other.²⁶⁻²⁸ Due to such parity-violation, spontaneous polymerization of D/L amino acids favors the L-isomer which is lower-energy than the D-form. Another model implicates autocatalysis and the differential crystallization ability of the crystal surfaces to which D and L-amino acids bind. Another piece of evidence indicates that enantiomers adsorb differentially onto chiral mineral surfaces resulting in an augmentation of pure L-isomer and thereby their incorporation into primordial life. Environmentally imposed physical asymmetry like circular polarized light and magnetic fields can cause preferential enhancement of the L-form in the D/L racemic mixture.²⁶⁻²⁸ It is also likely that a combination of these processes or other unknown events during early life may have resulted in chiral homogeneity favoring L-amino acids. Although L-amino acids are the predominant form, living organisms somehow evolved to induce biosynthetic and metabolic pathways for D-amino acids processing.

2.2.3 *D-Amino acids*

Initially D-amino acids were not considered to be naturally occurring and less important physiologically with isolated cases of detection reported largely in invertebrates.^{29, 30} Endogenously, D-amino

acids like D-Ala, D-Glu are incorporated into bacterial cell wall/peptidoglycans contributing to their overall structure as well as offering resistance to protease activity.^{22, 27, 28} In other cases D-amino acids like D-Asp in *Lactococcus* and *Enterococcus* and D-Ser in vancomycin-resistant *Staphylococcus* have been reported that allow them to potentially evade the effects of bactericides.^{22, 27, 28} Although they are not assimilated during ribosomal synthesis of proteins, D-amino acids like D-Ala, D-Phe, D-Val, D-Leu, D-Asn etc.²² (See Ref 22 for a full list of D-amino acids and the corresponding antibiotics) are integrated into natural antibiotic peptides through non-ribosomal pathways; and in neuropeptides of certain higher vertebrates where specific L-amino acids (L-Asp) undergo post-translational epimerization to the corresponding D-isomers.³¹ In vertebrates abundant quantities of D-Ser and D-Asp were reported in brain with proposed role in neurotransmission by regulating *N*-methyl-D-aspartate (NMDA) receptor activity.³¹⁻³³ Furthermore D-Asp has been reported in pineal gland, pituitary gland and adrenal gland and testis with proposed role in the synthesis and secretion of hormones and spermatogenesis.³³ D-amino acids also have specialized functions in that they have been shown to aid in bacterial spore germination as well as biofilm dispersal.^{22, 27, 28} Their detection is also of paramount importance in the food processing industry.^{27, 28}

Emergence of studies on the chemistry and biochemistry of D-amino acids as a field is fairly recent and the research mainly lagged behind in the previous years because of lack of proper ways of their detection and quantification.^{30, 33} However that idea quickly changed with the advent of improved analytical techniques like gas chromatography, high performance liquid chromatography and use of chiral columns that allow separation of D/L-racemic mixture and enabling detection of even trace amounts of D-amino acids.^{30, 33} Because of their wide distribution in nature and proposed roles for some in several crucial biological and biochemical processes, knowledge on the enzymes involved in their synthesis or metabolism can prove valuable.

2.2.4 Enzymes involved in α -amino acid metabolism

Turnover of proteins and peptides results in the generation of free amino acids that are recycled for utilization in key biochemical processes. Several enzymes have been discovered that act on the CH-

NH₂ group of donors. They have been classified on the basis of final electron acceptors and selected examples have been included as outlined in **Table 2.1**. Notable are the many flavin dependent enzymes like D-amino acid oxidase and D-aspartate oxidase from multiple sources, D-amino acid dehydrogenase and D-arginine dehydrogenase from bacterial sources, L-amino acid oxidase from multiple sources, L-aspartate oxidase, L-glutamate oxidase among others that act specifically upon the D or L-isomer but not both.

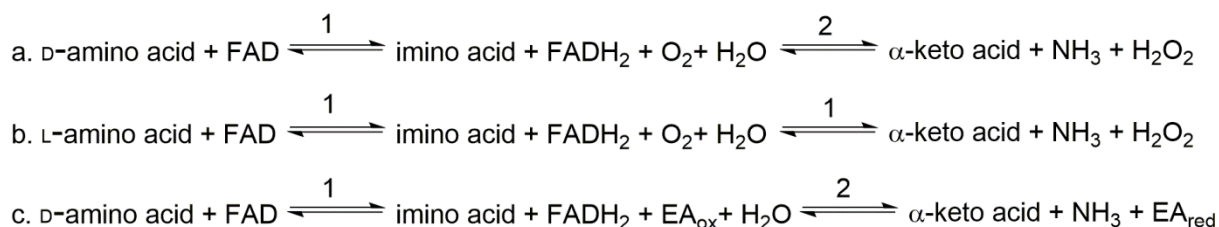
Table 2.1 Selected enzymes processing amino acids

Enzyme	Electron acceptor	Amino acid	EC number
Alanine dehydrogenase	NAD ⁺	L	1.4.1.1
Glutamate dehydrogenase	NAD ⁺	L	1.4.1.2
	NADP ⁺		1.4.1.3
Glycine dehydrogenase	cytochrome	-	1.4.2.1
D-aspartate oxidase	Oxygen	D	1.4.3.1
L-Amino acid oxidase	Oxygen	L	1.4.3.2
D-Amino acid oxidase	Oxygen	D	1.4.3.3
L-glutamate oxidase	Oxygen	L	1.4.3.11
L-aspartate oxidase	Oxygen	L	1.4.3.16
D-amino acid dehydrogenase	a quinone	D	1.4.5.1
Glutamate synthase	ferredoxin	L	1.4.7.1
D-arginine dehydrogenase	unknown	D	NC ^a

^aNot classified

One of the first discovered and widely studied model flavoenzymes is D-amino acid oxidase from pig kidney (pkDAAO) which is involved in the oxidative dehydrogenation of D-amino acids to iminoacids with concomitant flavin reduction (**Scheme 2.3a**). Apart from being one of the initial discoveries in the flavin field, pkDAAO has spurred myriad studies on several topics like the mode of dehydrogenation of D-amino acids in keeping with the versatility of the flavin cofactor, substrate specificity, physiological role of the enzyme and such. Interest in this enzyme has never dwindled mainly because of the controversy surrounding the accepted catalytic mechanism of amino acid dehydrogenation, its recent discovery in humans³⁰ and is the best structurally and mechanistically well characterized member in the class of en-

zymes involved in amino acid processing.^{7, 9, 34, 35} L-Amino acid oxidase (LAAO) catalyzes the “enantiomerically” opposite reaction to pkDAAO (**Scheme 2.3b**).³⁶ However, the mechanism of L-amino acid dehydrogenation has not been mechanistically established. Several crystal structures of LAAO are available from various sources which have been useful in proposing a catalytic mechanism for the enzyme in view of similarities with DAAO.^{36, 37} Apart from DAAO, another recently discovered enzyme that is emerging as a model for studies on amino acid oxidations is D-arginine dehydrogenase (PaDADH) from bacterial source (*Pseudomonas aeruginosa*).³⁸ It catalyzes the same reaction catalyzed by pkDAAO with D-arginine as the physiological substrate (**Scheme 2.3c**). Our knowledge on the mechanism of amino acid dehydrogenation by flavoenzymes has been further enhanced by the accumulating structural and mechanistic data of PaDADH.³⁹⁻⁴¹ The aim of this review is to summarize the structural and mechanistic data available thus far for each of these enzymes and formulate general framework for the oxidation of D- and L-amino acids so as to extend the formulated framework to other flavoenzymes proposed to catalyze similar reactions but lagging in mechanistic and/or structural characterization.



1 = Enzymatic

2 = Non-enzymatic

EA = Electron Acceptor

Scheme 2.3 General scheme of reactions catalyzed by (a.) DAAO, (b.) LAAO and (c.) DADH

2.3 Structural comparisons of D-amino acid oxidase, D-arginine dehydrogenase, L-amino acid oxidase and other related enzymes

pkDAAO catalyzes the oxidation of D-amino acids especially hydrophobic and aromatic ones, while PaDADH has high specificity for cationic and aromatic D-amino acid substrates with no activity against negatively charged residues.^{30, 34} LAAOs on the other hand accept most L-amino acids as substrates depending upon their source.^{36, 37} There are other D and L-amino acid oxidases that are more specific to individual D/L-amino acids (D/L-glutamate oxidase, D-aspartate oxidase, L-phenylalanine oxidase etc.). Although pkDAAO, PaDADH and LAAOs are involved in the dehydrogenation of D/L-amino acids, their sequence identity is counter-intuitively low. pkDAAO and PaDADH are involved in the oxidation of D-amino acids, yet, they share a low sequence identity of 17.2%;⁴¹ while enantiospecifically opposite pkDAAO and LAAO from *Rhodococcus opacus* share an identity of 25% and PaDADH and roLAAO share a meagre 16.4%.^{36, 41} Although their protein sequences are less identical, superimposition of their structures^{36, 37, 41} indicate a more preserved three-dimensional topology. Previous work on these enzymes establish the presence of a distinct substrate binding, flavin binding domains in all three enzymes with an additional helical domain in LAAOs;^{34, 36, 37, 41} Topology of the flavin binding domain is fairly preserved while subtle modifications in the substrate binding domain render differential specificity for D/L amino acid substrates. The active-site is generally located at the interface of the flavin and substrate binding domains with high homology of key active-site residues that dictate reactivity in these three different enzymes. Mirror symmetry along the plane of the isoalloxazine ring leads to the placement of the active-site residues on *Re* and *Si* faces of flavin. Such an instance is seen between pkDAAO and flavocytochrome b₂.³⁴ Another instance of symmetry arises when the substrates bind along the same face of isoalloxazine. In this situation the mirror symmetry of substrate binding sites lie along the plane perpendicular to isoalloxazine ring of the flavin. This type of spatial arrangement offers enantioselectivity to DAAOs/DADH and LAAOs.^{36, 41} Thorough analyses on the mirror symmetries between pkDAAO and LAAO from *Calloselasma rhodostoma* have been carried out by using inversion matrix software.³⁷ Comparison of PaDADH, pkDAAO and roLAAO can be found in ref 41.

2.3.1 Key conserved catalytic residues

DAAO

An important feature while considering the mode of catalysis of amino acids is the structural arrangement of catalytically relevant residues. Arrangements of these residues also have an impact on substrate specificity. Active site of pkDAAO (**Figure 2.2**) is defined by fairly hydrophobic residues such as the side chains of Ala49, Leu51, Ile215, Ile230, Tyr224 and Tyr228. The volume of active site cavity is 160 \AA^3 allowing only smaller hydrophobic residues to bind optimally. While the cavity is mainly hydrophobic, stabilization of substrate amino acid main chain carboxylate is provided by interactions with Arg283 and Tyr228; the substrate amine group is in hydrogen bonding interaction with the hydroxyl group of Tyr224 and a buried water molecule which has been conserved in the crystal structures of the eight subunits of pkDAAO. Model of D-Ala in the active site showed the importance of the zwitterionic form of the substrate for proper orientation of the substrate for optimal catalysis. Model of the corresponding L-configuration in the active-site showed unfavorable interactions with the flavin. Thus the active-site of D-amino acid oxidase is fine-tuned for small hydrophobic D-amino acids.³⁴

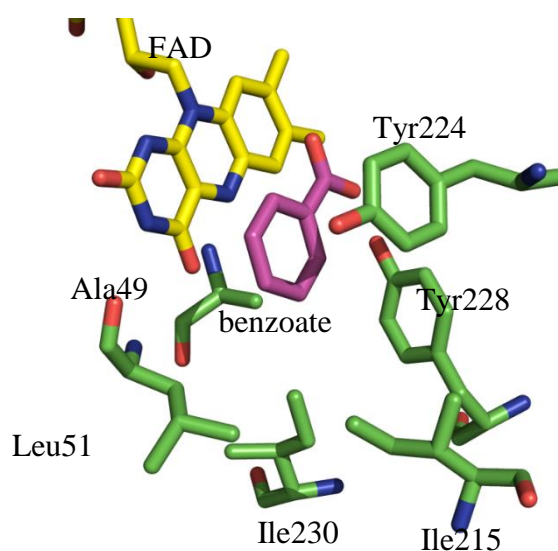


Figure 2.2 Active site of pkDAAO (PDB code:1KIF)

DADH

This enzyme has broader substrate specificity than pkDAAO. Multiple binding modes have been reported depending upon the various crucial interactions made by multiple substrates. D-Arg and D-Lys are the best substrates for the enzyme as judged by the large k_{cat}/K_m values (10^{-6} and $10^{-5} \text{ M}^{-1}\text{s}^{-1}$). The side chain of iminoarginine engages in a strong electrostatic interaction with Glu87 at the entrance of the substrate cavity as well as a hydrogen bond with Thr50 in the crystal structure of iminoarginine bound PaDADH (**Figure 2.3**). While iminohistidine interacts with His48 and the side chain is not long enough to make interactions with Glu87 and as a result, D-His ($10^3 \text{ M}^{-1}\text{s}^{-1}$) is not as good a substrate for PaDADH as D-Arg. In addition, similar to pkDAAO, hydrophobic walls formed due to the side chains of Tyr53, Met240, Val242 and Tyr249 engage in favorable van der Waals interactions with aliphatic and aromatic side chains. The main chain carboxylate is stabilized by two active site arginine residues, located at positions 222 and 305 and Tyr249. Tyr53 and a water molecule stabilize the imine group of iminoarginine in the crystal structure. The contacts between the main chain and the enzyme active site that are important for optimal catalysis are conserved between DADH and DAAO.

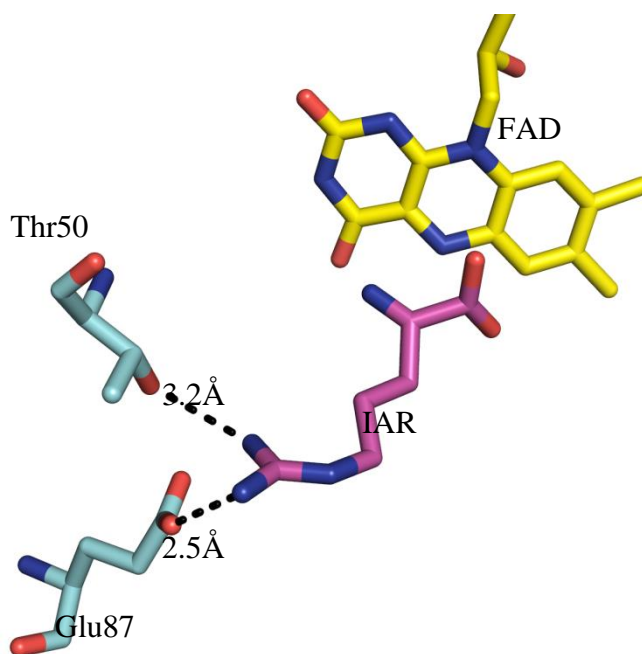


Figure 2.3 Interaction of iminoarginine (IAR) with Glu87 and Thr50 in PaDADH (PDB code: 3NYE)

LAAO

Structural features leading to active sites of crLAAO and roLAAO are slightly different resulting in subtle differences in substrate binding for the two LAAOs.^{36, 37} They are both characterized by broad substrate specificity. However substrates with branched and bulky side chains are restricted due to the volume of the active site in bacterial LAAO while for crLAAO, access to the substrate funnel which operates to orient and pack the substrate in the active site for catalysis may be a factor. Similar structural funnel has been also reported in yeast DAAO but not in pkDAAO.³⁷ The substrate funnel is however missing in bacterial LAAO which shares a 66% structural identity with crLAAO.³⁶ The absence of funnel seems to provide an advantage to roLAAO in the form of smaller K_m s compared to crLAAO, and substrate access seems limited only by diffusion.³⁶ Superposition of the active sites of ligand bound (amino benzoate) pkDAAO and crLAAO has been carried out using inversion matrix and generating the mirror image of liganded pkDAAO. Arg90 of crLAAO is equivalent to Arg283 of pkDAAO interacting with the carboxylate of amino benzoate. Ile430 of LAAO provided hydrophobic patch similar to Leu51 of DAAO. Furthermore, the mirror symmetry of the two active sites happens on the plane perpendicular to the isoalloxazine ring of the flavin which allows preservation of enantioselectivity.³⁷

2.3.2 Structural similarities and dissimilarities in DAAO, DADH, LAAO

In general, for optimal binding and catalysis of amino acids, a balance of hydrophobic and polar interactions seems suitable. The three enzymes in question exemplify such interactions as outlined in the previous sections. Hydrophobic active site is a common feature in all three enzymes as is the salt-bridge stabilization of the carboxylate group through arginine residues (90, 283 and 222 of LAAO, DAAO and DADH respectively). Further stabilization of the carboxylates of either the amino benzoate inhibitor or bound imino product through hydrogen bonding is offered by tyrosine residues, 371, 228 and 249 in LAAO, DAAO and DADH. The amino portion of the ligand is stabilized by hydrogen bonding interactions by His223 in LAAO and Tyr residues 224 and 53 in DAAO and DADH.^{34, 37, 41} The inversion matrix work done on DAAO and amino benzoate complex shows that the His223 of LAAO and Tyr224 of DAAO

lie in the same catalytic plane suggesting a common functionality in catalysis.³⁷ Tyr53 of DADH further is equivalent to Tyr224 in DAAO suggesting all the three residues are important catalytically. His223 which can exist in two alternative conformations as seen in the LAAO-amino benzoate and LAAO-citrate complexes has been proposed to be required for catalysis possibly as an active site base. There is however no direct evidence in favor of it. The histidine is fully conserved in all the LAAOs from different snake venoms, however in roLAAO the histidine is not conserved and instead two water molecules and Asp227 is found in the vicinity.³⁶ While in DAAO and DADH Tyr224 and Tyr53 are present in homologous position to the histidine. It has been proposed that similar to His223 in LAAO, Tyr224 of DAAO may have an important role in hydride transfer.³⁷ Mutagenic studies on Tyr53 (mutated to Phe) in DADH showed that catalysis is not significantly affected by the lack of hydroxyl group at that position ruling out its role as an active site base (Chapter 4, unpublished data). As the architecture of the active site of pkDAAO is very similar to PaDADH (**Figure 2.4**), the conclusion can be extended to pkDAAO. Furthermore, in yeast DAAO, the Tyr is replaced with an Ala in agreement with the previous conclusion. Recent covalent modification studies using L-propargylglycine on crLAAO reinforced the importance of His223 which is conserved in snake venom LAAOs.⁴² crLAAO differs from the other enzymes in question as it has a helical domain that is absent in DAAOs and DADH while it is projected away from the active site in roLAAO.^{34, 36, 37, 41} In crLAAO most of the residues in the helical domain line the funnel leading to the active site and His223 is part of that domain.³⁷ Chemical modification studies showed that His223 is the site of modification leading to irreversible inhibition of crLAAO.⁴² Therefore, active site His exclusive to snake venom LAAOs may or may not be an active site base in the wake of no mechanistic evidence. Examination of the active sites of pkDAAO, PaDADH and roLAAO shows the presence of water molecule(s) within a hydrogen bonding distance from the amine group of the ligand that needs to be deprotonated to allow further catalysis. In case of pkDAAO, the water molecule interacts with Tyr224, Gln53 and Gly313 and has been proposed to be a proton acceptor from the substrate amine.³⁴ In PaDADH, a proton relay can be envisioned between substrate amine, two water molecules connecting to His48 as mechanistic studies on this enzyme asserts the requirement of base for optimal catalysis while chemical

modification studies with DEPC suggest that an active site histidine is important for catalysis in PaDADH (Chapter 3 in this dissertation). In roLAAO, similar to PaDADH, two water molecules have been proposed to relay the amine proton to Asp227 that is present in the vicinity.³⁶

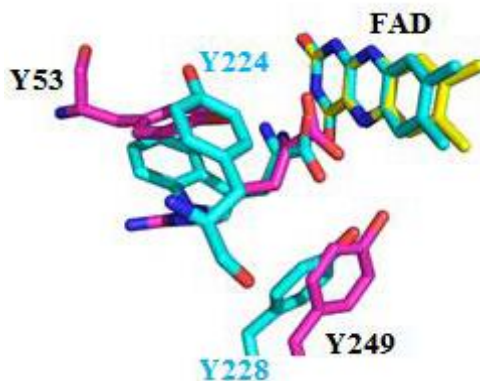


Figure 2.4 Conserved Tyr residues in pkDAAO (blue) and PaDADH (purple)

In any of the active site topologies, a base strong enough to abstract the α -proton from the amino acid substrate is lacking except in the case of crLAAO. But given the similarities of the active sites of crLAAO with roLAAO, pcDAAO, PaDADH, it seems more likely for these enzymes to operate via a common mechanistic pathway likely involving a hydride transfer (which will be described in the following section) in oxidizing the D/L-amino acid substrate.

2.4 Mechanism of amino acid dehydrogenation

The catalytic mechanism of flavin dependent C-N bond oxidations of amino acids can involve three catalytic mechanisms. One mechanism involves initial carbanion formation through the abstraction of α -H⁺ by a catalytic base, followed by removal of H⁺ from the $-\text{NH}_3^+$ group either by an active-site residue or solvent resulting in the rearrangement of electrons to reduce the flavin (**Scheme 2.4 a-b-c**). The mode of transfer of reducing equivalents to the flavin cofactor after the initiation of carbanion is not clear, although formation of N5 or C(4a) adducts with the flavin cofactor has been proposed ^{9, 43-46}. The mechanism requires that the cleavage of CH and NH bonds happen in two distinct steps with the CH bond

cleavage happening first followed by the adduct formation and the cleavage of NH leading to flavin reduction. The second mechanism involves nucleophilic attack of the lone pair of amine nitrogen at the electrophilic C(4a) site of flavin forming an adduct with a concomitant abstraction of $\alpha\text{-H}^+$ by the N5 atom of the flavin as seen in **Scheme 2.4, f-g-h**. Electronic rearrangement results in the breaking of the product imine from the reduced flavin⁴⁴. For a protonated amino acid, its deprotonation is essential prior to the attack at C(4a) atom of flavin. Therefore, this mechanism also requires for NH and CH bond cleavages to occur in separate steps. The third mechanism involves cleavage of NH bond to deprotonate the substrate amine thereby activating it for the transfer of a hydride directly from its $\alpha\text{-C}$ to the flavin cofactor (**Scheme 2.4 d-e**). Thus, the order of events starts with the removal of H^+ from the protonated amine followed by CH bond cleavage. If the cleavages are rate limiting then use of substrate and solvent kinetic isotope effects reporting on CH and NH bond cleavages can be exploited as useful probes to study the catalytic mechanism of substrate oxidation by flavin dependent oxidases, oxygenases and dehydrogenases.

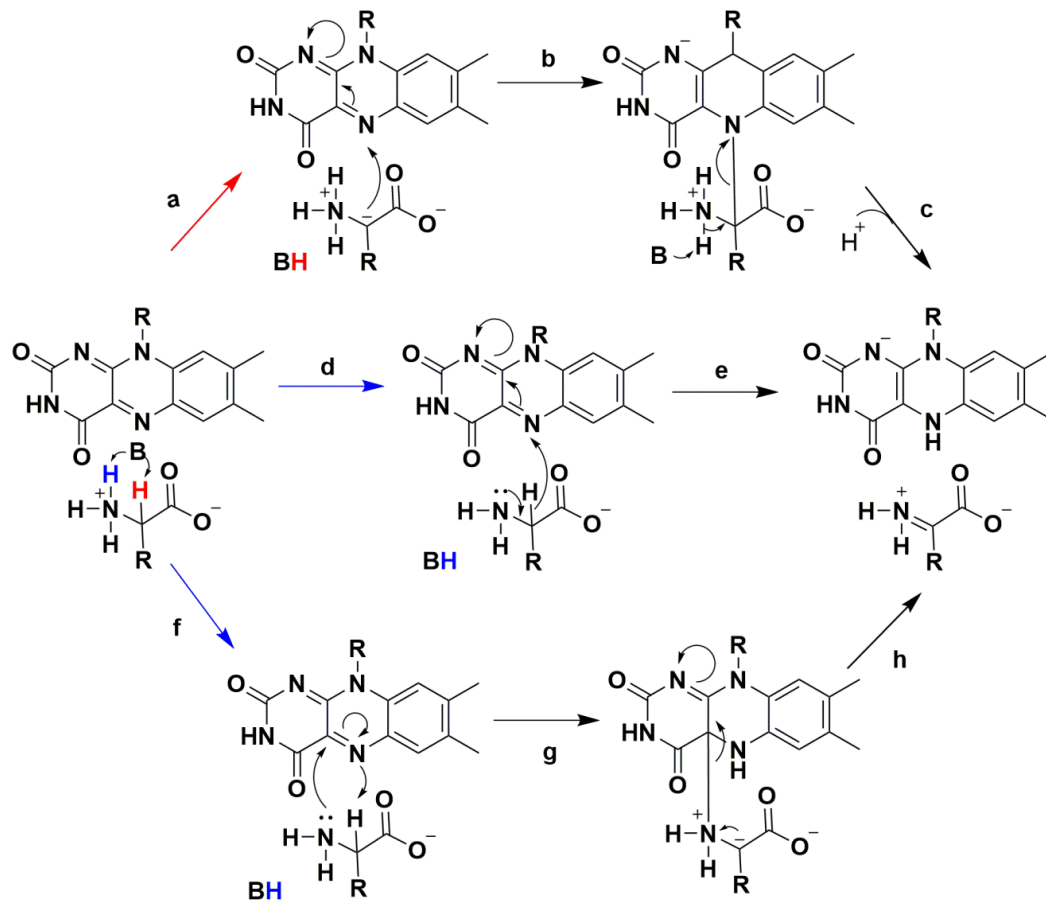
DAAO

D-Amino acid oxidase, a paradigm for amine oxidation in D-amino acids, glycine and N-methylated amino acids catalyzing enzymes^{9, 34, 47-51}, formation of carbanion has been accepted to be obligatory due to the oxygen dependent catalysis of HCl elimination from $\beta\text{-Cl}$ -alanine along with the generation of normal oxidation product, $\beta\text{-Cl}$ -pyruvate⁴⁶. Despite studies using 5-deazaFAD in D-amino acid oxidase demonstrating the transfer of α -hydrogen directly on to the flavin consistent with a hydride transfer mechanism⁵², mechanism involving carbanion was still recognized as being viable⁹. Deuterium and tritium kinetic isotope effects determined using D-alanine, D-serine and glycine suggested that the CH bond cleavage was fully rate limiting while the lack of solvent KIE was taken as being against concerted mechanism⁵³. This was consistent with a carbanion and a hydride transfer mechanism⁵³. However, with the availability of crystal structure of D-amino acid oxidase, the carbanion mechanism was rendered less credible as there was no base close to the $\alpha\text{-C}$ to extract its proton and initiate the reaction.³⁴ Furthermore, the use

of ^{15}N isotope effects suggested that rehybridization of substrate amine to imine was concomitant with the cleavage of CH bond which is consistent with a hydride transfer mechanism but not carbanion mechanism⁵⁴.

DADH

Bacterial DADH has broad substrate specificity compared to DAAOs. However, the arrangement of key residues proposed to be important for catalysis remains conserved among the two enzymes.⁴¹ Tyr53 and Tyr249 with ionizable side chains are positioned within 5 Å from the α -C while Tyr53 is ~ 4 Å from the product imine which is the site of deprotonation during substrate amino acid oxidation. Mutagenic studies on the two tyrosines ruled out any proposed role as active site base for these residues (Results from Chapter 4 in this dissertation). The binding as well as catalysis is not significantly affected by the replacement of Tyr to Phe at these sites. Tyr53 in PaDADH is equivalent in position to Tyr224 in pkDAAO which has been proposed to be a potential base.^{34, 37} Due to lack of direct mechanistic evidence and in the wake of the conclusions made in PaDADH, Tyr224 is less likely to be an active site base. Furthermore, the fact that the residue is not found conserved in the yeast DAAO makes the argument less favorable for Tyr224 in pkDAAO.



Scheme 2.4 Schematic representation of carbanion mechanism (a-b-c), hydride transfer (d-e) and polar nucleophilic attack (f-g-h) as catalyzed by amino acid oxidases and dehydrogenases. Scheme borrowed from Chapter 4

For catalytically slower D-Leu as substrate, molecular dynamics (MD) simulations on PaDADH showed that the binding free energy is much lower when a protonated (zwitterion) substrate is bound in the active site compared to the unprotonated form. This observation suggested that the zwitterionic form of the substrate is preferred for binding. Evidence in favor of this conclusion also comes from the K_d measurements which shows pH dependence with a pK_a of 9.6 with tight binding at pH below the measured pK_a . But at a pH above the pK_a the K_d value increases as does the rate constant for flavin reduction suggesting that for catalysis the protonated amino acid needs to be deprotonated. Use of deuterium substrate and solvent kinetic isotope effects demonstrated that the amine deprotonation and CH bond cleavages are

asynchronous. These results are consistent with hydride transfer, carbanion or polar nucleophilic mechanisms.³⁹ Mutagenic and isotope effects on the tyrosine mutants have been instrumental in settling the mechanism of D-amino acid oxidation as being most consistent with the transfer of a hydride ion from substrate onto the flavin in PaDADH. The lack of a strong base and any detectable intermediates along with concerted synchronous deuterium isotope effects in the tyrosine mutants played against the carbanion⁹ and polar nucleophilic mechanisms.^{8, 9} After the magnitude of mechanistic studies on DAAO, PaDADH has surfaced as another example of enzymes involved in amino acid processing with mechanistic and structural data favoring hydride transfer mechanism as the means of substrate oxidation.

LAAO

Mechanistic studies on LAAOs have lagged that of DAAOs and PaDADH. No direct mechanistic study probing the catalytic mechanism has been carried out on LAAOs. Within this context, it is interesting to note that LAAO from *Calloselasma adamanteus* has been shown to be reversibly inactivated at a pH above neutrality or upon freezing to -20 °C. Based on available crystal structures, active site topologies and in comparison with the mechanistic data available for enantiomerically opposite DAAO, hydride transfer mechanism from substrate L-amino acid to flavin has been proposed.^{36, 37} Base catalyzed hydride transfer has been proposed for crLAAO and His223 is proximal to the substrate amine to take up such a role.^{37, 42} However, a carbanion mechanism also cannot be ruled out in this scenario. Structural studies on crLAAO with bound inhibitors and substrates showed that His223 assumed different conformations strengthening the argument of its role as an active site base⁵⁵. However, mutagenic work on conserved His223 from crLAAO showed that the activity of His223Ser, His223Ala and His223Asn is comparable to the wild-type and the native crLAAO. Therefore, it seems likely that His223 may be important for substrate binding⁵⁵ but not as a catalytic base in the reductive half-reaction. Bacterial LAAO lacks an amino acid at the position homologous to His223 in snake venom LAAOs. Hydride transfer mechanism has been strongly favored due to the lack of a strong catalytic base in the vicinity of the amino acid substrate.³⁶ roLAAO shares highest structural identity with mono amine oxidase (MAO).³⁶ Notably, the

first step in the demethylation of methyl and dimethyl lysine by LSD1, a MAO enzyme has been shown to proceed via a hydride transfer mechanism using QM/MM studies.⁵⁶

2.5 Conclusion

The purpose of the review article is to bring to light the significance of D-amino acids and reflect upon the mechanistic and structural data available for amino acid oxidases in order to establish the most common mechanistic pathway adopted by this class of enzymes. Using DAAO, DADH and LAOs as models, common structural features have been highlighted in view of the available structural data and mechanistic conclusions have been drawn where necessary.

2.6 References

1. Ghisla, S., and Massey, V. (1986) New flavins for old: artificial flavins as active site probes of flavoproteins, *The Biochemical journal* 239, 1-12.
2. Ghisla, S., and Edmondson, D. E. (2001) Flavin Coenzymes, In *eLS*, John Wiley & Sons, Ltd.
3. Joosten, V., and van Berkel, W. J. H. (2007) Flavoenzymes, *Current Opinion in Chemical Biology* 11, 195-202.
4. Mattevi, A. (2006) To be or not to be an oxidase: challenging the oxygen reactivity of flavoenzymes, *Trends in biochemical sciences* 31, 276-283.
5. Massey, V. (2000) The chemical and biological versatility of riboflavin, *Biochemical Society transactions* 28, 283-296.
6. Ghisla, S., and Massey, V. (1989) Mechanisms of flavoprotein-catalyzed reactions, *European journal of biochemistry / FEBS* 181, 1-17.
7. Fitzpatrick, P. F. (2001) Substrate dehydrogenation by flavoproteins, *Accounts of chemical research* 34, 299-307.

8. Edmondson, D. E., Binda, C., and Mattevi, A. (2007) Structural insights into the mechanism of amine oxidation by monoamine oxidases A and B, *Archives of biochemistry and biophysics* 464, 269-276.
9. Fitzpatrick, P. F. (2010) Oxidation of amines by flavoproteins, *Archives of biochemistry and biophysics* 493, 13-25.
10. Sasabe, J., Miyoshi, Y., Suzuki, M., Mita, M., Konno, R., Matsuoka, M., Hamase, K., and Aiso, S. (2012) d-Amino acid oxidase controls motoneuron degeneration through d-serine, *Proceedings of the National Academy of Sciences* 109, 627-632.
11. Shi, Y., and Whetstone, J. R. (2007) Dynamic regulation of histone lysine methylation by demethylases, *Molecular cell* 25, 1-14.
12. Thomas, T., and Thomas, T. J. (2001) Polyamines in cell growth and cell death: molecular mechanisms and therapeutic applications, *Cellular and molecular life sciences : CMLS* 58, 244-258.
13. Wu, T., Yankovskaya, V., and McIntire, W. S. (2003) Cloning, Sequencing, and Heterologous Expression of the Murine Peroxisomal Flavoprotein, N1-Acetylated Polyamine Oxidase, *Journal of Biological Chemistry* 278, 20514-20525.
14. Edmondson, D. E., Mattevi, A., Binda, C., Li, M., Hubálek, F., and Abraham, D. J. (2003) Structure and Mechanism of Monoamine Oxidase, In *Burger's Medicinal Chemistry and Drug Discovery*, John Wiley & Sons, Inc.
15. Zaar, K., Kost, H. P., Schad, A., Volkl, A., Baumgart, E., and Fahimi, H. D. (2002) Cellular and subcellular distribution of D-aspartate oxidase in human and rat brain, *The Journal of comparative neurology* 450, 272-282.
16. Wolosker, H., D'Aniello, A., and Snyder, S. H. (2000) D-aspartate disposition in neuronal and endocrine tissues: ontogeny, biosynthesis and release, *Neuroscience* 100, 183-189.
17. Li, C., and Lu, C.-D. (2009) Arginine racemization by coupled catabolic and anabolic dehydrogenases, *Proceedings of the National Academy of Sciences* 106, 906-911.

18. Smith, B. C., and Denu, J. M. (2009) Chemical mechanisms of histone lysine and arginine modifications, *Biochimica et biophysica acta* 1789, 45-57.
19. Shih, J. C. (1991) Molecular basis of human MAO A and B, *Neuropsychopharmacology : official publication of the American College of Neuropsychopharmacology* 4, 1-7.
20. Gal, J. (2008) The discovery of biological enantioselectivity: Louis Pasteur and the fermentation of tartaric acid, 1857—A review and analysis 150 yr later, *Chirality* 20, 5-19.
21. Bentley, R. (2010) Chiral: a confusing etymology, *Chirality* 22, 1-2.
22. Cava, F., Lam, H., de Pedro, M. A., and Waldor, M. K. (2011) Emerging knowledge of regulatory roles of D-amino acids in bacteria, *Cellular and molecular life sciences : CMLS* 68, 817-831.
23. (1984) Nomenclature and Symbolism for Amino Acids and Peptides, *European Journal of Biochemistry* 138, 9-37.
24. Miller, S. L. (1953) A production of amino acids under possible primitive earth conditions, *Science (New York, N.Y.)* 117, 528-529.
25. Orgel, L. E. (2004) Prebiotic chemistry and the origin of the RNA world, *Critical reviews in biochemistry and molecular biology* 39, 99-123.
26. Podlech, J. (2001) Origin of organic molecules and biomolecular homochirality, *Cellular and molecular life sciences : CMLS* 58, 44-60.
27. Friedman, M. (2010) Origin, microbiology, nutrition, and pharmacology of D-amino acids, *Chemistry & biodiversity* 7, 1491-1530.
28. Friedman, M. (1999) Chemistry, nutrition, and microbiology of D-amino acids, *Journal of agricultural and food chemistry* 47, 3457-3479.
29. Corrigan, J. J. (1969) D-amino acids in animals, *Science (New York, N.Y.)* 164, 142-149.
30. Pione, M. S. (2000) D-Amino acid oxidase: new findings, *Cellular and molecular life sciences : CMLS* 57, 1732-1747.

31. Fujii, N., Kaji, Y., and Fujii, N. (2011) D-Amino acids in aged proteins: analysis and biological relevance, *Journal of chromatography. B, Analytical technologies in the biomedical and life sciences* 879, 3141-3147.
32. Yoshimura, T., and Goto, M. (2008) D-amino acids in the brain: structure and function of pyridoxal phosphate-dependent amino acid racemases, *The FEBS journal* 275, 3527-3537.
33. Ohide, H., Miyoshi, Y., Maruyama, R., Hamase, K., and Konno, R. (2011) D-Amino acid metabolism in mammals: biosynthesis, degradation and analytical aspects of the metabolic study, *Journal of chromatography. B, Analytical technologies in the biomedical and life sciences* 879, 3162-3168.
34. Mattevi, A., Vanoni, M. A., Todone, F., Rizzi, M., Teplyakov, A., Coda, A., Bolognesi, M., and Curti, B. (1996) Crystal structure of D-amino acid oxidase: a case of active site mirror-image convergent evolution with flavocytochrome b2, *Proceedings of the National Academy of Sciences of the United States of America* 93, 7496-7501.
35. Todone, F., Vanoni, M. A., Mozzarelli, A., Bolognesi, M., Coda, A., Curti, B., and Mattevi, A. (1997) Active site plasticity in D-amino acid oxidase: a crystallographic analysis, *Biochemistry* 36, 5853-5860.
36. Faust, A., Niefind, K., Hummel, W., and Schomburg, D. (2007) The structure of a bacterial L-amino acid oxidase from *Rhodococcus opacus* gives new evidence for the hydride mechanism for dehydrogenation, *Journal of molecular biology* 367, 234-248.
37. Pawelek, P. D., Cheah, J., Coulombe, R., Macheroux, P., Ghisla, S., and Vrielink, A. (2000) The structure of L-amino acid oxidase reveals the substrate trajectory into an enantiomerically conserved active site, *The EMBO journal* 19, 4204-4215.
38. Li, C., and Lu, C. D. (2009) Arginine racemization by coupled catabolic and anabolic dehydrogenases, *Proceedings of the National Academy of Sciences of the United States of America* 106, 906-911.

39. Yuan, H., Xin, Y., Hamelberg, D., and Gadda, G. (2011) Insights on the mechanism of amine oxidation catalyzed by D-arginine dehydrogenase through pH and kinetic isotope effects, *Journal of the American Chemical Society* 133, 18957-18965.
40. Yuan, H., Fu, G., Brooks, P. T., Weber, I., and Gadda, G. (2010) Steady-state kinetic mechanism and reductive half-reaction of D-arginine dehydrogenase from *Pseudomonas aeruginosa*, *Biochemistry* 49, 9542-9550.
41. Fu, G., Yuan, H., Li, C., Lu, C. D., Gadda, G., and Weber, I. T. (2010) Conformational changes and substrate recognition in *Pseudomonas aeruginosa* D-arginine dehydrogenase, *Biochemistry* 49, 8535-8545.
42. Mitra, J., and Bhattacharyya, D. (2013) Irreversible inactivation of snake venom l-amino acid oxidase by covalent modification during catalysis of l-propargylglycine, *FEBS open bio* 3, 135-143.
43. Gadda, G., Edmondson, R. D., Russell, D. H., and Fitzpatrick, P. F. (1997) Identification of the naturally occurring flavin of nitroalkane oxidase from *fusarium oxysporum* as a 5-nitrobutyl-FAD and conversion of the enzyme to the active FAD-containing form, *J Biol Chem* 272, 5563-5570.
44. Hamilton, G. A., and Brown, L. E. (1970) Model reactions and a general mechanism for flavoenzyme-catalyzed dehydrogenations, *Journal of the American Chemical Society* 92, 7225-7227.
45. Walsh, C. T., Krodel, E., Massey, V., and Abeles, R. H. (1973) Studies on the Elimination Reaction of d-Amino Acid Oxidase with α -Amino- β -chlorobutyrate : FURTHER EVIDENCE FOR ABSTRACTION OF SUBSTRATE α -HYDROGEN AS A PROTON, *Journal of Biological Chemistry* 248, 1946-1955.
46. Walsh, C. T., Schonbrunn, A., and Abeles, R. H. (1971) Studies on the mechanism of action of D-amino acid oxidase. Evidence for removal of substrate -hydrogen as a proton, *J Biol Chem* 246, 6855-6866.

47. Trickey, P., Wagner, M. A., Jorns, M. S., and Mathews, F. S. (1999) Monomeric sarcosine oxidase: structure of a covalently flavinylated amine oxidizing enzyme, *Structure* 7, 331-345.
48. Ilari, A., Bonamore, A., Franceschini, S., Fiorillo, A., Boffi, A., and Colotti, G. (2008) The X-ray structure of N-methyltryptophan oxidase reveals the structural determinants of substrate specificity, *Proteins* 71, 2065-2075.
49. Job, V., Marcone, G. L., Pilone, M. S., and Pollegioni, L. (2002) Glycine oxidase from *Bacillus subtilis*. Characterization of a new flavoprotein, *J Biol Chem* 277, 6985-6993.
50. Khanna, P., and Schuman Jorns, M. (2001) Characterization of the FAD-containing N-methyltryptophan oxidase from *Escherichia coli*, *Biochemistry* 40, 1441-1450.
51. Leys, D., Basran, J., and Scrutton, N. S. (2003) Channelling and formation of 'active' formaldehyde in dimethylglycine oxidase, *Embo J* 22, 4038-4048.
52. Hersh, L. B., and Jorns, M. S. (1975) Use of 5-deazaFAD to study hydrogen transfer in the D-amino acid oxidase reaction, *J Biol Chem* 250, 8728-8734.
53. Denu, J. M., and Fitzpatrick, P. F. (1994) Intrinsic primary, secondary, and solvent kinetic isotope effects on the reductive half-reaction of D-amino acid oxidase: evidence against a concerted mechanism, *Biochemistry* 33, 4001-4007.
54. Kurtz, K. A., Rishavy, M. A., Cleland, W. W., and Fitzpatrick, P. F. (2000) Nitrogen Isotope Effects As Probes of the Mechanism of d-Amino Acid Oxidase, *Journal of the American Chemical Society* 122, 12896-12897.
55. Moustafa, I. M., Foster, S., Lyubimov, A. Y., and Vrielink, A. (2006) Crystal structure of LAAO from *Calloselasma rhodostoma* with an L-phenylalanine substrate: insights into structure and mechanism, *Journal of molecular biology* 364, 991-1002.
56. Karasulu, B., Patil, M., and Thiel, W. (2013) Amine oxidation mediated by lysine-specific demethylase 1: quantum mechanics/molecular mechanics insights into mechanism and role of lysine 661, *Journal of the American Chemical Society* 135, 13400-13413.

3 pH AND KINETIC ISOTOPE EFFECTS OF D-ARGININE DEHYDROGENASE WITH MULTIPLE SUBSTRATES

Contribution: Directing undergraduates' (Jacob Ball and Quan Bui) research, KIE measurements

3.1 Abbreviations

PaDADH, *Pseudomonas aeruginosa* D-arginine dehydrogenase; PMS, phenazine methosulfate; DEPC, diethyl pyrocarbonate.

3.2 Highlights

- Leucine is a non-sticky substrate for the enzyme
- Arginine, lysine and methionine are sticky substrates for the enzyme
- A group with $pK_a \geq 7.9$, likely Glu-79, is required to bind cationic but not zwitterionic substrates
- A catalytic base with $pK_a \sim 9.5$ is required for substrate oxidation, possibly His-48 or Tyr-53

3.3 Abstract

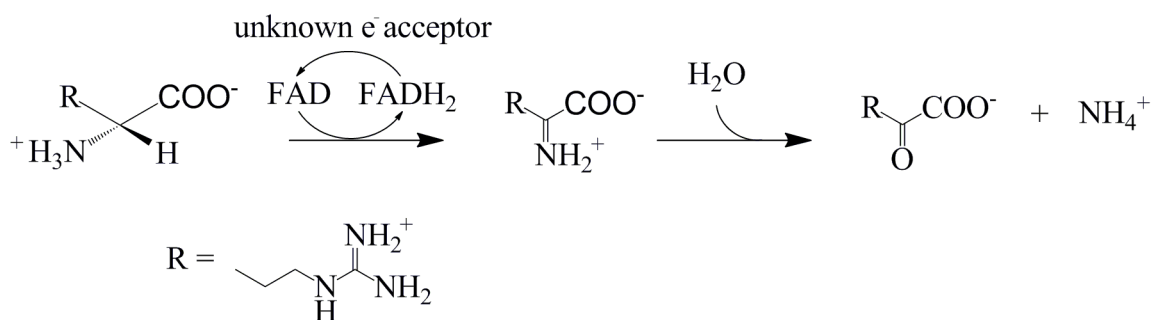
Pseudomonas aeruginosa D-arginine dehydrogenase (PaDADH) catalyzes the oxidation of D-arginine to iminoarginine, which is non-enzymatically hydrolyzed to 2-ketoarginine and ammonia. All D-amino acids with the exception of D-aspartate and D-glutamate are substrates for the enzyme, with the highest k_{cat}/K_m values displayed by D-arginine and D-lysine. Here, we have used pH and kinetic isotope effects to investigate how cationic and zwitterionic substrates bind to and are oxidized by PaDADH. The effects of pH on k_{cat} and k_{cat}/K_m were determined with cationic substrates D-arginine and D-lysine and the zwitterionic substrates D-methionine and D-leucine. An unprotonated group with apparent $pK_a \geq 7.9$ is required for binding cationic substrates, but not zwitterionic substrates. This group is likely Glu-87, whose carboxylate is ≤ 2.8 Å from the imino side chain of iminoarginine. An unprotonated group with pK_a of

~9.5 acts as general base for amine oxidation with cationic and zwitterionic substrates, possibly His-48 or Tyr-53. Lack of pH effects on the kinetic isotope effects for the rate constant of flavin reduction k_{red} with D-leucine established 9.5 as the intrinsic $\text{p}K_{\text{a}}$, and D-leucine as a slow, non-sticky substrate. D-Arginine, D-lysine and D-methionine were significantly stickier than D-leucine as indicated by apparent $\text{p}K_{\text{a}} < 9.5$ in both $k_{\text{cat}}/K_{\text{m}}$ and k_{cat} .

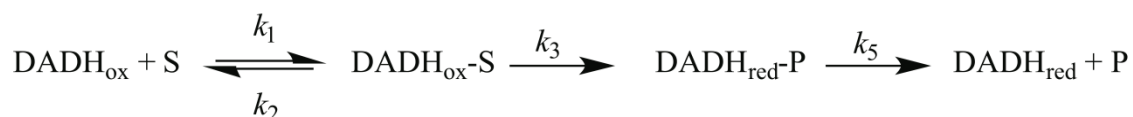
3.4 Introduction

Pseudomonas aeruginosa D-arginine dehydrogenase (PaDADH) catalyzes the flavin-mediated, oxidative deamination of D-arginine to iminoarginine, followed by the non-enzymatic hydrolysis in solution of the imino product to give 2-ketoarginine and ammonia (**Scheme 3.1**).⁽¹⁾ All the standard D-amino acids except for D-glutamate, D-aspartate, or glycine are oxidized by the enzyme,^(1, 2) with D-arginine and D-lysine displaying rate constants for substrate capture of 10^5 - $10^6 \text{ M}^{-1}\text{s}^{-1}$.⁽²⁾ L-Amino acids are not substrates for PaDADH.⁽²⁾ The enzyme is a strict dehydrogenase because during turnover it reacts with an electron acceptor other than molecular oxygen, presumably ubiquinone *in vivo*.⁽³⁾ Steady-state kinetics is consistent with a Ping-Pong Bi-Bi kinetic mechanism, as demonstrated with D-arginine or D-histidine as substrate and phenazine methosulfate (PMS) as electron acceptor.⁽³⁾ In the reductive half-reaction the enzyme-bound flavin (PaDADH_{ox}) is reduced to hydroquinone with concomitant oxidation of the amino acid to the imino acid (PaDADH_{ox}-P), as shown in **Scheme 3.2**. In the oxidative half-reaction the reduced flavin is oxidized (*in vitro*) by PMS (**Scheme 3.3**). Flavin reduction is irreversible with D-histidine or D-leucine as substrate, as demonstrated by rapid kinetics.⁽³⁾ With D-arginine, however, the reaction is too fast and cannot be studied in a stopped-flow spectrophotometer.⁽³⁾ Amine oxidation has been studied with D-leucine, which is amenable to mechanistic investigation using a stopped-flow spectrophotometer, with pH, substrate and solvent kinetic isotope effects, as well as computational studies.⁽⁴⁾ Free energy calculations and the pH profile for K_{d} are consistent with the enzyme binding preferentially the zwitterionic form of D-leucine. After isomerization of the enzyme-substrate complex, amine deprotonation triggers the ox-

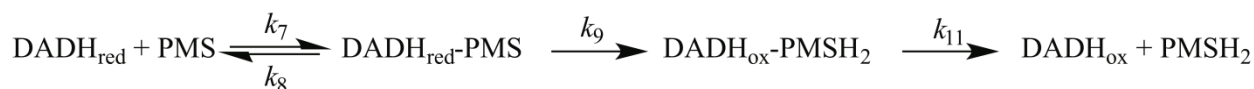
idation reaction, with cleavages of the NH and CH bonds of D-leucine occurring asynchronously, as suggested by multiple deuterium kinetic isotope effects on the rate constant for flavin reduction.⁽⁴⁾ In this respect PaDADH is similar to proline dehydrogenase,⁽⁵⁾ but different from other flavin-dependent amine oxidases, such as D-amino acid oxidase or monomeric sarcosine oxidase, for which amine oxidation occurs from the anionic substrate.⁽⁶⁾



Scheme 3.1 Oxidation of D-Arginine by PaDADH.



Scheme 3.2 Reductive Half-reaction of PaDADH.



Scheme 3.3 Oxidative Half-reaction of PaDADH.

The three-dimensional structures of PaDADH in complex with iminoarginine or iminohistidine, or in the unliganded form have been previously solved at high resolution (1.06-1.3 Å), along with an atomic-resolution structure of a 4-methyl-2-pentanone-FAD adduct in the enzyme co-crystallized with D-leucine.^(2, 7) The structure with iminoarginine underlines the importance of the side chain carboxylate of Glu-87 for binding the cation of the iminoarginine side chain, as shown in **Figure 3.1**.⁽⁷⁾ Two tyrosine residues,

i.e., Tyr-53 and Tyr-249, with the aid of Met-240 and Val-242 arrange into a hydrophobic pocket that surrounds the central part of the iminoarginine side chain. The imine of the ligand is connected to His-48 through two intervening water molecules (**Figure 3.1B**). The ligand C α atom is close to the flavin N(5) atom, presumably indicating where the C α atom of the amino acid substrate resides during catalysis. The structure of the enzyme in complex with iminohistidine demonstrates that the imidazole of the ligand is present in two alternate conformations, with H-bonding interactions with the side chains of His-48, Thr-50, and either Glu-87 or Gln-336. A mobile loop, composed of residues 50-56, is present in two alternate conformations in the unliganded and product-bound enzyme structures.⁽²⁾ This flexible loop forms an active site lid and is proposed to play an important role for substrate specificity and recognition, allowing the enzyme to accommodate bulky substrates like phenylalanine or tryptophan.⁽²⁾

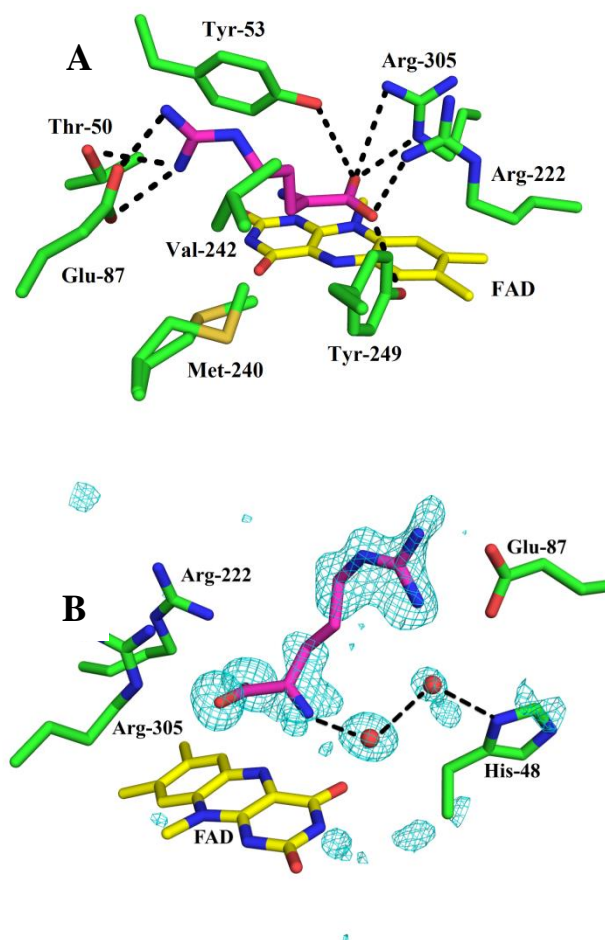


Figure 3.1 Interactions of iminoarginine with active site residues of PaDADH. C atoms are colored green for each of the PaDADH active site residues and magenta for iminoarginine. FAD is represented by its

isoalloxazine ring with the C atoms colored yellow. H-bond and ionic interactions are shown as dashed lines. Two water molecules in the binding site are shown as red spheres. For clarity, panels A and B focus on different interactions. Note that the side chains of Met-240 and Val-242 are present in two alternate conformations. The $F_o - F_c$ omit map of the ligand and two interacting water molecules is indicated in panel B as blue mesh and contoured at 3.5σ .

In this study, we have used mechanistic approaches to investigate further the reaction of amine oxidation catalyzed by PaDADH. Effects of pH were determined on the steady-state kinetic parameters with selected substrates and on the kinetic isotope effects associated with flavin reduction using D-leucine. The results shed light on the ionization states of groups that are relevant to amine oxidation and provide further mechanistic clues on the catalytic mechanism for amine oxidation by PaDADH.

3.5 Experimental Procedures

Materials

D-Methionine and D-leucine were purchased from Sigma-Aldrich (St. Louis, MO). D-Arginine and D-lysine were obtained from Alfa-Aesar (Ward Hill, MA). D-Leucine_{d10} was obtained from CDN Isotopes (Pointe-Claire, Canada). PaDADH was prepared as described previously.^(2, 3) All other reagents used were of the highest purity commercially available.

Steady-state Kinetics

The steady-state kinetic parameters for D-arginine, D-lysine, and D-methionine were measured polarographically on a computer-interfaced O₂ electrode by using the method of initial rates. The enzyme does not react with O₂, hence as electron acceptor we used PMS, which spontaneously reacts in its reduced form with molecular oxygen.⁽⁸⁾ The reaction was initiated by the addition of the enzyme, with final concentrations ranging from 5 nM to 2 μM depending on pH and the substrate used, yielding a reaction

volume of 1 mL. Substrate concentrations ranged from 0.01-100 mM for D-arginine, 0.25-250 mM for D-lysine, and 1-186 mM for D-methionine, ensuring that the K_m values determined were within the range of substrate concentrations used at any given pH. The assays were carried out at 25 °C in 20 mM sodium pyrophosphate (pH 8.5-10.0), 20 mM sodium phosphate (pH 6.0-8.5) or 20 mM piperazine (pH 4.75-6.0). The concentration of PMS was kept fixed at 1 mM to ensure full saturation of the enzyme ($K_m = 10 \mu\text{M}$), as previously described.^(2, 3) Data for D-leucine were taken from Yuan *et al.*⁽⁴⁾

Kinetic Isotope Effects

The reductive half-reaction of PaDADH with D-leucine was monitored using an SF-61DX2 Hi-Tech KinetAsyst high performance stopped-flow spectrophotometer thermostated at 25 °C. The observed first-order rate constants for flavin reduction (k_{obs}) were determined at varying concentrations of D-leucine or D-leucine_{d10} between 0.5 and 50 mM under pseudo first-order conditions using the buffer system described above at pH 7.0, 8.5, and 10.0. Multiple measurements typically differed by $\leq 5\%$.

Chemical Modification of PaDADH by DEPC

PaDADH (1.5 μM) was incubated with 1.5 mM DEPC in the absence and presence of 8.9 mM phenyl-guanidine, a competitive inhibitor of the enzyme with K_{is} of 0.9 mM in 20 mM sodium pyrophosphate, pH 9.5 and 25 °C. Hydroxylamine (200 mM final) was added directly to the DEPC-inactivated enzyme after 60 min incubation. The enzymatic activity was assayed with 2 mM D-arginine as substrate by withdrawing aliquots from the various reaction mixtures at different times. Due to fast hydrolysis of DEPC in aqueous buffered solutions, which affects the kinetics of enzyme inactivation, the time courses of inactivation are not shown and only data at a fixed time are reported.

Data Analysis

Kinetic data were analyzed with KaleidaGraph software (Synergy Software, Reading, PA) and the Kinetic Studio Software Suite (Hi-Tech Scientific, Bradford on Avon, U.K.). Stopped-flow traces were

fit to eq 1, which describes a single exponential process where k_{obs} represents the observed first-order rate constant for flavin reduction at any given concentration of substrate, t is time, A is the absorbance at 446 nm at any given time, B is the amplitude of the absorbance change, and C is the absorbance at infinite time which in this case is the non-zero absorbance of the fully reduced enzyme. Kinetic parameters for the reductive half-reactions were determined by using eq 2, where k_{obs} is the observed first-order rate constant for the reduction of the enzyme-bound flavin at any given concentration of substrate (S), k_{red} is the limiting first-order rate constant for flavin reduction at saturating concentrations of substrate, and $^{app}K_d$ is the apparent dissociation constant for binding of the substrate to the enzyme.

The apparent steady-state kinetic parameters at varying substrate concentrations were determined by using the Michaelis-Menten equation for a single substrate. Previous results demonstrated a Ping Pong Bi-Bi steady-state kinetic mechanism for PaDADH for both the fast substrate arginine and the slow substrate histidine, with a K_m value for PMS of $\sim 10 \mu\text{M}$.⁽³⁾ Consequently, when the steady-state kinetic parameters were determined at a fixed concentration of 1 mM PMS in this study, they approximate well the true k_{cat} , K_m , and k_{cat}/K_m values for the amino acid substrate.

The pH profiles of the k_{cat} values for D-arginine and k_{cat} and k_{cat}/K_m values for D-methionine were fit to eq 3, which describes a curve that increases with increasing pH with slope of +1 and a limiting value (C) at high pH. The pH profiles of the k_{cat}/K_m values for D-arginine and D-lysine were fit to eq 4, which describes a curve that increases with increasing pH with slope of +2, a limiting value (C) at high pH and two indistinguishable pK_a values. The pH profiles of the k_{cat} values for D-lysine were fit using eq 5, which describes a curve that increases with increasing pH to an intermediate value (C_I) and it increases further to a limiting pH-independent value (C_H) at high pH with slopes of +1.

$$A = B \exp(-k_{obs}t) + C \quad (1)$$

$$k_{obs} = \frac{k_{red}S}{^{app}K_d + S} \quad (2)$$

$$\log(k_{cat}, k_{cat}/K_m) = \log \frac{C}{1+10^{(pK_a-pH)}} \quad (3)$$

$$\log(k_{cat}/K_m) = \log \frac{C}{1+10^{(pK_a-pH)^2}} \quad (4)$$

$$\log(k_{cat}) = \log \left(\frac{C_I}{1+10^{(pK_{a1}-pH)}} + \frac{C_H}{1+10^{(pK_{a2}-pH)}} \right) \quad (5)$$

3.6 Results

k_{cat}/K_m and k_{cat} pH-Profiles with Cationic Substrates

The pH-dependences of the steady-state kinetic parameters k_{cat}/K_m and k_{cat} were determined with D-arginine or D-lysine as substrate to establish relevant ionizations of groups involved in binding or catalysis with cationic substrates, i.e., carrying a positive charge on the side chain. As shown in **Figure 3.2**, the k_{cat} pH-profile with D-arginine increased to a limiting value at high pH, defining the requirement for an unprotonated group for catalysis. With D-lysine as substrate a similar pattern was seen at low pH, with an unprotonated group required for catalysis having a pK_a similar to that seen with D-arginine, although the enzyme could not be saturated with D-lysine below pH 6.0 (**Figure 3.2**). Despite similar k_{cat} values with the two substrates up to pH 7.5, turnover with D-lysine was significantly faster than with D-arginine at high pH, with a pH-profile identifying two plateaus at intermediate and high pH with D-lysine. Both D-lysine and D-arginine had k_{cat}/K_m pH-profiles increasing to limiting values with increasing pH (**Figure 3.2**). However, the ascending limbs clearly showed the presence of two unprotonated groups rather than the single one seen in the k_{cat} pH-profiles. The apparent pK_a values and the pH-independent, limiting values of k_{cat}/K_m and k_{cat} determined with D-arginine and D-lysine are summarized in **Table 3.1**.

Table 3.1 pH Effects on k_{cat}/K_m and k_{cat} of PaDADH.

	k_{cat}/K_m			k_{cat}		
	$\text{p}K_{\text{a}1}$	$\text{p}K_{\text{a}2}$	$(k_{\text{cat}}/K_m)_{\text{H}^+} (\text{M}^{-1}\text{s}^{-1})$	$\text{p}K_{\text{a}1}$	$\text{p}K_{\text{a}2}$	$(k_{\text{cat}})_{\text{H}^+} (\text{s}^{-1})$
<i>cationic substrates</i>						
D-arginine	7.3 ^{b,c}	7.3 ^{b,c}	2,700,000 ($\pm 400,000$)	6.2 ^{b,d}	–	150 (± 20)
D-lysine	7.9 ^{b,c}	7.9 ^{b,c}	590,000 ($\pm 140,000$)	$\sim 6.2^e$	9.3 ^{f,g}	400 (± 100)
<i>zwitterionic substrates</i>						
D-methionine	7.7 ^{b,d}	–	35,000 ($\pm 7,000$)	6.9 ^{b,d}	–	190 (± 20)
D-leucine ^h	$\sim 9.5^{d,i}$	–	$\sim 11,000^i$	$\sim 9.5^{d,i}$	–	$\sim 100^i$

^a pH-independent limiting value at high pH.

^b (± 0.1).

^c Determined by using eq 4.

^d Determined by using eq 3.

^e Inferred by visual inspection of Figure 5A.

^f (± 0.3).

^g Determined by using eq 5.

^h From Yuan *et al.*⁽⁴⁾

ⁱ Approximate value, due to plateau being not well defined.

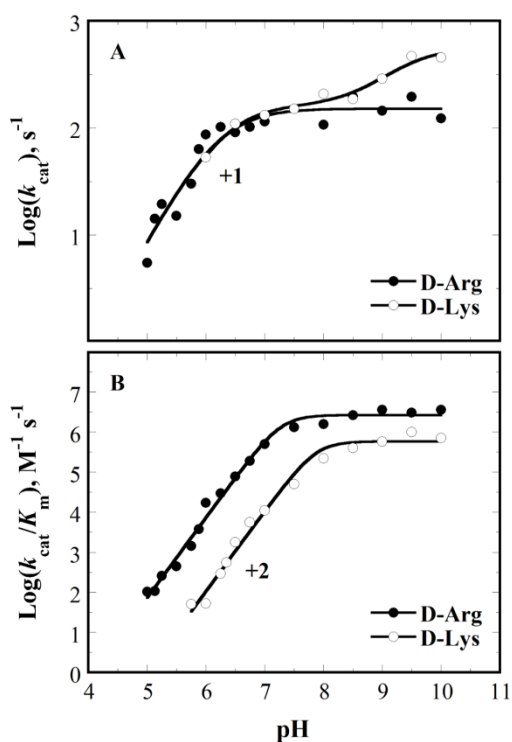


Figure 3.2 pH-profiles of k_{cat} (A) and k_{cat}/K_m (B) with D-arginine (●) and D-lysine (○). PaDADH activity was measured at varying concentrations of D-arginine or D-lysine and 1 mM PMS at 25 °C. Curves represent fits of the data to eqs 3-5.

k_{cat}/K_m and k_{cat} pH-Profiles with Zwitterionic Substrates

The pH-dependences of the steady-state kinetic parameters k_{cat}/K_m and k_{cat} were determined with D-methionine or D-leucine as substrate to establish relevant ionizations of groups involved in binding or catalysis with zwitterionic substrates, i.e., not carrying a positive charge on the side chain. With both D-methionine and D-leucine, the pH-profiles of the k_{cat} and k_{cat}/K_m values increased with increasing pH, reaching limiting values at high pH, and demonstrating the requirement for a single unprotonated group for catalysis (**Figure 3.3**). **Table 3.1** summarizes the apparent pK_a values and the pH-independent, limiting values of k_{cat}/K_m and k_{cat} determined with D-methionine and D-leucine.

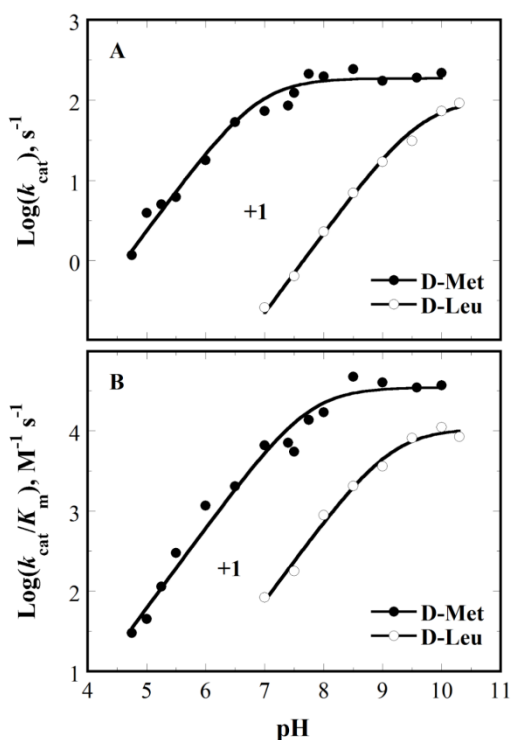


Figure 3.3 pH-profiles of k_{cat} (A) and k_{cat}/K_m (B) with D-methionine (●) and D-leucine (○). PaDADH activity was measured at varying concentrations of D-methionine or D-leucine and 1 mM PMS at 25 oC. Curves represent fits of the data to eq 3.

^Dk_{red} pH-Profile with D-Leucine

The pH-dependence of the kinetic isotope effects on the rate constant for flavin reduction at saturating substrate (k_{red}) was determined with D-leucine to establish if the latter is a slow substrate for PaDADH for which apparent and intrinsic $\text{p}K_{\text{a}}$ values are identical. Flavin reduction was followed at 446 nm upon mixing the enzyme with varying concentrations of D-leucine in a stopped-flow spectrophotometer, yielding monophasic traces (**Figure 3.4** shows the case of pH 8.5, with pH 7.0 and 10.3 being similar). The $^{\text{D}}k_{\text{red}}$ values were computed from the ratio of the k_{red} values with D-leucine and D-leucine- d_{10} determined by plotting the observed rate constants for flavin reduction as a function of substrate concentration. As illustrated in **Table 3.2**, the $^{\text{D}}k_{\text{red}}$ had similar values in the pH range from 7.0 to 10.3.

Chemical Modification with DEPC

The effect of DEPC on the enzymatic activity of PaDADH was determined to evaluate whether His-48 is important for catalysis. Incubation of the enzyme for 30 min with 1.5 mM DEPC at pH 9.5 and 25 °C resulted in 75% decrease of enzymatic activity with 2 mM D-arginine from 119 s^{-1} to 29 s^{-1} . The enzymatic activity decreased by only 15%, from 125 s^{-1} to 104 s^{-1} , when the 1.5 mM DEPC treatment was carried out in the presence of the competitive inhibitor phenyl-guanidine (8.9 mM, $K_{\text{is}} = 0.9$ mM at pH 9.5 and 25 °C, data not shown). These data are consistent with chemical modification by DEPC occurring at the active site of the enzyme. The DEPC-inactivated enzyme regained ~100% of its initial activity, i.e., 121 s^{-1} , when treated with 200 mM hydroxylamine, consistent with histidine being the target of DEPC modification.⁽⁹⁾

Table 3.2 pH Effects on Kinetic Isotope Effects with D-Leucine.

pH	$^{\text{D}}k_{\text{red}}$
7.0 ^a	4.6 (± 0.9)
8.5 ^b	5.2 (± 0.4)
10.3 ^c	5.1 (± 0.1)

Experimental conditions: 20 mM ^asodium phosphate and ^bsodium pyrophosphate in H₂O at 25 °C with between 0.5 to 5 mM D-leucine and D-leucine- d_{10} .
^c From Yuan *et al.*⁽⁴⁾

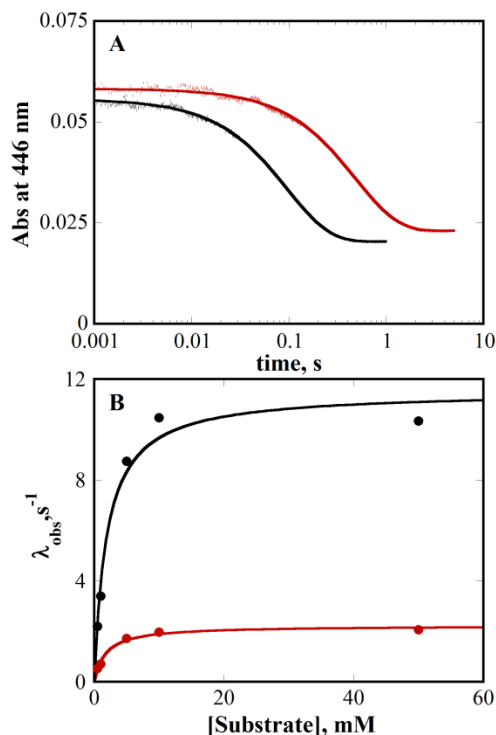


Figure 3.4 Kinetic isotope effects on k_{red} at pH 8.5 with D-leucine (black) and D-leucine_{d10} in (red). Panel A shows representative time courses for the light and heavy substrate at 50 mM substrate concentration; the traces were fit to eq 1. Panel B shows the concentration dependences of the observed rate constants for flavin reduction at different substrate concentrations of protiated and deuterated leucine

3.7 Discussion

The substrates of PaDADH, which displays broad specificity being able to oxidize most of the D-amino acids except D-aspartate, D-glutamate and glycine,⁽²⁾ can be classified as cationic and zwitterionic, depending on the presence of a charge on the side chain. In this study, we have used D-arginine, D-lysine, D-methionine and D-leucine to investigate mechanistically how cationic and zwitterionic substrates bind to and are oxidized by PaDADH. Insights on the roles played by several functional groups in the active site of the enzyme have emerged from the investigation, as discussed below.

The unprotonated side chain of Glu-87 is important for binding cationic substrates through an electrostatic interaction with the substrate side chain. This conclusion is supported by pH profiles of the steady-state kinetic parameters and X-ray structures of the enzyme in complex with the iminoarginine

product. While a single unprotonated group is required to achieve maximal $k_{\text{cat}}/K_{\text{m}}$ values at high pH with the zwitterionic substrates D-methionine and D-leucine, two groups are seen in the $k_{\text{cat}}/K_{\text{m}}$ pH-profiles with the cationic substrates D-arginine and D-lysine. The extra unprotonated group must be involved in substrate binding rather than catalysis, since it is not seen in the k_{cat} pH-profiles, which show the requirement for a single unprotonated group required for catalysis with both cationic and zwitterionic substrates. Further support for Glu-87 interacting with the side chain of the cationic substrates comes from the X-ray structures of the enzyme in complex with iminoarginine and one of the two alternate conformations of iminohistidine,⁽²⁾ showing the carboxylate chain of Glu-87 at ≤ 2.8 Å away from the guanido and ϵ -amino groups of the cationic products of reaction.

The $\text{p}K_{\text{a}}$ of Glu-87 is perturbed by the protein microenvironment to a value ≥ 7.9 , as suggested by the $k_{\text{cat}}/K_{\text{m}}$ pH-profiles with the cationic substrates D-arginine and D-lysine. The intrinsic $\text{p}K_{\text{a}}$, however, cannot be estimated accurately because different $\text{p}K_{\text{a}}$ values were determined with D-arginine and D-lysine. Since $\text{p}K_{\text{a}}$ values determined from $k_{\text{cat}}/K_{\text{m}}$ pH-profiles refer to ionizations of the free enzyme or substrate, but not of enzyme-substrate complexes,⁽¹⁰⁾ the different values determined with D-arginine and D-lysine reflect the stickiness of these substrates, which refers to the propensity of the enzyme-substrate complex to catalyze amine oxidation rather than releasing the substrate to bulk solvent (i.e., k_3/k_2 in **Scheme 3.2**). Since substrate stickiness perturbs apparent $\text{p}K_{\text{a}}$ values outward in $k_{\text{cat}}/K_{\text{m}}$ pH-profiles,⁽¹⁰⁾ D-arginine, with a $\text{p}K_{\text{a}}$ of 7.3, is stickier than D-lysine, with $\text{p}K_{\text{a}}$ of 7.9. However, no conclusion on the stickiness of D-lysine can be drawn with the data available, preventing the determination of the intrinsic $\text{p}K_{\text{a}}$ value of Glu-87¹.

An unprotonated group with intrinsic $\text{p}K_{\text{a}}$ of ~ 9.5 is required for catalysis with both cationic and zwitterionic substrates, as suggested by the pH profiles of the steady-state kinetic parameters. Both k_{cat}

¹ Since Glu-87 does not interact with the side chain of D-leucine, the perturbations of the apparent $\text{p}K_{\text{a}}$ of Glu-87 and of the proposed general base participating in catalysis, which is instead common to all substrates oxidized by PaDADH, are not the same. For this reason, while the $\Delta\text{p}K_{\text{a}}$ values attributed to the chemical step of catalysis allows the determination of the intrinsic $\text{p}K_{\text{a}}$ value of the base (*vide infra*), the same cannot be done to establish the intrinsic $\text{p}K_{\text{a}}$ value of Glu-87.

and k_{cat}/K_m with D-arginine, D-lysine, D-methionine and D-leucine increased to limiting values with increasing pH. This establishes the requirement for an unprotonated group acting in the chemical step of amine oxidation rather than in substrate binding, since k_{cat} excludes binding steps because the enzyme is saturated with the substrate.⁽¹¹⁾ Previous solvent kinetic isotope effects ruled out the possibility of the $\text{p}K_a$ being that of the substrate amine, since amine deprotonation occurs in the step probed by k_{red} .⁽⁴⁾ The linear decrease with decreasing pH in both k_{cat} and k_{cat}/K_m with all the tested substrates is consistent with the unprotonated group acting as general base catalyst rather than electrostatic catalyst, since in the latter case the kinetic parameters would approach a limiting, lower value at low pH. The apparent $\text{p}K_a$ values determined in the k_{cat} and k_{cat}/K_m pH profiles with D-leucine approximate well the intrinsic $\text{p}K_a$ of the general base, since D-leucine is a slow, non-sticky substrate for PaDADH. This conclusion comes from the pH-independence of the $^{\text{D}}k_{\text{red}}$ value for the reduction of the enzyme-bound flavin with D-leucine between pH 7.0 and 10.3, where both k_{cat} and k_{cat}/K_m depend on pH, which establishes that the enzyme-substrate complex is not committed to catalysis and that D-leucine is not a sticky substrate.⁽¹²⁾ Independent support for D-leucine being a slow substrate is provided by the comparison of the $\text{p}K_a$ of ~ 9.5 determined for k_{cat}/K_m with the $\text{p}K_a$ of 9.6 recently reported for the k_{red} pH-profile with D-leucine.⁽⁴⁾ A reasonable candidate for the role of general base in the active site of PaDADH is His-48, which is bridged to the ligand imine through two water molecules in the PaDADH complex with iminoarginine. Support for His-48 being required for catalysis comes from the effect of DEPC treatment on PaDADH, resulting in loss of enzymatic activity due to chemical modification of the active site of the enzyme that could be completely reversed by treatment of the inactivated enzyme with hydroxylamine.⁽⁹⁾ His-48 is the histidine residue closest to the active site. Previous studies on other enzymes have indeed established that hydroxylamine commonly reverses DEPC modification of histidine residues.⁽⁹⁾ An alternate possibility is that Tyr-53 is the general base, being located on the mobile loop 50-56 with its hydroxyl at ≤ 3.8 Å away from the imine of iminoarginine.⁽²⁾

D-Arginine is considerably stickier than D-leucine, followed by D-methionine and D-lysine, as suggested by the perturbations of the apparent $\text{p}K_a$ values in the k_{cat}/K_m pH-profiles from the intrinsic value

of ~ 9.5 determined with D-leucine. Substrate stickiness can be computed by using eq 6, where ΔpK_a is the difference between the apparent and intrinsic pK_a values. As expected from the k_{cat}/K_m of $10^6 \text{ M}^{-1}\text{s}^{-1}$, D-arginine is the stickiest substrate, with k_3/k_2 of 160, likely due to the optimization of the active site with key residues involved in binding, such as Tyr-53, Arg-222, Tyr-249, Arg-305 and, most importantly, Glu-87. Interestingly, D-methionine is as sticky as D-lysine, with comparable k_3/k_2 ratios of 60 and 40, respectively, despite lack of interaction of its side chain with Glu-87. This is possibly due to the S atom establishing anion- π interactions with the phenols of both Tyr-53 and Tyr-249.⁽¹³⁾

$$\Delta pK_a = \log\left(1 + \frac{k_3}{k_2}\right) \quad (6)$$

The cationic side chains of the iminoarginine and iminolysine products contribute to their stickiness compared to products lacking a positive charge. This conclusion is supported by the pH-profiles of the k_{cat} values, showing apparent pK_a values with D-arginine and D-lysine ~ 3 pH units lower than the intrinsic value of ~ 9.5 determined with D-leucine. Perturbations of pK_a values in k_{cat} pH-profiles are symptomatic of a kinetic step other than the chemical step of catalysis being at least partially rate-determining for the overall turnover of an enzyme saturated with substrates.⁽¹⁰⁾ Since PaDADH operates through a Ping-Pong Bi-Bi kinetic mechanism in steady-state and previous studies established that the oxidative half-reaction with PMS as electron acceptor is fast,⁽⁴⁾ the only first-order kinetic step other than amine oxidation in the reductive half-reaction of the enzyme is product release (k_5 in **Scheme 3.2**). Most likely product stickiness with cationic substrates is due to the interaction of the positive charge present on the side chain of the ligand with the carboxylate of Glu-87, as suggested by the structures of the enzyme in complex with iminoarginine. The similar pK_a perturbations seen with D-arginine and D-lysine suggest that the interaction of the carboxylate of Glu-87 with the side chain of the ligand has the same effect on the rate of turnover of PaDADH irrespective of the presence of an ϵ -amino or guanido group on the product side chain. The increase in k_{cat} from $\sim 150 \text{ s}^{-1}$ to 400 s^{-1} seen in the pH-profile with D-lysine above pH 9.3 is in

agreement with product stickiness with D-lysine being due to its cationic side chain, since at high pH the latter is expected to be unprotonated, thereby making product release fast. Interestingly, iminomethionine is also considerably stickier than iminoleucine, as suggested by the apparent pK_a of 6.9 compared to the intrinsic $pK_a \sim 9.5$. Since both lack a cationic side chain, the stickiness of iminomethionine cannot be due to electrostatic interactions with Glu-87. Rather, potential anion- π interaction of the ligand S atom with the aromatic rings of Tyr-53 and Tyr-249 are likely responsible for the stickiness of iminomethionine,⁽¹³⁾ as also proposed for D-methionine.

In conclusion, we have used pH profiles, kinetic isotope effects, and chemical modification to investigate the mechanism of amine oxidation in PaDADH. The enzyme is able to oxidize both cationic and zwitterionic D-amino acids, providing a unique tool to discern the structural-functional relationships for broad substrate specificity. This study established: *a*) The importance of Glu-87, with $pK_a \geq 7.9$ for binding cationic substrates carrying a charge on the side chain; *b*) The general base that deprotonates the amine substrate has a pK_a of ~ 9.5 , with structural data suggesting either His-48 or Tyr-53; and *c*) Cationic substrates and products are sticky, resulting in steady-state turnover being primarily populated of substrate and product complexes rather than free enzyme. Future studies will use site-directed mutagenesis to mechanistically investigate several of the amino acid residues identified in the active site of PaDADH by the structural-functional investigation presented here, including His-48, Tyr-53, Glu-87 and Tyr-249.

3.8 Acknowledgements

The authors thank Irene T. Weber and Yuan-Fang Wang for insightful discussions.

3.9 References

1. Li, C., and Lu, C. D. (2009) Arginine racemization by coupled catabolic and anabolic dehydrogenases, *Proc Natl Acad Sci U S A* 106, 906-911.

2. Fu, G., Yuan, H., Li, C., Lu, C. D., Gadda, G., and Weber, I. T. (2010) Conformational changes and substrate recognition in *Pseudomonas aeruginosa* D-arginine dehydrogenase, *Biochemistry* 49, 8535-8545.
3. Yuan, H., Fu, G., Brooks, P. T., Weber, I., and Gadda, G. (2010) Steady-state kinetic mechanism and reductive half-reaction of D-arginine dehydrogenase from *Pseudomonas aeruginosa*, *Biochemistry* 49, 9542-9550.
4. Yuan, H., Xin, Y., Hamelberg, D., and Gadda, G. (2011) Insights on the mechanism of amine oxidation catalyzed by D-arginine dehydrogenase through pH and kinetic isotope effects, *Journal of the American Chemical Society* 133, 18957-18965.
5. Serrano, H., and Blanchard, J. S. (2013) Kinetic and Isotopic Characterization of L-Proline Dehydrogenase from *Mycobacterium tuberculosis*, *Biochemistry*.
6. Fitzpatrick, P. F. (2010) Oxidation of amines by flavoproteins, *Archives of biochemistry and biophysics* 493, 13-25.
7. Fu, G., Yuan, H., Wang, S., Gadda, G., and Weber, I. T. (2011) Atomic-resolution structure of an N5 flavin adduct in D-arginine dehydrogenase, *Biochemistry* 50, 6292-6294.
8. Gadda, G., and McAllister-Wilkins, E. E. (2003) Cloning, expression, and purification of choline dehydrogenase from the moderate halophile *Halomonas elongata*, *Appl Environ Microbiol* 69, 2126-2132.
9. Miles, E. W. (1977) [41] Modification of histidyl residues in proteins by diethylpyrocarbonate, In *Methods in Enzymology* (Hirs, C. H. W., and Serge, N. T., Eds.), pp 431-442, Academic Press.
10. Cleland, W. W. (1982) The use of pH studies to determine chemical mechanisms of enzyme-catalyzed reactions, *Methods Enzymol* 87, 390-405.
11. Cleland, W. W. (1963) The kinetics of enzyme-catalyzed reactions with two or more substrates or products. I. Nomenclature and rate equations, *Biochimica et biophysica acta* 67, 104-137.
12. Cleland, W. W. (1982) Use of isotope effects to elucidate enzyme mechanisms, *CRC critical reviews in biochemistry* 13, 385-428.

13. Meyer, E. A., Castellano, R. K., and Diederich, F. (2003) Interactions with aromatic rings in chemical and biological recognition, *Angewandte Chemie* 42, 1210-1250.

4 MECHANISTIC AND COMPUTATIONAL STUDIES ON THE REDUCTIVE HALF-REACTION OF TYROSINE TO PHENYLALANINE ACTIVE SITE VARIANTS OF D-ARGININE DEHYDROGENASE

(This chapter also has contribution by Dr. Sarah Sirin (computational analysis))

4.1 Abbreviations

PaDADH; D-Arginine Dehydrogenase, KIE; Kinetic Isotope Effects, FAD; Flavin Adenine Dinucleotide IAR; Iminoarginine, DAAO; D-amino acid Oxidase, PLP; Pyridoxal Phosphate, MD; Molecular Dynamics, QM/MM; Quantum Mechanical/Molecular Mechanical.

4.2 Abstract

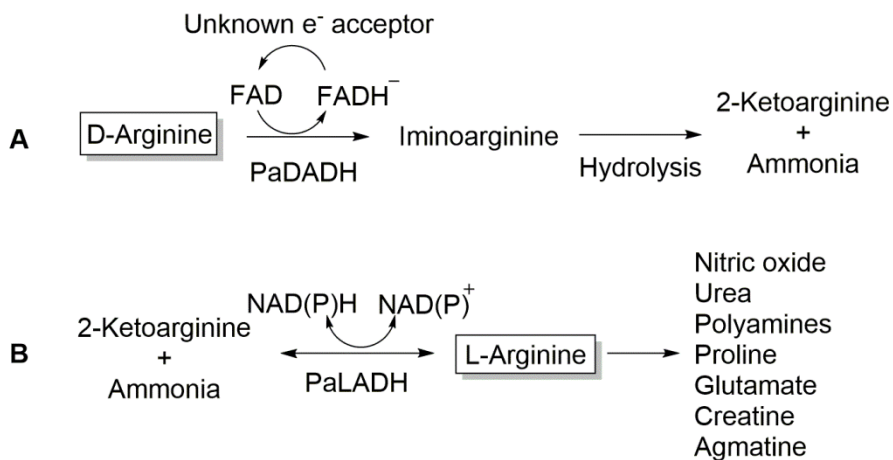
The flavin-mediated enzymatic oxidation of a CN bond in amino acids can occur through hydride transfer, carbanion or polar nucleophilic mechanisms. Previous results with D-arginine dehydrogenase from *Pseudomonas aeruginosa* (PaDADH) using multiple kinetic isotope effects (KIEs) and computational studies established preferred binding of the substrate protonated on the α -amino group, with the cleavages of the NH and CH bonds occurring in asynchronous fashion, consistent with the three possible mechanisms. The hydroxyl groups of Y53 and Y249 are $\leq 4\text{\AA}$ from the imino and carboxylate groups of the reaction product iminoarginine, suggesting participation in binding and catalysis. In this study, we have investigated the reductive half-reactions of the Y53F and Y249F variants of PaDADH using substrate and solvent KIEs, solvent viscosity and pH effects and QM/MM computational approaches to gain insights on the catalytic roles of the protein hydroxyl groups and evaluate whether the mutations affect the transition state for substrate oxidation. Both Y53F and Y249F enzymes oxidized D-arginine with steady-state kinetic parameters similar to wild-type enzyme. Rate constants for flavin reduction (k_{red}) with D-leucine, a slow substrate amenable to rapid kinetics, were <3 -fold than wild-type with similar $\text{p}K_{\text{a}}$ values for an unprotonated group of ~ 10.0 . Similar $\text{p}K_{\text{a}}$ values were also observed for $^{\text{app}}K_{\text{d}}$ in the Y53F, Y249F

and wild-type enzymes. However, cleavage of the substrate NH and CH bonds in the mutants occurs in synchronous fashion, as suggested by multiple KIEs on k_{red} . These data can be reconciled with a hydride transfer mechanism, but not with carbanion and polar nucleophilic mechanisms.

4.3 Introduction

Pseudomonas aeruginosa D-arginine dehydrogenase (PaDADH) is a member of a structural family consisting of D-amino acid oxidase, sarcosine oxidase, dimethyl glycine oxidase, and glycine oxidase.¹⁻⁷ The enzyme, along with L-arginine dehydrogenase (PaLADH) is part of a recently discovered, two-enzyme system involved in D- to L-arginine racemization in pseudomonads and related species (**Scheme 4.1**).^{8,9} Prior to this discovery, racemization between D- and L-amino acids was known to be catalyzed only by single PLP-dependent or -independent racemases.¹⁰ PaDADH is an FAD-dependent enzyme that oxidizes D-arginine to iminoarginine, which is then hydrolyzed non-enzymatically to 2-ketoarginine and ammonia (**Scheme 4.1A**).⁸ The latter are substrates for the NAD(P)H-dependent PaLADH for the synthesis of L-arginine (**Scheme 4.1B**). L-Arginine is shuttled through different pathways to yield physiologically important compounds in bacteria¹¹ as well as mammals¹² (**Scheme 4.1B**). Although PaDADH is primarily involved in arginine metabolism in *P. aeruginosa*, the enzyme has broad substrate specificity for D-amino acids except D-aspartate, D-glutamate, and glycine.⁹

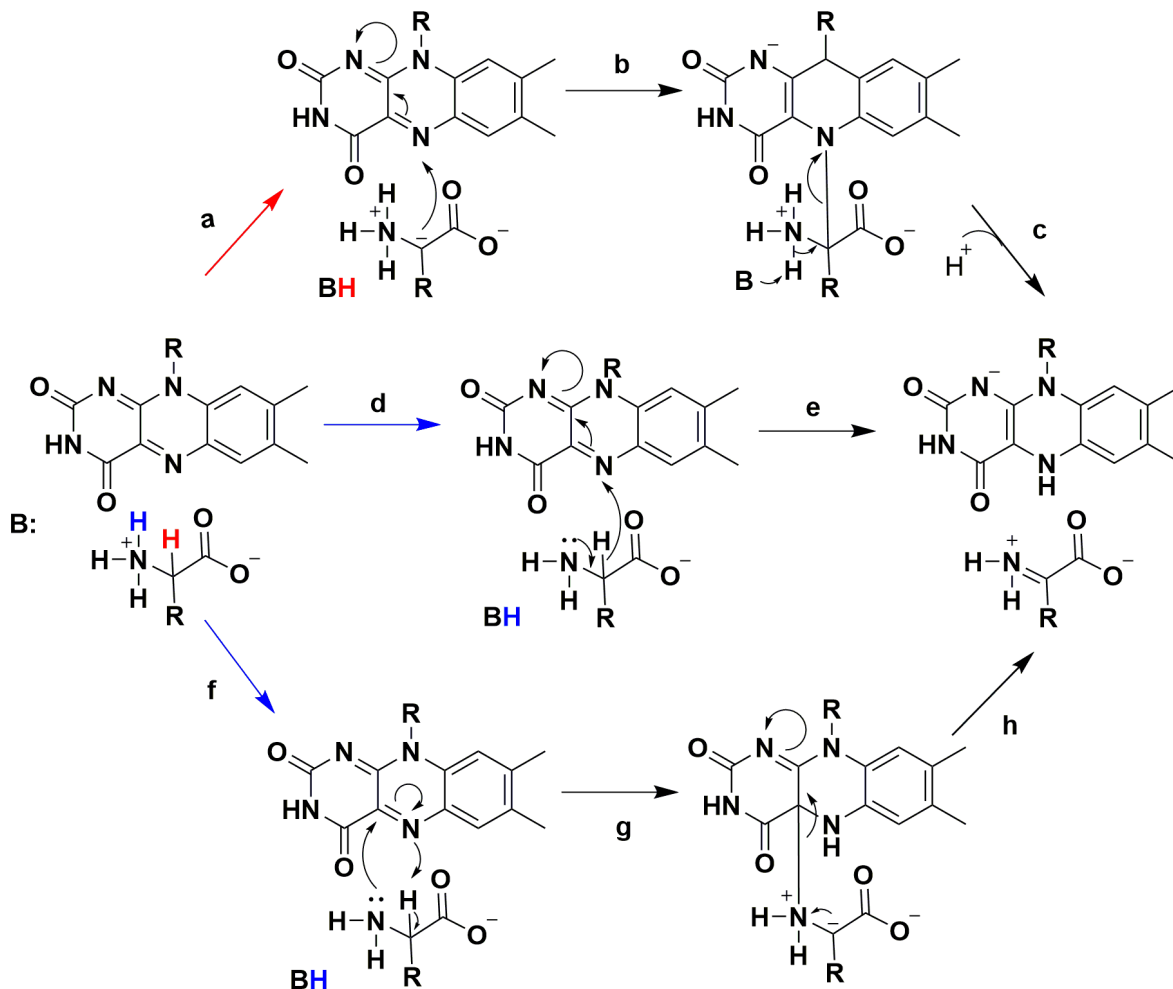
The FAD-mediated oxidation of the CN bond in PaDADH was recently investigated with D-leucine, a catalytically slow substrate for the enzyme.¹³ With arginine, the mechanistic analysis is precluded since >85% of the reaction happens within the mixing time of the stopped-flow spectrophotometer (i.e., 2.2 ms).¹⁴ Deuterium kinetic isotope effects (KIE) and solvent effects (isotope, pH and viscosity) in combination with molecular dynamics simulations are consistent with preferred binding to the enzyme of D-leucine protonated on the α -amino group.¹³ Multiple deuterium KIE on the rate constant for flavin reduction (k_{red}) established that cleavages of the NH and CH bonds occur in asynchronous fashion. Three mechanisms for CN bond oxidation are consistent with the available data



Scheme 4.1 Schematic illustration of D- to L-arginine racemization in *P. aeruginosa* and possible fates of L-arginine.

If a strong active site base abstracts the substrate α -proton with $pK_a \sim 17$,¹⁵ the resulting carbanion would react with the flavin N5 atom forming a covalent N5-flavin adduct (**Scheme 4.2, a-b-c**).^{1,16-20} Alternatively, a polar nucleophilic attack of the lone pair of electrons of the substrate α -amine at the flavin C4a atom may form a covalent C4a-flavin adduct (**Scheme 4.2, f-g-h**).²¹ In both mechanisms, cleavage of the substrate NH bond would occur stepwise to CH bond cleavage, either before (**f**) or after (**c**) formation of a covalent adduct with the flavin. If deprotonation of the substrate α -amine occurs first, it would trigger CH bond cleavage through the transfer of a hydride ion from the substrate to the flavin N5 atom (**Scheme 4.2, d-e**). While in principle the transfer of a single electron and a hydrogen atom from the substrate to the flavin is possible, mechanistic studies have yet to demonstrate in flavoproteins the transient existence of the resulting radical species in reactions with physiological substrates.

During reduction of PaDADH with D-leucine¹³ or D-histidine¹⁴ no reaction intermediates characteristic of flavin C4a and N5 adducts, i.e., with absorbance maxima in the 360 to 400 nm region, were reported, consistent with a hydride transfer mechanism. However, carbanion and polar nucleophilic mechanisms could not be ruled out solely based on these observations since flavin adducts that decay faster than they form, would not accumulate.



Scheme 4.2 Possible mechanisms for CN bond oxidation by PaDADH: carbanion (a-b-c), hydride transfer (d-e) and polar nucleophilic attack (f-g-h).

Steady-state and rapid kinetics pH-profiles with D-leucine demonstrated in PaDADH the requirement for catalysis of an unprotonated group with pK_a of 9.6.^{13,22} A protonated group with pK_a of ~ 10.3 favors the binding of the substrate to the enzyme.¹³ X-ray crystallography of the enzyme in complex with iminoarginine or iminohistidine showed that Y53 is suitably positioned in the active site to deprotonate the substrate α -amine,^{13,22} being on a mobile loop with its hydroxyl oxygen atom at ≤ 3.8 Å from the imine of iminoarginine (**Figure 4.1**). The side chain of Y249 interacts with the substrate carboxylate at a distance of ~ 2.8 Å, suggesting that Y249 may be the protonated group that facilitates substrate binding (**Figure 4.1**).

In this study, we have individually replaced Y53 and Y249 with phenylalanine to investigate the roles of their hydroxyl groups in catalysis and binding in PaDADH and gain insights on the relative timing of CH and NH bond cleavage. To this end, we used steady-state and rapid reaction kinetics, pH and solvent effects, deuterium substrate, solvent and multiple KIE, and QM/MM computational approaches. The results presented allow us to rule out two of the three possible reaction mechanisms and establish how CN bond oxidation is achieved in PaDADH, thereby advancing knowledge of amino acid oxidation catalyzed by flavin-dependent enzymes.

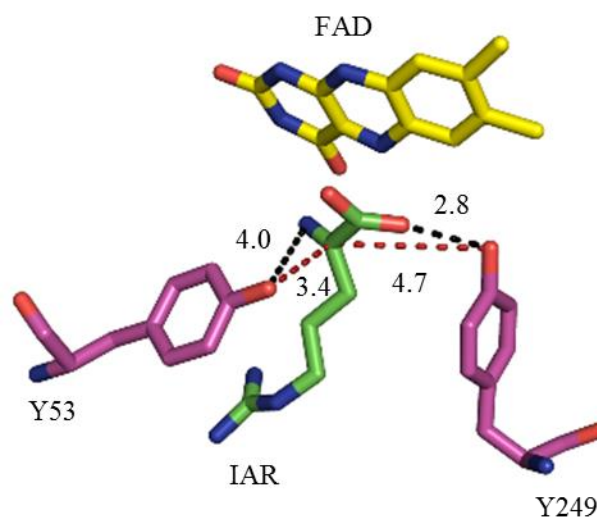


Figure 4.1 The active site of PaDADH in complex with iminoarginine at 1.3 Å resolution (PDB: 3NYE). The distances in Å of the hydroxyl oxygen atom of Y53 and Y249 to the imine nitrogen atom or carboxylate oxygen atom of the reaction product are shown in black, whereas those to the C_α atom are in red.

4.4 Experimental Procedures

Materials. *Escherichia coli* Rosetta(DE3)pLysS was from Novagen (Madison, WI). QIAprep Spin Miniprep kit was obtained from Qiagen (Valencia, CA), QuickChange site-directed mutagenesis kit was purchased from Stratagene (La Jolla, CA). Oligonucleotides for site-directed mutagenesis and sequencing of the mutant genes were obtained from Sigma Genosys (The Woodlands, TX). D-Arginine and phenazine methosulfate (PMS) were purchased from Sigma-Aldrich (St. Louis, MO). D-Leucine was

obtained from Alfa Aesar and D-leucine- d_{10} was obtained from CDN isotopes (Canada). 99.9% deuterium oxide was purchased from Cambridge Isotope Laboratories, Inc. (Andover, MA). All other reagents used were obtained in their highest purity commercially available.

Site-directed Mutagenesis, Expression, and Purification of the Y53F and Y249F Enzymes. The Y53F and Y249F enzymes were prepared by site-directed mutagenesis using the cloned wild-type gene pET20b(+)/PA3863 as template. Site-directed mutagenesis was performed as per the manufacturer's manual using the QuickChange kit. DMSO was added at a final concentration of 5% to ensure proper separation of double stranded DNA template. Each mutation was confirmed through sequencing the gene using an Applied Biosystems Big Dye Kit on an Applied Biosystems model ABI377 DNA sequencer, at the DNA Core Facility of Georgia State University. Rosetta(DE3)pLysS cells were transformed via heat-shock. All steps of protein expression and purification were carried out at 4 °C using the published protocol for the wild-type enzyme.¹⁴

Steady-State Kinetics. Steady-state kinetic parameters with D-arginine (0.01-3.0 mM) were determined by measuring initial rates of reaction with an oxygen electrode in the presence of 1 mM PMS ($K_m = 10 \mu\text{M}$) as electron acceptor in 20 mM Tris-Cl, pH 8.7 and 25 °C, as previously described.¹⁴ As for the wild-type enzyme, both Y53F and Y249F enzymes showed no oxygen consumption in absence of PMS, indicating that the mutations did not confer oxidase activity to the enzyme.

Reductive Half-Reaction. Reductive half-reactions were carried out using an SF-61DX2 Hi-Tech KinetAsyst high performance stopped-flow spectrophotometer at 25 °C. For substrate, solvent, and multiple KIE, as well as pH and solvent viscosity effects, the published protocols and buffers previously used for the wild-type enzyme were employed.¹³ Final concentrations of D-leucine and enzyme were 0.1-50 mM and $\sim 10 \mu\text{M}$ to ensure pseudo first-order kinetic conditions. KIE were carried out in 20 mM

EDTA, pH 10.5 and 25 °C, in either H₂O or 99.9% D₂O with D-leucine and D-leucine-*d*₁₀ as substrates, as previously described for the wild-type enzyme.¹³

Computational Characterization. Computational models of the reactant were prepared based on wild-type crystal structures of PaDADH (PDB accession codes: 3NYC and 3NYE).²³ To model the open, substrate free configuration of PaDADH 3NYC was used, which corresponds to 70% occupancy of the ligand free open conformer²². The Y53 side chain rotamer corresponding to the open configuration was modeled after removing the imino product. For all other amino acids with multiple rotamers, side chains with higher occupancies were used. For the closed, substrate bound PaDADH configuration, we used the 3NYE crystal structure because it has 100% occupancy of the product²² and transformed the imino-arginine product to the D-arginine or D-leucine substrate. For both open and closed models, the isoalloxazine ring was modeled in its oxidized form, which is the state prior to substrate oxidation. Missing hydrogen atoms were added and optimized using the Protein Preparation Wizard²⁴ in Maestro.²⁵ *In silico* PaDADH variants with Y249F and Y53F single point mutations were generated using Residue Scanning module of BioLuminate²⁶ for substrate-free, D-leucine, and D-arginine bound configurations. PaDADH binding sites of open configurations were characterized using SiteMap²⁷ by first calculating the binding site volume as beads placed on a 1 Å grid and determining the local hydrophobic-hydrophilic character.

QM/MM geometry optimizations for all Pa-DADH models were performed at the B3LYP/6-31G* and B3LYP/cc-pVDZ+ levels of theory, as implemented in QSite.²⁸ For substrate-free models, the QM regions included the Y53(F), Y249(F) side chains, and the isoalloxazine ring of flavin cofactor (**Figure 4.2a**). For substrate-bound configurations, D-leucine/arginine substrates were also included in QM region, as illustrated in **Figure 4.2b**. The rest of the system was treated using the OPLS2005^{29,30} molecular mechanics force field. Local electrophilicity was predicted for the C4a and N5 atoms based on computed global electrophilicity power of the system and the regional Fukui functions. Fukui functions can be used to describe the electron density in a frontier atomic orbitals,^{31,32} while the global electrophilicity

of a system is a quantitative approximation of the likelihood of a system to accept electrons, and is calculated as electronegativity squared divided by twice the chemical hardness.³³⁻³⁵

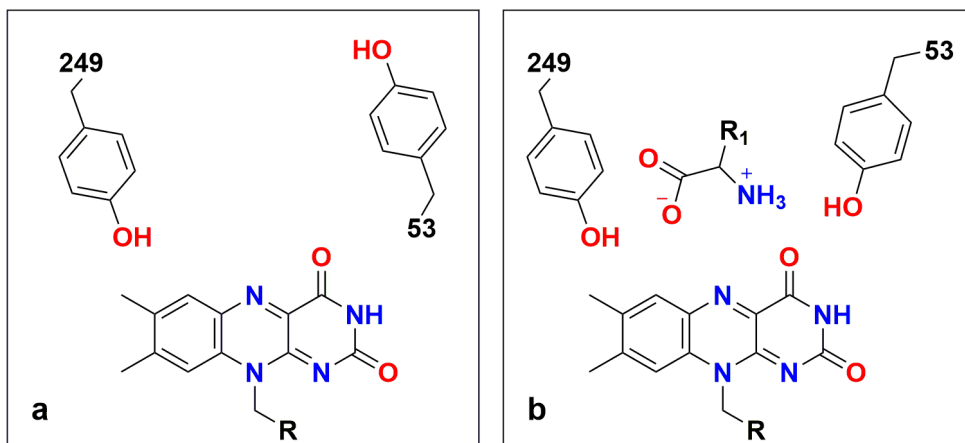


Figure 4.2 Illustration of the QM region in (a) open, substrate free, and (b) closed, substrate bound configurations. R1 in panel b denotes the D-leucine and D-arginine side chains. For simplicity, only wild-type PaDADH is shown.

Data Analysis. Data were fit with the KaleidaGraph software (Synergy Software, Reading, PA), Enzfitter software (Biosoft, Cambridge, U.K.), Kinetic Studio Software Suite (Hi-Tech Scientific, Bradford on Avon, U.K.) or the global-fitting analysis software SPECFIT/32.

Time-resolved flavin reductions were fit to eqs 1 and 2, which describe single and double exponential processes for flavin reduction. k_{obs} , k_{obs1} and k_{obs2} are the first-order rate constants associated with the absorption changes at 446 nm at a given concentration of substrate, t is time, A is the absorbance at 446 nm at any given time, B , B_1 and B_2 are the amplitudes of the absorption changes, and C is the absorbance at infinite time to account for the non-zero absorbance of the reduced enzyme.

$$A = B \exp(-k_{\text{obs}} t) + C \quad (1)$$

$$A = B_1 \exp(-k_{\text{obs1}} t) + B_2 \exp(-k_{\text{obs2}} t) + C \quad (2)$$

Reductive half-reaction kinetic parameters were determined by using eqs 3 and 4, which describe hyperbolic trends with and without a y-intercept. k_{obs} is the observed first-order rate constant for the reduction of the flavin at any given concentration of substrate (S), k_{red} is the limiting first-order rate constant for flavin reduction at saturating concentrations of substrate, k_{rev} is the limiting first-order rate constant for the reverse of flavin reduction, and $^{\text{app}}K_d$ is the apparent equilibrium constant for dissociation of the enzyme-substrate complex into free enzyme and substrate.

$$k_{\text{obs}} = \frac{k_{\text{red}}S}{^{\text{app}}K_d + S} + k_{\text{rev}} \quad (3)$$

$$k_{\text{obs}} = \frac{k_{\text{red}}S}{^{\text{app}}K_d + S} \quad (4)$$

Substrate deuterium KIEs were calculated using eq 5, which applies for a KIE on the k_{red} value. Solvent deuterium and multiple KIEs were calculated using eq 6, which describes a KIE on the k_{red} value and a solvent effect on the K_d value due to pH. F_i represents the fraction of heavy atom $^{\text{D}}k_{\text{red}}$ is the KIE on k_{red} , and $^{\text{SE}}(K_d)$ is the solvent effect due to pH on the apparent K_d value elicited by substituting H_2O with D_2O at those pL values where K_d is not pH-independent.¹³

$$k_{\text{obs}} = \frac{k_{\text{red}}S}{(K_d + S)[1 + F_i(D_{k_{\text{red}}} - 1)]} \quad (5)$$

$$k_{\text{obs}} = \frac{k_{\text{red}}S}{K_d \left[1 + F_i \left(\frac{D_{k_{\text{red}}}}{^{\text{SE}}(K_d)} \right) - 1 \right] + S [1 + F_i(D_{k_{\text{red}}} - 1)]} \quad (6)$$

The pH dependences of the k_{red} values were fit using eq 7, where $k_{\text{red}(\text{lim})}$ represents the pH-independent limiting value for flavin reduction at high pH and $\text{p}K_a$ is the apparent value for the ionization of a group that must be unprotonated for flavin reduction.

$$\log k_{red} = \log \left(\frac{k_{red(lim)}}{1+10^{pKa-pH}} \right) \quad (7)$$

The pH dependence of the k_{rev} value with Pa-DADH-Y53F was fit using eq 8 describing a curve with two plateau regions; where $k_{rev(L)}$ and $k_{rev(H)}$ indicate lower and higher limiting values at low and high pH respectively and k_a is the dissociation constant of the ionizable groups.

$$\log k_{rev} = \log \left(\frac{k_{rev(L)} + k_{rev(H)} \times (10^{pH-pKa})}{1+10^{pH-pKa}} \right) \quad (8)$$

The pH dependences of the K_d values were fit using eq 9, which describes a curve with a slope of +1 at high pH and a plateau region that defines a limiting, pH-independent K_d value at low pH, i.e., $K_{d(lim)}$.

$$\log K_d = \log \left(K_{d(lim)} \times (1 + 10^{pH-pKa}) \right) \quad (9)$$

4.5 Results

Purification of the Y53F and Y249F Enzymes. Y53 and Y249 of PaDADH were mutated to phenylalanine using site-directed mutagenesis and the resulting proteins were expressed and purified to high levels following the same procedure previously used for the wild-type enzyme.¹⁴ The Y53F enzyme exhibited a UV-visible absorption spectrum similar to wild-type (**Figure 4.3**), whereas the Y249F variant was present in two forms that could be separated on a DEAE-Sepharose column: a yellow fraction containing FAD (**Figure 4.3**) and a green fraction, containing a modified form of FAD (data not shown). The yellow fraction was enzymatically active, whereas the green fraction was inactive. Hence, this work focuses on the yellow fraction; the inactive green fraction is currently under investigation and will be discussed in future work. Both the Y53F and Y249F enzymes oxidized D-arginine, with steady-state kinetic parameters at 1 mM PMS similar to the wild-type enzyme at pH 8.7 (**Table 4.1**).

Table 4.1 Apparent Steady-State Kinetic Parameters for wild-type, Y53F, and Y249F PaDADH.

Enzyme	$^{app}k_{cat}/K_m$ ($M^{-1}s^{-1}$)	$^{app}K_m$ (mM)	$^{app}k_{cat}$ (s^{-1})
Wild type ^a	$3.4 (\pm 0.3) \times 10^6$	0.06 (± 0.01)	204 (± 6)
Y53F ^b	$1.2 (\pm 0.1) \times 10^6$	0.36 (± 0.01)	420 (± 4)
Y249F ^b	$3.4 (\pm 0.3) \times 10^6$	0.06 (± 0.01)	204 (± 6)

Experimental conditions: ^aTaken from Fu *et.al.*³⁵

^b20 mM Tris-HCl, pH 8.7, 25 °C and 1 mM PMS; 0.01-3mM D-Arginine

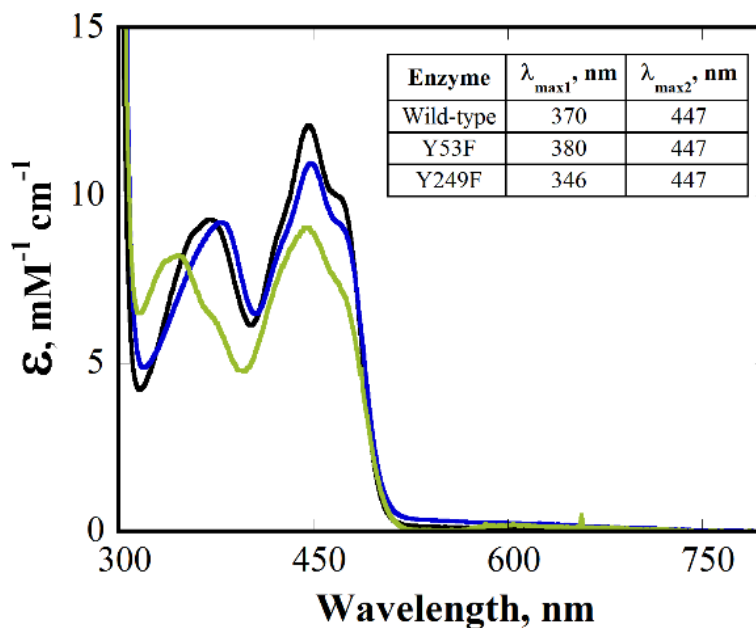


Figure 4.3 UV-Visible absorption spectra of the Y53F (blue), Y249F (green), and wild-type PaDADH (black) in 20 mM Tris-Cl, 10% glycerol, pH 8.7 and 22 °C.

pH Profiles of k_{red} . The reductive half-reaction with D-arginine in the Y53F and Y249F enzymes was too fast to be studied in a stopped-flow spectrophotometer, with >80% of the flavin being completely reduced within the mixing time of the instrument (i.e., 2.2 ms). This was previously observed in the wild-type enzyme.¹⁴ The reaction was thus investigated with D-leucine as the reducing substrate, for which data for the wild-type enzyme are available to compare and contrast. Flavin reduction was monitored at 446 nm upon mixing PaDADH ($\sim 10 \mu M$) with varying concentrations of D-leucine ($\geq 100 \mu M$) to ensure pseudo-first order conditions. With the exception of the Y249F enzyme at pH ≥ 10.0 , the

stopped-flow traces with both mutant enzymes were best fit to single exponential processes at any pH (Figure 4.4).

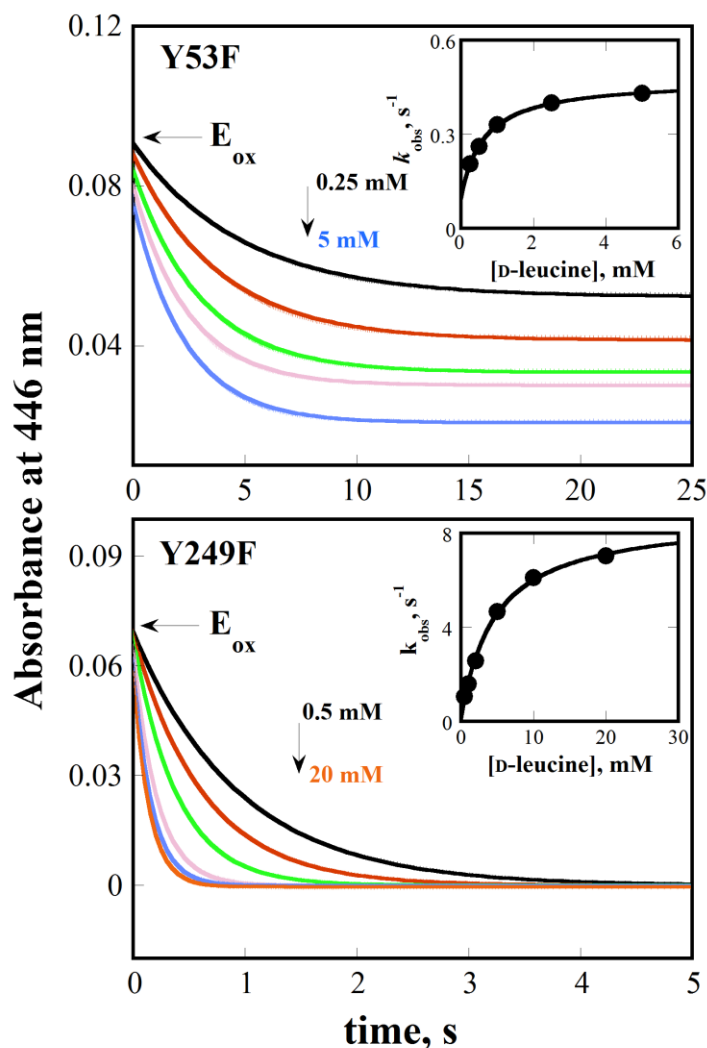


Figure 4.4 Reductive half-reactions for the Y53F and Y249F enzymes with D-leucine. Stopped-flow traces at 446 nm at varying D-leucine concentrations are shown for Y53F at pH 8.0 (top panel) and Y249F at pH 9.0 (bottom panel); E_{ox} is the absorbance of the enzymes in the oxidized state after mixing with buffer. Insets show the concentration dependences of k_{obs} with the best fit of the data points obtained with eqs 3 and 4 for the Y53F and Y249F enzymes, respectively.

At high pH, the Y249F enzyme showed biphasic flavin reduction with a slow phase independent of D-leucine concentration, which accounted for ~10% absorption change. This was probably due to partially damaged enzyme, since the Y249F enzyme was relatively unstable at high pH. With both enzymes, observed rate constants for flavin reduction (k_{obs}) increased hyperbolically with increasing substrate concentration, defining limiting rate constants for flavin reduction at saturating concentration of D-leucine (k_{red}) (**Figure 4.4 insets**). For the Y53F enzyme, y-intercepts significantly different from zero were obtained by fitting the data to eq 3, consistent with reversible flavin reduction (**Figure 4.4 inset**).³⁶ A similar pattern was seen with the Y249F enzyme at $\text{pH} \leq 8.0$, whereas the y-intercepts with the latter enzyme were negligible at $\text{pH} \geq 8.5$ (**Figure 4.4 inset**). With both enzymes the reversibility was more prominent at low pH due to a progressive decrease in the k_{red} values (**Figure 4.5**). In contrast, previous results with the wild-type enzyme demonstrated negligible y-intercepts in the same pH range from 7.0 to 10.5.¹³

The k_{red} values for the Y53F and Y249F enzymes increased with increasing pH (**Figure 4.5**), defining apparent $\text{p}K_{\text{a}}$ values not significantly different from the value of 9.6 previously determined for the wild-type enzyme (**Table 4.2**). The estimated pH-independent k_{red} values with both mutant enzymes were <3-fold lower than in the wild-type enzyme (**Table 4.2**), indicating that neither Y53 nor Y249 is essential for amine oxidation. With the Y53F enzyme, the k_{rev} increased with increasing pH between limiting values at low and high pH of $0.05 (\pm 0.01) \text{ s}^{-1}$ and $0.7 (\pm 0.1) \text{ s}^{-1}$, respectively, defining a $\text{p}K_{\text{a}}$ of $9.1 (\pm 0.2)$ (**Figure 4.5**). The $^{\text{app}}K_{\text{d}}$ values were pH-independent below pH 8.5 and increased with increasing pH (**Figure 4.6**), defining apparent $\text{p}K_{\text{a}}$ values slightly lower than in the wild-type enzyme (**Table 4.2**). While the pH-independent $^{\text{app}}K_{\text{d}}$ for the Y249F enzyme was similar to wild-type, the value for the Y53F enzyme was 7-fold lower (**Table 4.2**).

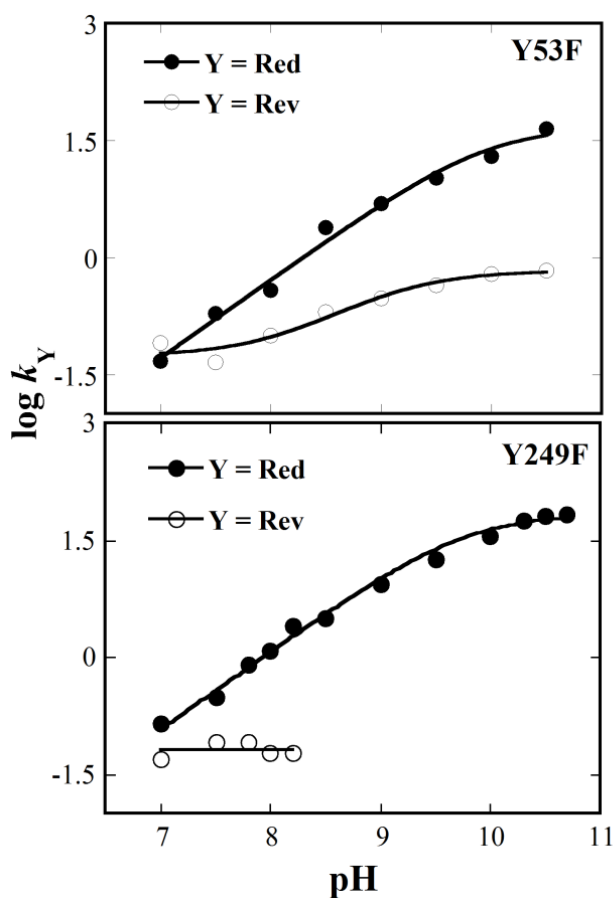


Figure 4.5 Effects of pH on k_{red} and k_{rev} of the Y53F (top panel) and Y249F enzymes (bottom panel) with D-leucine. The k_{red} values (●) were fit with eq 7, whereas the k_{rev} values (○) were fit with eq 8 for the Y53F enzyme. The horizontal line in the plot of the Y249F enzyme is the average of the k_{rev} values.

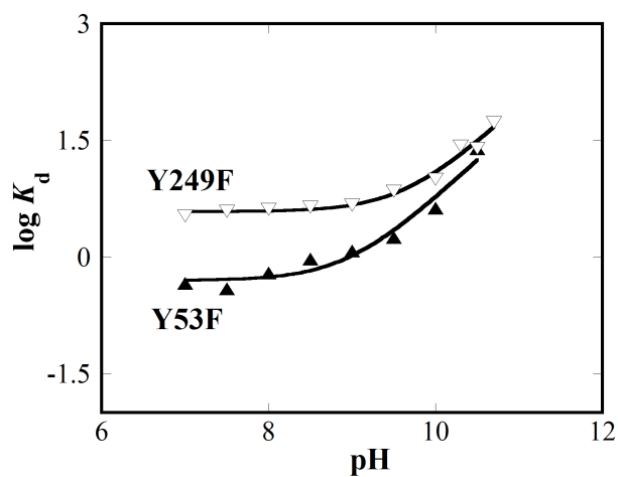


Figure 4.6 Effects of pH on ${}^{app}K_d$ of the Y53F and Y249F enzymes with D-leucine. Data points were fit with eq 9.

Table 4.2 pH Dependence of k_{red} and K_{d} in wild type, Y53F, and Y249F PaDADH.

Enzyme	$k_{\text{red}}(\text{lim}), \text{s}^{-1}$	$\text{p}K_{\text{a}} (k_{\text{red}})$	$K_{\text{d}}(\text{lim}), \text{mM}$	$\text{p}K_{\text{a}} (K_{\text{d}})$
Wild type ^a	133 (± 5)	$\sim 9.6^b$	3.5 (± 0.3)	10.3 (± 0.1)
Y53F	$\sim 50^b$	$\sim 10.0^b$	0.5 (± 0.1)	9.0 (± 0.1)
Y249F	$\sim 70^b$	$\sim 9.8^b$	3.5 (± 0.3)	9.6 (± 0.1)

^aTaken from Yuan *et.al.*¹²

^bApproximate value as the plateau is not well defined

Substrate Deuterium KIEs on k_{red} . Substrate deuterium KIEs were measured with D-leucine and D-leucine- d_{10} at pL 10.5 to gain insights on the status of the CH bond in the transition state for amine oxidation catalyzed by the Y53F and Y249F enzymes. $^{\text{D}}k_{\text{red}}$ values >4 were observed in aqueous buffered solutions with both the Y53F and Y249F enzymes (**Table 4.3**). Upon substitution of H_2O with D_2O , the substrate deuterium KIE increased slightly in the Y53F enzyme, whereas it decreased slightly in the Y249F enzyme. The changes, however, were not significant within standard deviation (**Table 4.3**).

Solvent Deuterium KIEs on k_{red} . Solvent deuterium KIEs were measured at pL 10.5 to probe the status of the substrate NH bond in the transition state for amine oxidation catalyzed by the Y53F and Y249F enzymes. The high pL was chosen because k_{red} is independent of pL in the wild-type¹³ and the mutant enzymes (**Table 4.2**), thereby eliminating possible artifactual effects due to different ionization of relevant groups in H_2O and D_2O . The data were fit to eq 6, which allows for the determination of the $^{\text{D}_2\text{O}}k_{\text{red}}$ values while accounting for solvent effects due to pH on the $^{\text{app}}K_{\text{d}}$ values, as previously carried out for wild-type PaDADH.¹³ Small but significant $^{\text{D}_2\text{O}}k_{\text{red}}$ values with magnitudes similar to wild-type PaDADH were determined for both mutant enzymes (**Table 4.3**). Since D_2O is $\sim 25\%$ more viscous than H_2O , there exists the possibility that the small $^{\text{D}_2\text{O}}k_{\text{red}}$ values could be due to viscosity rather than isotope effects. This was assessed by determining the effect of solvent viscosity on the rate constant for flavin reduction in the absence and presence of 10% glycerol, which provides viscosity at 25 °C equivalent to that of D_2O . The solvent viscosity effect on k_{red} , expressed as $k_{\text{red}}/k_{\text{red}}(\text{glycerol})$, was 1.06 (± 0.04) for the Y53F enzyme and 0.94 (± 0.01) for the Y249F enzyme, consistent with the $^{\text{D}_2\text{O}}k_{\text{red}}$ values arising from

KIE and not solvent viscosity effects, as previously established for the wild-type enzyme.¹³ Substitution of D-leucine with D-leucine-*d*₁₀ resulted in a slight increase in the ^{D2O}*k*_{red} value with the Y53F enzyme and no changes with the Y249F enzyme (**Table 4.3**).

Multiple KIEs on *k*_{red}. Multiple deuterium isotope effects (^{D,D2O}*k*_{red}) were carried out to dissect the contributions of the hydroxyl groups of Y53 and Y249 on the relative timing of CH and NH bond cleavages in the transition state(s) for amine oxidation catalyzed by the mutant enzymes. The ^{D,D2O}*k*_{red} values for both Y53F and Y249F enzymes at pL 10.5 are summarized in **Table 4.3**. The ^{D,D2O}*k*_{red} is similar within standard deviation to the product of the individual deuterium isotope effects ^D(*k*_{red})_{H2O} × ^{D2O}(*k*_{red})_H for Y53F and Y249F mutant enzymes. In contrast, in the wild-type enzyme the multiple KIE was slightly lower than the product of the individual ones (**Table 4.3**).¹³

Table 4.3 KIEs on *k*_{red} in the Y53F and Y249F enzymes ^a

KIE	Y249F ^b	Y53F ^b	Wild type ^a
^D (<i>k</i> _{red}) _{H2O}	4.7 (±0.1)	4.2 (±0.4)	5.1 (±0.1)
^D (<i>k</i> _{red}) _{D2O}	4.3 (±0.1)	5.0 (±0.2)	4.7 (±0.1)
^{D2O} (<i>k</i> _{red}) _H	1.3 (±0.1)	2.1 (±0.1)	1.8 (±0.1)
^{D2O} (<i>k</i> _{red}) _D	1.3 (±0.1)	2.3 (±0.1)	1.6 (±0.1)
^{D, D2O} (<i>k</i> _{red})	5.7 (±0.1)	12 (±2)	7.8 (±0.1)
^D (<i>k</i> _{red}) _{H2O} · ^{D2O} (<i>k</i> _{red}) _H	6.1 (±0.2)	9 (±1)	9.0 (±0.2)

Experimental conditions: ^aFrom Yuan *et.al.*¹²;

^b20 mM EDTA, pL 10.5, 25 °C

Time Resolved Absorption Spectroscopy. The reductive half-reaction of the Y53F and Y249F enzymes, as well as wild-type PaDADH, were further studied at pH 10.5 in a stopped-flow spectrophotometer equipped with a photo-diode-array detector. Irrespective of D-leucine or D-leucine-*d*₁₀ as substrate, flavin reduction occurred without transient accumulation of any flavin-derived intermediate, as indicated by the stopped-flow traces at any wavelength between 300 and 700 nm (**Figure S1**).

Relative Flavin Electrophilicity at the C4a and N5 Atoms. The active site of PaDADH was mapped computationally for hydrophilic and hydrophobic characteristics as described in the methods section. Initially, this was done with the Y53F, Y249F and wild-type enzymes in the absence of substrate to reveal any possible effects of mutagenesis on the binding pocket and substrate recognition (**Figure 4.7**). The hydrophilic regions were further characterized as hydrogen bond donor and acceptor regions, colored blue and red, respectively. In the substrate free state, the Y249F mutation changes the hydrogen bond donor character near the flavin N5 atom compared to wild-type, while no changes were seen in the Y53F enzyme.

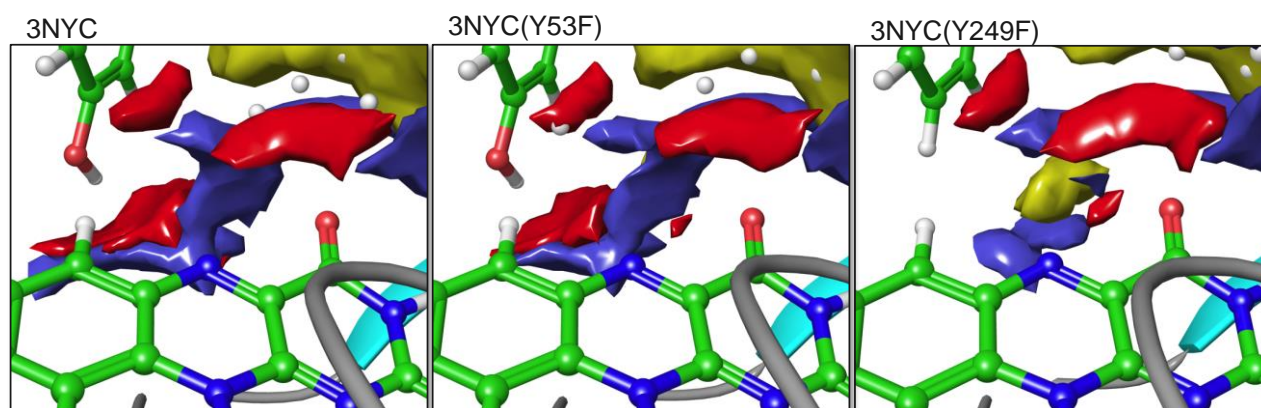


Figure 4.7 Electrophilicity of the substrate binding sites close to the flavin C4a and N5 atoms in wild-type, Y53F and Y249F PaDADH. Hydrophilic regions are divided into hydrogen-bond donor (blue) and acceptor regions (red), whereas hydrophobic regions are shown in yellow. The white spheres denote SiteMap points that are placed into 1 Å grid and used to calculate the binding site volume used to evaluate the binding site.

Since the X-ray crystallographic structure of PaDADH previously resolved demonstrated that in the enzyme-iminoarginine complex the loop containing Y53 is in a closed conformation, as opposed to the open conformation seen in the substrate free enzyme, local electrophilicity indexes were computed also for the ligand-bound enzyme. This showed that the flavin N5 atom was a better electrophile than the flavin

C4a atom, irrespective of the starting configurations, presence or absence of substrate and substrate identity (**Figure S2-3**).

4.6 Discussion

A previous study of the reductive half-reaction of wild-type PaDADH using substrate and solvent KIEs established that the oxidation of D-leucine to the imino product 4-methyl-2-oxopentanoate occurs through the asynchronous cleavages of the substrate NH and CH bonds.¹³ Thus, amino acid oxidation could take place via hydride transfer, a carbanion or a polar nucleophilic mechanism (**Scheme 4.2**). Here, we have investigated the reductive half-reactions of the Y53F or Y249F variants of PaDADH using substrate and solvent KIEs, solvent viscosity and pH effects and QM/MM computational approaches. The mutations were selected because in the X-ray crystallographic structure of the wild-type enzyme in complex with the reaction product iminoarginine the hydroxyl groups of the two tyrosines are ≤ 4 Å from the imino and carboxylate moieties of the ligand, suggesting participation in catalysis and binding.^{13,22}

The cleavages of the NH and CH bonds of D-leucine catalyzed by the Y53F and Y249F variants of PaDADH occur in synchronous fashion, consistent with a hydride transfer mechanism for flavin reduction. Strong evidence for a hydride transfer mechanism, in which the substrate amine proton is in flight in the transition state for CH bond cleavage, comes from the deuterium multiple KIEs on the k_{red} value determined with both mutant enzymes. In the transition state for amino acid oxidation, substrate deuterium KIEs directly probe the status of the CH bond, whereas solvent deuterium KIEs report on the status of the substrate NH bond. The $^{\text{D}}k_{\text{red}}$ values are >4 in both enzymes, consistent with CH bond cleavage contributing to the transition state leading to amino acid oxidation. Similarly, $^{\text{D}_2\text{O}}k_{\text{red}}$ values >1 were determined with both mutant enzymes, suggesting that NH bond cleavage also contributes to the transition state for amino acid oxidation. With the Y53F enzyme, the $^{\text{D}, \text{D}_2\text{O}}k_{\text{red}}$ obtained with D-leucine in water and D-leucine- d_{10} in D_2O is 12, which is similar to, if not slightly larger than, the product of the individual substrate and solvent deuterium KIEs with a value of 9 (**Table 4.3**). With the Y249F enzyme, the $^{\text{D},$

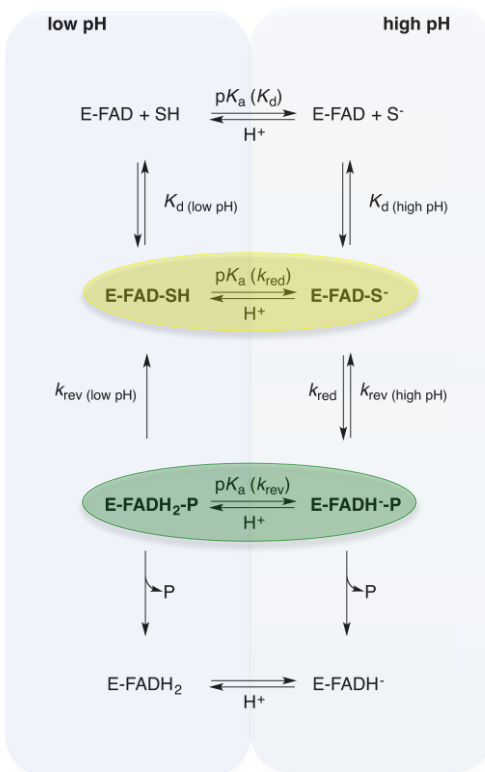
$^{D_2O}k_{red}$ is the same of the product of the individual KIEs, i.e., 5.7 vs. 6.1. This is consistent with the two bonds probed by the substrate and solvent KIEs being cleaved in concerted, synchronous fashion.³⁶ In contrast, a stepwise mechanism in which the two bonds are cleaved in two separate kinetic steps, such as in carbanion and polar nucleophilic mechanisms, is not consistent with the observed results because a multiple deuterium KIE significantly smaller than the product of the individual deuterium KIEs is expected in this case.³⁶ Consistent with a hydride transfer mechanism of reaction, QM/MM computations demonstrate that the flavin N5 atom accepting the hydride ion from the amino acid substrate is a better electrophile than the C4a atom, which has been proposed to be more reactive in other flavoprotein oxidases, such as monomamine oxidase.²¹

Despite Y53 is suitably positioned in the active site of the enzyme to deprotonate the substrate α -amine,^{13,22} this residue is not the catalytic base with pK_a of 9.6 that triggers the hydride transfer reaction to the flavin. Evidence in support of this conclusion comes from the reductive half-reaction determined with D-leucine as substrate, showing only a <3-fold decrease in the limiting value for k_{red} at high pH in the Y53F enzyme as compared to the wild-type. Although the limited stability of the mutant enzyme at pH >10.5 hampered an accurate determination of the pK_a value, the pH profile for k_{red} in the Y53F enzyme demonstrates that an unprotonated group is still required for flavin reduction. These results are consistent with Y53 not being the catalytic base in PaDADH. Similar conclusions are drawn for Y249 based on the results of the rapid reaction studies on the Y249F enzyme, showing a <3-fold decrease in the pH-independent k_{red} value at high pH and the presence of a pK_a similar to that of the wild-type enzyme for an unprotonated group required for catalysis. Thus, site-directed mutagenesis showed that neither tyrosine is responsible for the pK_a of 9.6 in wild-type PaDADH. Previous studies on wild-type PaDADH using molecular dynamics simulations showed that the pK_a of D-leucine increases upon binding to the enzyme, consistent with preferred binding of the zwitterionic form of the substrate.¹³ Since substrate deprotonation is required for the hydride transfer reaction, it is likely that the pK_a of ~10.0 seen in the pH profile of k_{red} for the Y53F enzyme, and 9.6 in the wild-type PaDADH, reflects the deprotonation of the amino acid substrate in the oxidized enzyme-substrate complex (**Scheme 4.3**). The alternate

possibility of H48 acting as catalytic base appears less likely, although it cannot be ruled out at this stage, because its side chain is separated by two intervening water molecules from the α -imine of the reaction product in the crystal structure of the enzyme in complex with iminoarginine.³⁷ The anionic form of the amino acid substrate as the productive species that undergoes oxidation was previously proposed for D-amino acid oxidase based on mechanistic, structural and computational studies.¹

The side chain hydroxyl of Y249 is not involved in substrate binding in wild-type PaDADH, as previously proposed based on its location in the crystal structure of the enzyme in complex with iminoarginine. Thus, the pK_a of 10.3 seen in the pH profile of the $^{app}K_d$ value previously reported for the wild-type enzyme is assigned to the substrate α -amino group (**Scheme 4.3**). Evidence for this conclusion comes from the pH profile of the $^{app}K_d$ value determined in a stopped-flow spectrophotometer for the Y249F enzyme, with a pH-independent $^{app}K_d$ value of 3.5 mM that is identical to that of the wild-type enzyme.¹³ Replacement of Y249 with phenylalanine results in a shift of the pK_a from 10.3 to 9.6, underlining the importance of establishing pH effects when comparing kinetic parameters of mutant and wild-type enzymes.³⁸ The Y53F enzyme also shows a perturbed pK_a for $^{app}K_d$, with a value of 9.0. Interestingly, substrate binding in the Y53F is 7-fold tighter than in the wild-type enzyme, as indicated by the pH-independent $^{app}K_d$ value of 0.5 mM compared to 3.5 mM at low pH. This may be the result of increased hydrophobic interactions between the benzene moiety of F53 and the hydrophobic side chain of D-leucine.

Conversion of the oxidized enzyme-amino acid complex to the reduced enzyme-imino acid complex in PaDADH becomes reversible upon removing the hydroxyl group from either Y53 or Y249. This is in contrast to the wild-type enzyme, for which irreversible flavin reduction was previously established.¹³ Evidence for reversible flavin reduction comes from the reductive half-reactions of the Y53F and Y249F enzymes with D-leucine at low pH, showing non-zero y -intercepts in the plots of the observed rates of flavin reduction (k_{obs}) as a function of the concentration of substrate. This behavior is observed over a limited pH range in the Y249F enzyme, i.e., 7.0 to 8.2, with the rate constant for the reverse of



Scheme 4.3 The reductive half-reaction catalyzed by the Y53F enzyme with D-leucine ^a

^aFAD, oxidized flavin; FADH⁻, anionic hydroquinone; FADH₂, neutral hydroquinone; SH, zwitterionic D-leucine; S⁻, anionic D-leucine; P, imino leucine product; yellow oval, enzyme-substrate complex; green oval, enzyme-product complex

the flavin reduction reaction (k_{rev}) becoming negligible compared to k_{red} , and therefore not amenable to measurement, as the pH increases >8.2. However, with the Y53F enzyme reversible flavin reduction is observed throughout the pH range from 7.0 to 10.5 used in the experiment, allowing for a mechanistic analysis of the reductive half-reaction in the latter mutant enzyme. Reversible flavin reduction in the oxidation of amino acids was previously reported in D-amino acid oxidase from *Trigonopsis variabilis* using *p*-substituted phenylglycine substrates and glycine oxidase from *Bacillus subtilis* with proline as substrate.^{3,39}

The k_{red} and k_{rev} values determined with the Y53F enzyme do not simply reflect the same kinetic step in the forward and reverse direction because if this were the case one would expect superimposable pH

profiles for $\log k_{\text{red}}$ and $\log k_{\text{rev}}$ according to the principle of microscopic reversibility. The minimal kinetic mechanism for the reductive half-reaction shown in **Scheme 4.3** is consistent with the observed results. At high pH, the Michaelis complex of the oxidized enzyme and anionic substrate is competent for the subsequent hydride transfer reaction. The resulting reduced enzyme-product complex then partitions between the (true) reverse of the flavin reduction step, yielding the initial oxidized enzyme-substrate complex, and the release of the reaction product from the reduced enzyme. Due to the high pH, the anionic hydroquinone is both the species that is formed in the k_{red} step and that goes through the k_{rev} step. At low pH, instead, the Michaelis complex involves the zwitterionic substrate, which is deprotonated within the oxidized enzyme-substrate complex to allow for the subsequent hydride transfer reaction. The enzyme-bound flavin in the resulting reduced enzyme-product complex is immediately protonated due to the low pH, presumably in a rapid equilibrium fashion. This yields a reduced enzyme-product complex of the neutral hydroquinone, which partitions between the reverse of the flavin reduction step and the release of the product from the reduced enzyme. In this case, however, conversion of the oxidized enzyme-substrate complex to the reduced enzyme-product complex and the opposite reaction do not proceed through the same pathway since in the former the substrate and reduced flavin are unprotonated and in the latter they are protonated (**Scheme 4.3**). The $\text{p}K_{\text{a}}$ of 9.1 that is established in the pH profile of k_{rev} is therefore assigned to the ionization of the flavin N1 atom in the reduced enzyme. For comparison, reduced FMN has $\text{p}K_{\text{a}}$ values between 5.8 and 7.0 when bound to flavodoxin from *Megaspahera elsdonii*, or *Desulfovibrio vulgaris*,⁴⁰ and 6.7 when free in solution,⁴¹ as previously established through optical or redox determinations.

4.7 Conclusions

In summary, through the use of mechanistic and computational approaches and site-directed mutagenesis we have demonstrated that the FAD-mediated oxidation of the substrate CN bond in PaDADH occurs via hydride transfer. The mutant enzymes lacking hydroxyl groups in the active site, which were engineered through mutagenesis of Y53 and Y249 to phenylalanine, stabilize transition states for the

amino acid oxidation reaction in which the substrate NH and CH bonds are cleaved in synchronous fashion. In contrast, the transition state is asynchronous in the wild-type enzyme, as previously reported.¹³ The change in the relative timing for NH and CH bond cleavage can be rationalized for a hydride transfer reaction, because removal of the protein hydroxyl groups would destabilize partial charge accumulation on the CN bond in the transition state. Both carbanion and nucleophilic mechanisms cannot be reconciled with the results of the mutant and wild-type enzymes unless one assumed that the removal of either protein hydroxyl group have a dramatic change in the mechanism of the reaction, which seems very improbable. A similar conclusion was proposed for flavocytochrome b2, based on mutagenesis and mechanistic studies using KIEs.⁴² Hydride transfer mechanisms have been recently discussed for D-amino acid oxidase and sarcosine oxidase,¹ which belong to the same structural family of D-arginine dehydrogenase. Thus, as more studies using mutagenesis, kinetic, structural and computational approaches are carried out evidence in favor of hydride transfer as the most likely mechanism for amino acid oxidation by flavoproteins is accumulating. PaDADH is further emerging as a model system along with the well-characterized D-amino acid oxidase^{1,7} for the study of flavin-dependent amino acid oxidation, as evidenced by the mechanistic and structural data from this and previous studies.^{13,14,37}

4.8 Acknowledgements

The authors would like to thank Lydia Law for the preparation of the Y249F mutant of PaDADH, Dr. Dale Edmondson, Dr. Elvira Romero, and Jacob Ball for critical reading of the manuscript. The authors would also like to acknowledge schrödinger IT for providing computational resources.

4.9 References

- (1) Fitzpatrick, P. F. *Arch. Biochem. Biophys.* 2010, 493, 13.
- (2) Ilari, A.; Bonamore, A.; Franceschini, S.; Fiorillo, A.; Boffi, A.; Colotti, G. *Proteins* **2008**, 71, 2065.
- (3) Job, V.; Marccone, G. L.; Pilone, M. S.; Pollegioni, L. *J. Biol. Chem.* **2002**, 277, 6985.
- (4) Khanna, P.; Schuman Jorns, M. *Biochemistry* **2001**, 40, 1441.

- (5) Leys, D.; Basran, J.; Scrutton, N. S. *EMBO J.* **2003**, 22, 4038.
- (6) Trickey, P.; Wagner, M. A.; Jorns, M. S.; Mathews, F. S. *Structure* **1999**, 7, 331.
- (7) Mattevi, A.; Vanoni, M. A.; Todone, F.; Rizzi, M.; Teplyakov, A.; Coda, A.; Bolognesi, M.; Curti, B. *Proc. Natl. Acad. Sci. U. S. A.* **1996**, 93, 7496.
- (8) Li, C.; Lu, C.-D. *Proc. Natl. Acad. Sci. U. S. A.* **2009**, 106, 906.
- (9) Li, C.; Yao, X.; Lu, C. D. *Microbiology* **2010**, 156, 60.
- (10) Yoshimura, T.; Esak, N. *J. biosci. and bioeng.* **2003**, 96, 103.
- (11) Lu, C. D. *Appl. microbiol. and biotechnol.* **2006**, 70, 261.
- (12) Morris, S. M. *J. Nutri.* **2004**, 134, 2743S.
- (13) Yuan, H.; Xin, Y.; Hamelberg, D.; Gadda, G. *J. Am. Chem. Soc.* **2011**, 133, 18957.
- (14) Yuan, H.; Fu, G.; Brooks, P. T.; Weber, I.; Gadda, G. *Biochemistry* **2010**, 49, 9542.
- (15) Stroud, E. D.; Fife, D. J.; Smith, G. G. *J. of Org. Chem.* **1983**, 48, 5368.
- (16) Porter, D. J. T.; Voet, J. G.; Bright, H. J. *J. Biol. Chem.* **1973**, 248, 4400.
- (17) Gadda, G.; Edmondson, R. D.; Russell, D. H.; Fitzpatrick, P. F. *J. Biol. Chem.* **1997**, 272, 5563.
- (18) Hamilton, G. A.; Brown, L. E. *J. Am. Chem. Soc.* **1970**, 92, 7225.
- (19) Walsh, C. T.; Krodel, E.; Massey, V.; Abeles, R. H. *J. Biol. Chem.* **1973**, 248, 1946.
- (20) Walsh, C. T.; Schonbrunn, A.; Abeles, R. H. *J. Biol. Chem.* **1971**, 246, 6855.
- (21) Edmondson, D. E.; Mattevi, A.; Binda, C.; Li, M.; Hubálek, F.; Abraham, D. J. In *Burger's Med. Chem. and Drug Disc.*; John Wiley & Sons, Inc.: 2003.
- (22) Fu, G.; Yuan, H.; Li, C.; Lu, C. D.; Gadda, G.; Weber, I. T. *Biochemistry* **2010**, 49, 8535.
- (23) Sastry, G. M.; Inakollu, V. S.; Sherman, W. J. *J. Chem. Info. and Model.* **2013**.
- (24) Maestro, version 9.6, Schrödinger, LLC: New York, NY, 2013.
- (25) BioLuminate, version 1.1, Schrödinger, LLC New York, NY, 2013.
- (26) SiteMap, version 2.9, Schrödinger, LLC: New York, NY, 2013.
- (27) QSite, version 6.1, Schrödinger, LLC: New York, NY, 2013.
- (28) Jorgensen, W. L.; Tirado-Rives, J. J. *J. Am. Chem. Soc.* **1988**, 110, 1657.

- (29) Kaminski, G. A.; Friesner, R. A.; Tirado-Rives, J.; Jorgensen, W. L. *J. of Phys. Chem. B* **2001**, 105, 6474.
- (30) Parr, R. G.; Szentpály, L. v.; Liu, S. *J. Am. Chem. Soc.* **1999**, 121, 1922.
- (31) Domingo, L. R.; Aurell, M. J.; Pérez, P.; Contreras, R. *J. of Phys. Chem. A* **2002**, 106, 6871.
- (32) Ayers, P. W.; Parr, R. G. *J. Am. Chem. Soc.* **2000**, 122, 2010.
- (33) Chattaraj, P. K.; Parr, R. G. In *Chemical Hardness*; Springer: 1993, p 11.
- (34) Pearson, R. G. *Proc. Natl. Acad. Sci. U. S. A.* **1986**, 83, 8440.
- (35) Strickland, S.; Palmer, G.; Massey, V. *J. Biol. Chem.* **1975**, 250, 4048.
- (37) Edmondson, D. E.; Gadda, G. In *Protein Engineering Handbook*; Wiley-VCH Verlag GmbH & Co. KGaA: 2008, p 1
- (36) Cleland, W. W. *CRC Crit. Rev. Biochem.* **1982**, 13, 385.
- (38) Pollegioni, L.; Blodig, W.; Ghisla, S. *J. Biol. Chem.* **1997**, 272, 4924.
- (39) Yalloway, G. N.; Mayhew, S. G.; Malthouse, J. P.; Gallagher, M. E.; Curley, G. P. *Biochemistry* **1999**, 38, 3753.
- (40) Draper, R. D.; Ingraham, L. L. *Arch. Biochem. Biophys.* **1968**, 125, 802.
- (41) Sobrado, P.; Fitzpatrick, P. F. *Biochemistry* **2003**, 42, 15208.

5 BIOCHEMICAL AND STRUCTURAL CHARACTERIZATION OF GREEN FLAVIN FROM MUTANT VARIANT OF D-ARGININE DEHYDROGENASE

(This chapter also has contributions by Dr. Alexander Spring (NMR), Dr. Sarah Sirin (computational analysis))

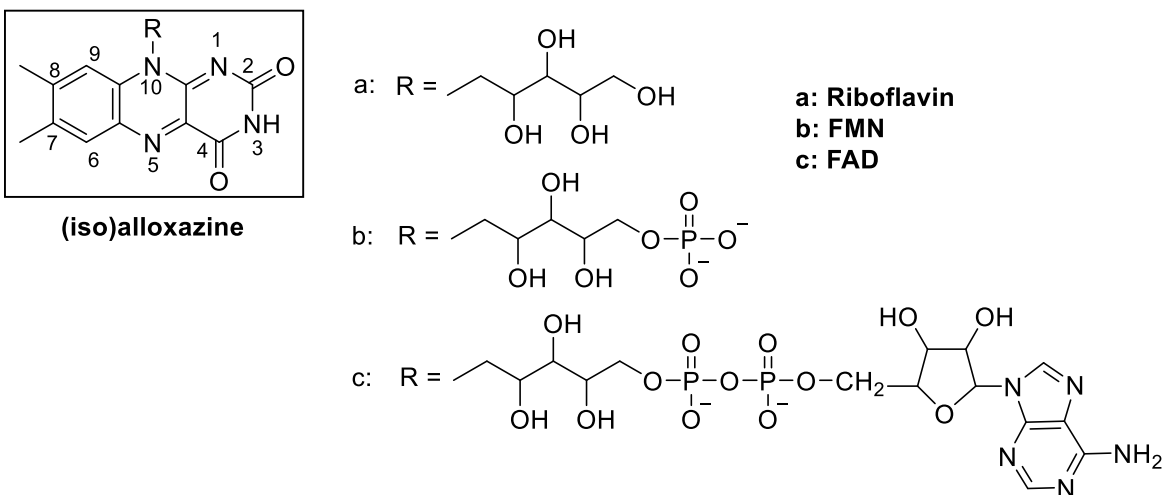
5.1 Abbreviations

DADH, D-arginine dehydrogenase; TMAD, Trimethylamine dehydrogenase; AMID, apoptosis-inducing factor-homologous mitochondrion-associated inducer of death; TCA, trichloroacetic acid; TFA, trifluoroacetic acid;

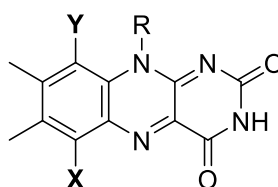
5.2 Introduction

Flavin adenine dinucleotide and flavin mononucleotide (FMN) are vitamin B₂ derived cofactors that are incorporated into many enzymes for catalytic activity (**Scheme 5.1**). Flavoenzymes are yellow in color and are found to be involved in multitude of reactions ranging from cell growth, DNA repair, apoptosis, etc.¹ The reactive center of flavins is the conjugated-aromatic (iso)alloxazine ring system (**Scheme 5.1**). The (iso)alloxazine moiety is formed by the fusion of xylene, pyrazine and pyrimidine rings. This configuration confers chemical versatility to flavins which is further fine-tuned by the protein active site allowing the isoalloxazine to participate in one or two electron redox reactions. The spectral properties and reactivity of flavins are greatly affected when functional groups like CH, OH, SH, NH₂, SCN, Cl, and Br were introduced synthetically to different sites, including N1, O2, O4 N5, C6, C7, C8, C9 and N10, of the (iso)alloxazine ring. These synthetic modified flavins were used as probes to elucidate chemical mechanisms of flavoenzymes.²⁻⁸ Around that time, the first instance of a natural modification on the (iso)alloxazine – was reported in two enzymes in 1974 by Ghisla *et.al*. One is the native electron transferring flavoprotein from bacterial, *Peptostreptococcus elsdenii* with a modification of the FAD cofactor at the 6th

position on the (iso)alloxazine by a hydroxyl functional group (**Scheme 5.2**). The same modification on the FMN cofactor was also reported in pig liver glycolate oxidase.⁹ Since then, there have been other reports of hydroxylated flavins at the 6th position in a variety of aerobic and anaerobic, as well as prokaryotic and eukaryotic organisms (**Table 5.1**). In general the flavin cofactors in these enzymes were partially hydroxylated and the hydroxylated flavin – enzyme complex was reported to be catalytically inactive. The functional relevance of this partial hydroxylation however remains to be discerned.



Scheme 5.1 Chemical structure of flavins



X = OH, SH, N₃; **Y** = H

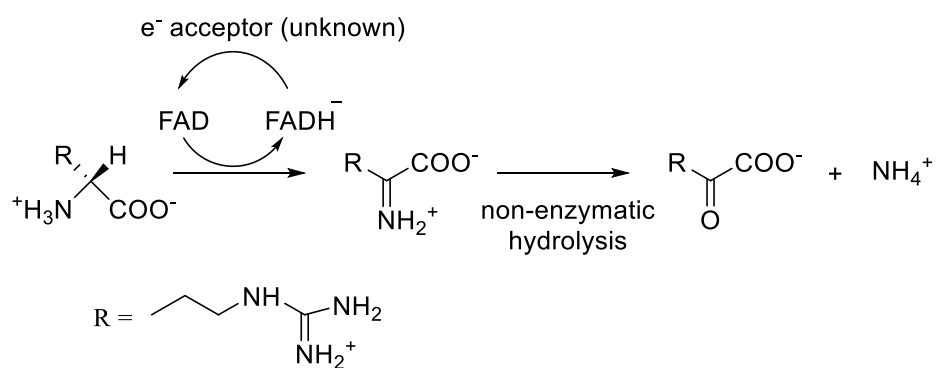
Y = OH; **X** = H

Scheme 5.2 Some modifications of the (iso)alloxazine moiety resulting in long wavelength absorbance and green coloration.

Note that the 'R' functional group is the same as seen in **Scheme 5.1**.

In the current study, mutagenesis work on recombinant D-arginine dehydrogenase isolated from *Pseudomonas aeruginosa* resulted in a variant enzyme with similar characteristics described in other enzyme systems summarized in Table 5.1.¹⁰ The wild-type enzyme is mainly involved in the oxidation of D-arginine, while displaying broad substrate specificity for other neutral and hydrophobic D-amino acids (**Scheme 5.3**).^{11, 12} Crystallographic and mechanistic data of the wild-type enzyme suggested that several active site residues might engage in important polar and non-polar interactions for facilitating D-amino acid oxidation by the FAD cofactor.^{11, 13-15} One such interaction that is part of the proposed binding pocket involving Y249, R222 and R305, is the polar interaction between the phenolic oxygen atom of Y249 and the carboxylate moiety of the imino product, which is conserved across the different enzyme-imino product complexes.^{11, 13} Mutagenesis of Y249 to phenylalanine resulted in a variant enzyme that could be differentiated into yellow and green fractions. The yellow fraction retained the activity of the wild-type enzyme and has been characterized for its role in amine oxidation (Chapter 4), while the green fraction had spectral properties similar to that previously reported for other enzymes (**Table 5.1**). Notwithstanding, studies of synthetic flavins with modifications made at the 6th or 9th positions of the (iso)alloxazine with either OH, SH, N₃ have also been shown to have very similar spectral properties.^{4, 7} Therefore, in the current study the green fraction from DADH-Y249F enzyme was subject to further biochemical and computational characterization.

Here, we used a combination of UV-visible absorbance spectroscopy, liquid chromatography, ¹H, and ¹³C NMR, mass spectrometry approaches to unequivocally establish the site and functional group involved in the modification of the cofactor. Furthermore, computational approaches were employed to gain insights about the novel-cofactor isolated from PaDADH at the molecular level.



Scheme 5.3 General reaction mechanism of PaDADH.

Table 5.1 Enzymes with 6 OH flavins.

Enzyme	Native/ recombinant	Source	Type	Cofactors	Activity of 6-OH-Flavin	Year
Electron-transferring flavo- protein (ETF) ²	Native	<i>Peptostreptococcus elsdenii</i>	Bacterial (Gram- positive anerobic)	FAD & 6-OH-FAD	Inactive	1974
Glycolate oxidase ²	Native	Pig liver	Mammalian	FMN & 6-OH-FMN	Inactive	1974
D-aspartate oxidase ¹⁶	Native	Beef Kidney	Mammalian	FAD & 6-OH-FAD	Inactive	1987
D-aspartate oxidase ¹⁷	Native	<i>Octopus vulgaris</i>	Molluscan	FAD & 6-OH-FAD	Inactive	1994
Cellobiose dehydrogenase ¹⁸	Native	<i>Humicola insolens</i>	Fungal	Heme, FAD & 6- OH-FAD	Partially active	1999
Cellobiose quinone dehydro- genase ¹⁹	Native	<i>Sporotrichum pulverulentum</i>	Fungal	FAD & 6-OH-FAD	Partially active	1986
TMAD ²⁰	Native	Methylophilus methylotrophus	Bacterial	Fe-S cluster, FMN & 6-OH-FMN	Inactive	1997
TMAD ²⁰	Recombinant	Methylophilus methylotrophus	Bacterial	Fe-S cluster, FMN & 6-OH-FMN	Inactive	1997
TMAD W355L ²⁰	Recombinant	Methylophilus methylotrophus	Bacterial	Fe-S cluster, FMN & 6-OH-FMN	Inactive	1997
^a TMAD C30A ^{21, 22}	Recombinant	Methylophilus methylotrophus	Bacterial	Fe-S cluster, FMN	Inactive ^a	1996
^b AMID ²³	Recombinant	<i>Homo sapiens</i>	Mammalian	6-OH-FAD	Active	2005

^a6 -OH FMN is formed during turnover with excess substrate (trimethylamine or dimethylamine)

^bapoptosis-inducing factor-homologous mitochondrion-associated inducer of death

5.3 Experimental Procedures

Materials

Rosetta(DE3)pLysS, an expression strain of *E.coli* was purchased from Novagen (Madison, WI). BSA and MgCl₂ were obtained from Promega (Madison, WI). QIAprep Spin Miniprep kit has been obtained from Qiagen (Valencia, CA), QuickChange site-directed mutagenesis kit has been obtained from Stratagene (La Jolla, CA), oligonucleotides for site-directed mutagenesis and sequencing of the mutant genes were obtained from Sigma Genosys (The Woodlands, TX). D-Arginine, Luria-Bertani agar, Luria-Bertani broth, chloramphenicol, IPTG, lysozyme, sodium hydrosulfite (dithionite), Phenazine methosulfate (PMS) and phenylmethanesulfonyl fluoride (PMSF) have been purchased from Sigma-Aldrich (St. Louis, MO). D-Leucine has been obtained from Alfa Aesar. The mutant of DADH-Y249F has been prepared and expressed as described previously. The un-tagged mutant enzyme was purified using the protocol described for wild-type enzyme involving a DEAE-Sepharose Fast Flow column. All other reagents used were obtained in their highest purity commercially available.

Reverse-phase HPLC

The cofactors from DADH-Y249F were extracted by acid precipitation using 10% trichloroacetic acid stock at a final concentration of 7% in the sample mixture. The reaction was allowed to proceed for 30 min on ice-bath and in dark and the sample was centrifuged at 10,000 X g rpm for 10 minutes. The supernatant which was at a pH \leq 1 was yellow and the process as stated above was repeated one more time on the pellet to ensure maximal extraction of the chromophores from the enzyme. The supernatant was retained for further purification using SCL-10A VP SHIMADZU reverse-phase HPLC capable of diode array detection. The stationary phase was μ Bondapak C18

column (15 cm x 4.6 mm) and the mobile phase was H₂O + 0.01% TFA as solvent A and 5% acetonitrile + 0.01% TFA as solvent B. Blank run was performed at a 5 to 100% gradient of solvent B from 0 to 60 min and at 100% B for 10 min to ensure the column is free of any debris from the previous runs. The C18 column was then equilibrated in 5% solvent B prior to loading a sample volume of 1.4 mL onto it via a 2mL sample loop. The elution conditions are the same as the blank run and the flow rate for all runs was 0.5 mL/min. Wavelengths of 446 and 421 nm were monitored for FAD and the modified cofactor.

¹H and ¹³C NMR Studies

NMR experiments were conducted on a Bruker Avance 600 MHz spectrometer equipped with a 5 mm QXI ¹H (³¹P, ¹³C, ¹⁵N) probe (Bruker). 1D ¹H spectra were collected using the watergate W5 pulse sequence for water suppression (Liu, 1998). A 100 ms mixing time was used for TOCSY spectra. Heteronuclear ¹H-¹³C HSQC spectra were processed with a shifted squared sine bell multiplication in both dimensions (SSB=2). For all NMR experiments, samples were prepared in 10 mM sodium phosphate (pH 7.0) and referenced to 4,4-dimethyl-4-silapentane-1-sulfonic acid (DSS) at 25 °C, unless otherwise stated. Sample concentrations of HPLC purified modified FAD and FAD varied based on purification yields but generally ranged from 15 to 30 μM for the modified FAD and 100 μM for FAD samples; synthesized FAD and 6-OH-FAD sample concentrations were 300 μM.

Mass Spectrometry

Molecular mass of the cofactors was analyzed using mass spectrometry in the negative electrospray ionization (ESI) mode at the Mass Spectrometry Laboratory of the Georgia State University. The samples retrieved from NMR analyses were passed through HPLC to eliminate the high salt and the DSS reference added to the samples. Accurate mass analysis was carried out using a Thermal Fisher Orbitrap Elite mass spectrometer equipped with ESI source in negative ion mode. The samples were analyzed with an LC-MS profile without the use of column. The sample was eluted isocratically with 20% ACN in H₂O and 0.1% HCOOH at a flow rate of 8 μ L/min.

Spectroscopic Studies

The modified cofactor extracted from DADH-Y249F by TCA precipitation and purification using HPLC as described in the previous sections was subjected to SpeedVac for \sim 14 hours to remove the acetonitrile-H₂O mixture from the sample. The powder was resuspended in 20 mM sodium phosphate and -20 mM sodium pyrophosphate buffer at pH 6.0. The concentration of the purified 6-OH-FAD cofactor was calculated using the extinction coefficient of 19.6 mM⁻¹cm⁻¹ at 422 nm at pH 5.6 for free 6-OH-FAD.⁹ The effect of pH on the absorbance spectra of the buffered 6-OH FAD was measured by titration with 0.5 M KOH at 15 °C.

The reactivity of enzyme bound 6-OH-FAD was measured spectroscopically by monitoring the absorbance change between 500-800 nm regions. The concentration of 6-OH-FAD was calculated using the extinction coefficient for free 6-OH-FAD.⁹ The fraction of DADH-Y249F containing FAD and 6-OH-FAD as cofactors was allowed to react with 1mM D-arginine and 13 mM D-leucine in 20 mM Tris-HCl, pH 8.7 at 25 °C.

Data Analyses

Data from UV-visible spectroscopy, NMR studies, mass spectrometry were analyzed using Xcalibur 2.2. softwares and KaleidaGraph software (Synergy Software, Reading, PA). Schemes 1, 2 and 3 were generated using CambridgeSoft ChemBioDraw from PerkinElmer.

The pH dependence of absorbance at 585 nm for purified 6-OH-FAD from DADH-Y249F was fit to equation 1, where C_L and C_H represent pH independent limiting values for the absorbance at 585 nm at low and high pH respectively.

$$Abs_{585\text{ nm}} = \frac{C_L + C_H}{1 + 10^{pKa - pH}} \quad (1)$$

5.3.1 Computational Methods

The computational models were based on the X-ray crystal structure of DADH (PDB accession code: 3NYC). All missing side chains and hydrogen atoms were added using Protein Preparation Wizard.²⁴⁻²⁷ Protonation states of ionizable amino acid side chains were determined using PROPKA²⁸ and hydrogen bond networks were subsequently optimized via restrained energy minimization. Residue scanning module of BioLuminate,^{29, 30} which uses a rotamer library in Prime³¹ for side-chain sampling and the VSGB2.0³²⁻³⁴ implicit solvent model with the OPLS2005³⁵⁻³⁷ force field for energy evaluations, was used to generate DADH-Y249F variant. For both wild type and Y249F variants, FAD molecule was modified to its 6-OH-FAD form. The resultant 4 models were geometry optimized using Prime with OPLS2005 force field and VSGB solvent model. Sitemap³⁸ was used to characterize the active sites of the generated DADH variants. Watermap³⁹ was used to calculate the properties, such as location, free energy, enthalpy, and entropy, of structural waters within the binding cavity through a combination of molecular dynamics, solvent clustering, and statistical thermodynamic analysis. Each model was optimized using QSite⁴⁰, in which the QM region was described using B3LYP/6-31G* and included (iso)alloxazine

ring of bound FAD. Local electrophilicity flavin was calculated using as described earlier in Chapter 4.

5.4 Results

Purification and Spectral Properties of DADH-Y249F

Purification of DADH-Y249F enzyme was carried out using the protocol for wild-type enzyme and 10% glycerol was included in all steps of the purification to minimize the loss of non-covalently bound cofactor. The enzyme loaded on a DEAE sepharose column had two distinct bands, a green band and below it, a yellow band, in 20 mM Tris-HCl at pH 8.0. This yellow portion eluted first under the gradient of a high salt buffer (20 mM Tris-HCl + 500 mM NaCl, pH 8). The enzyme was collected in two major fractions, which were a predominant yellow and a green fraction. The absorption spectrum of the yellow fraction was identical to wild type, suggesting that this fraction is enriched with unmodified FAD (**Figure 5.1**). The chromophore of green fraction showed broad absorption at the long wavelengths between 500 to 800 nm. Additionally, the peaks at 450 to 370 regions for FAD were blue shifted by about 30 to 40 nm for the green chromophore. The yellow fraction had apparent kinetic properties very similar to the wild-type enzyme (Refer to Chapter 4). Full separation of the enzyme bound green chromophore from the yellow fraction was not achieved and as a result activity assay on the oxygen electrode using PMS as *in vitro* electron acceptor used for yellow fraction of DADH-Y249F was not useful in this case.

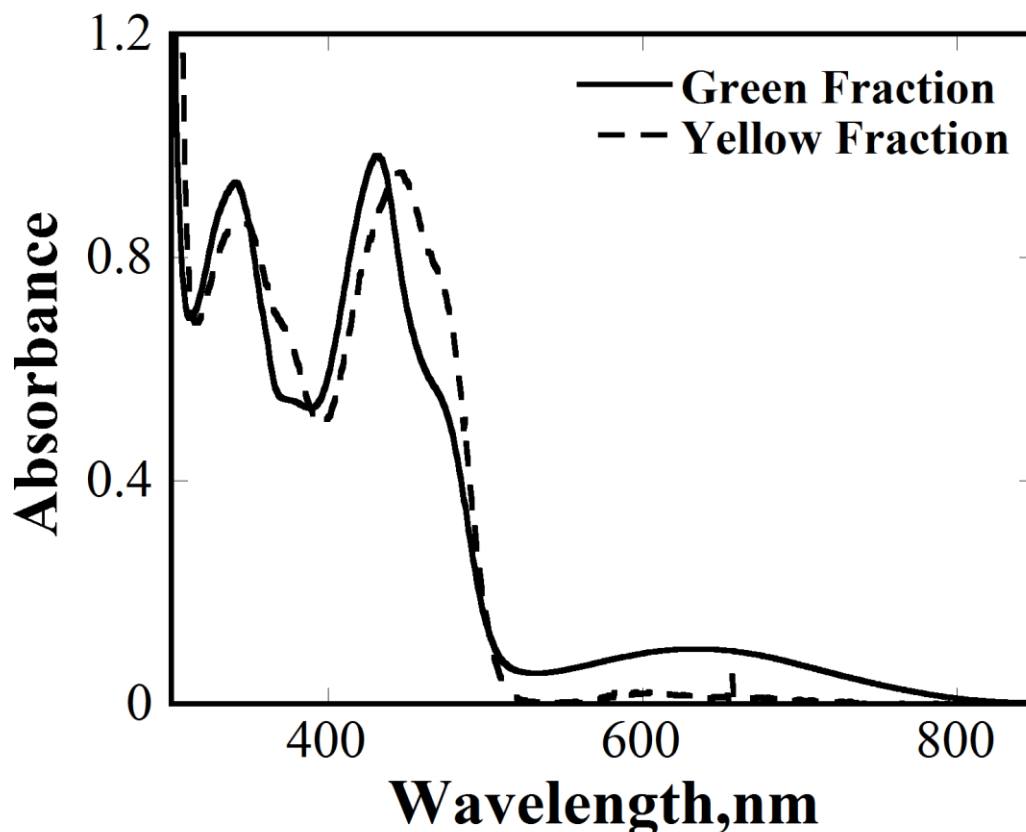


Figure 5.1 UV-visible absorbance spectrum of green and yellow fractions. The dashed curve represents the spectrum of the fraction of DADH-Y249F enriched predominantly by the green chromophore after DEAE-Sephacrose fractionation with peaks at 340, 430 and ~625 nm; the solid curve represents the spectrum of DADH-Y249F enriched by FAD as cofactor with peaks at 346 and 446 nm. The conditions at which either spectrum were recorded are 20 mM Tris-HCl + 10% glycerol, pH 8.7 at 22 °C. At the same conditions the wild-type had peaks at 370 and 447 nm.

Isolation of Chromophores from PaDADH-Y249F

In order to establish the identity of the green chromophore from PaDADH-Y249F, the cofactor was extracted from the enzyme and purified for further characterization. The enzyme was subjected to acid precipitation using TCA to isolate the cofactor (see Methods for details). The extracted green cofactor was separated from FAD using reverse-phase HPLC: FAD eluted first

with a retention time (t_R) of ~21 minutes as judged by the UV-visible absorbance spectrum (**Figure 5.2, B**). The second chromophore eluted in two peaks with retention times starting approximately at 22 and 24 minutes. The first fraction contained trace amount of FAD while the second fraction was well separated (**Figure 5.2, A**). The pH of the cofactor samples was around 1 due to the presence of TFA and all samples collected were yellow. On adjusting the pH close to 7, the spectral properties of FAD remained unchanged, however, the spectrum of the other cofactor changed as seen in **Figure 5.2A, inset**. The color of the sample also changed from yellow to pale green. The absorbance spectrum of the cofactor at neutral pH had peaks at 325, 427 and ~600 nm, and resembled that of modified FAD chromophore with a hydroxylation at the 6th position of the (iso)alloxazine ring moiety.^{4, 7, 9} However, hydroxylation at the 9th position of the (iso)alloxazine is also characterized by broad absorbance in the 500 to 800 nm region with additional peaks at 440 and 332 nm.⁷ So we had to further examine and establish whether the collected sample was hydroxylated at the 6th or the 9th position.

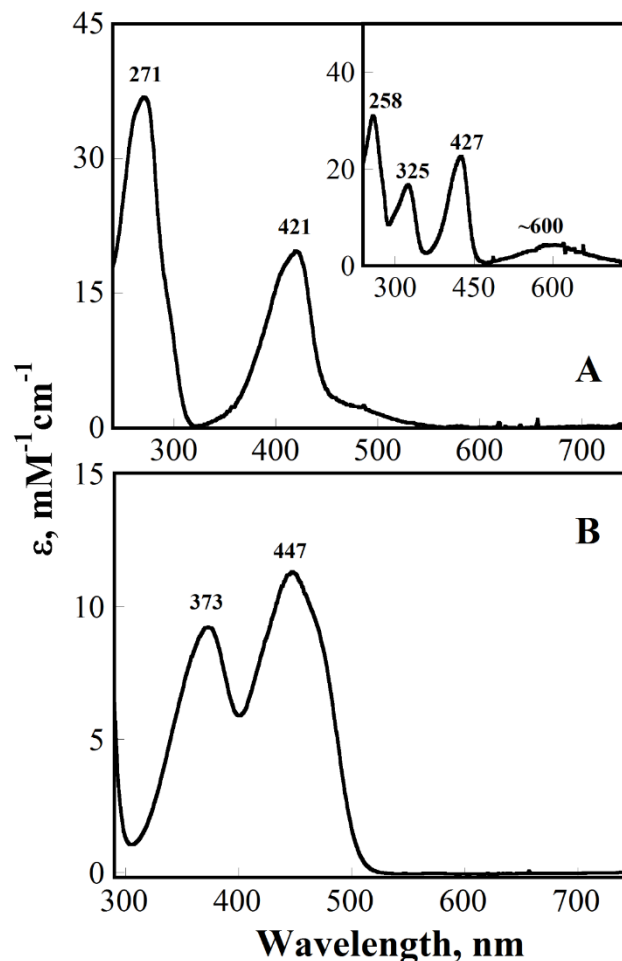


Figure 5.2 UV-visible absorbance spectrum of chromophores obtained from HPLC. Panel A: spectrum of modified FAD with a retention time of ~ 24 min on the C18 column at pH of 1.0 and inset shows the spectrum of the same sample after the pH has been adjusted to 7.5. Panel B: spectrum of FAD after elution from the C18 column with a retention time of ~ 21 min. Both chromophore samples contained 0.1% trifluoro acetic acid and \sim acetonitrile at a pH of 1.0 following HPLC purification.

¹H and ¹³C-NMR Analyses of the Purified Chromophores from DADH-Y249F

The extracted and purified chromophores were analyzed using NMR to directly establish the hydroxylation site on the (iso)alloxazine ring. Published NMR spectra of FAD were used to

determine the peak assignment of the purified FAD samples and they were compared to control samples of similarly treated commercially obtained FAD (Biological Magnetic Resonance Data Bank). As expected, the (iso)alloxazine ring protons for the unmodified FAD at positions 6 and 9 were easily identified at 7.62 and 7.85 ppm, respectively and matched the published spectra.

The aromatic region of the purified modified-FAD sample from DADH-Y249F and synthesized 6-OH-FAD exhibit identical major resonances. The major difference between the modified and native FAD spectra is the lack of an aromatic proton resonance. The three resonances of the modified sample correlate to the adenosine 2 and 8 protons and the remaining (iso)alloxazine proton. **(Figure 5.3)** It is anticipated that adenine at the 2nd and 8th positions will not exhibit large chemical shift perturbations due to the (iso)alloxazine hydroxyl modification; comparison of the HSQC spectra of the synthesized 6-OH -FAD and FAD reveal that the adenine 2 and 8 protons are indeed not impacted by the modification, indicating the 3rd aromatic resonance belongs to the (iso)alloxazine proton. To further verify the remaining aromatic resonance as the (iso)alloxazine proton, a TOCSY spectrum was used to identify coupling between the (iso)alloxazine proton and the methyl group. Coupling was observed between the remaining aromatic peak at 6.75 ppm and a methyl resonance at 2.42 ppm allowing for the unambiguous determination that the remaining aromatic resonance is the remaining (iso)alloxazine proton. **(Figure 5.4)** Lastly, in order to determine the sample's identity as 6-OH-FAD, the isoalloxazine methyl groups' chemical shifts were used to characterize the (iso)alloxazine hydroxylation pattern. Previous studies of (iso)alloxazine ring system substitutions found that the methyl resonances at positions 7 and 8 are sensitive to hydroxylation at positions 6 and 9 and exhibit different changes in chemical shifts as a result of the hydroxyl additions. This trait can be used to characterize the hydroxylated (iso)alloxazine ring system.² The observed difference of 0.23 ppm between the two methyl groups is consistent with

hydroxylation at the 6th position establishing the (iso)alloxazine substitution as a 6-OH modification (**Figure 5.4**).

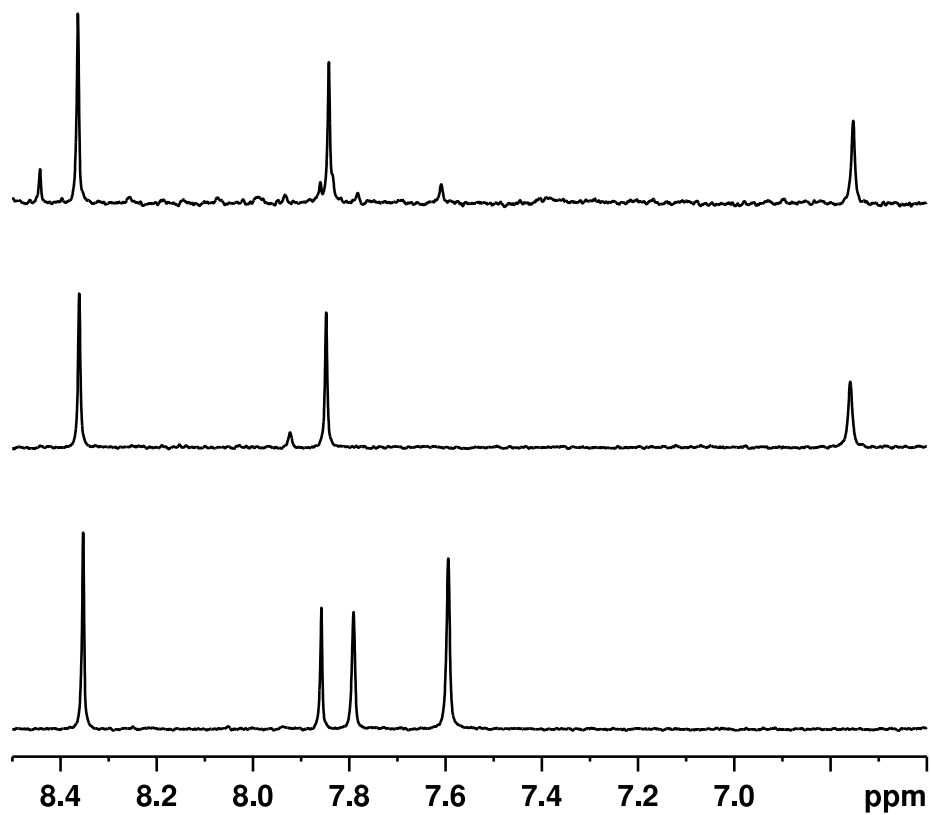


Figure 5.3 ¹H NMR of bottom = FAD, middle = synthesized 6-OH-FAD, top = HPLC purified 6-OH-FAD.

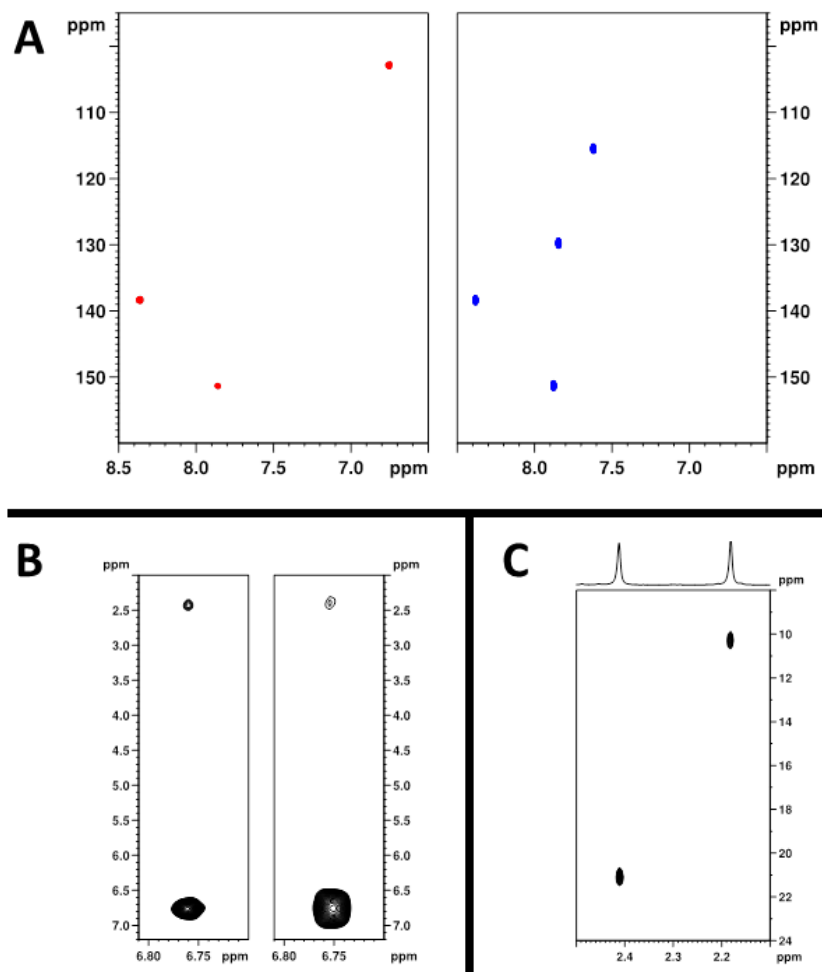


Figure 5.4 A) HSQC spectra of aromatic regions of synthesized 6-OH (left) and FAD (right). B) slices from TOCSY spectra showing coupling between position 9 of the (iso)alloxazine ring and the adjacent methyl protons (left synthesized, right HPLC purified). C) HSQC spectrum of 6-OH-FAD methyl protons. Separation between methyl protons is 0.24 ppm.

Mass Spectrometry of the Purified Chromophores from DADH-Y249F

Mass spectrometry analyses were carried out on the FAD and the modified FAD chromophores extracted from PaDADH-Y249F as well as the standard 6-OH-FAD in order to establish the molecular weight of the modified FAD chromophore from PaDADH-Y249F. The m/z of FAD

analyzed in the ESI negative mode was 784.2 (data not shown), which agrees well with the molecular weight of 785.5 Da for the FAD cofactor. Modified FAD and the standard 6-OH-FAD analyzed in the same conditions had m/z of 800.1, which corresponds to a molecular weight of 801 Da (**Figure 5.5**). The difference in molecular weight between the FAD and the modified FAD cofactor is 16 Da, which corresponds well with the addition of $-OH$ functional group.

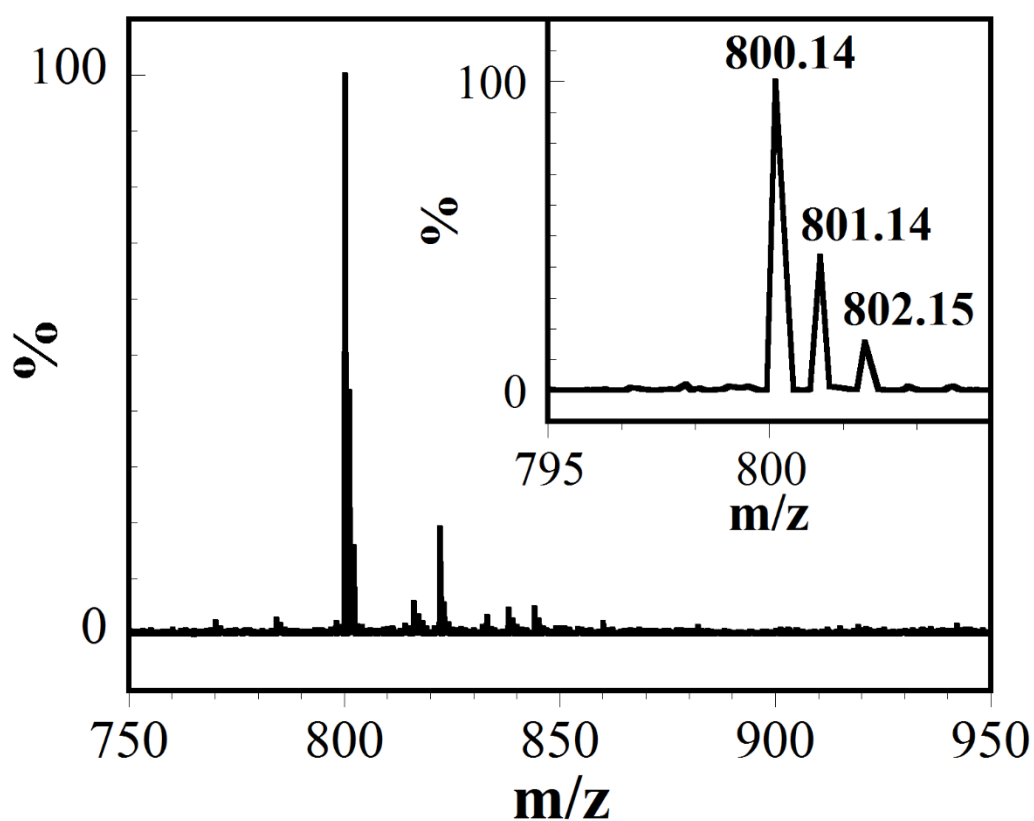


Figure 5.5 Negative ion ESI mass spectrum of the modified flavin isolated from DADH-Y249F enzyme. The peak at m/z 800.14 corresponds to the $(M-H)^{1-}$ ion expected for OH-FAD. Inset shows an expansion of the $(M-H)^{1-}$ ion region (m/z 795-805) of the mass spectrum.

Determination of Ionizable groups on Modified FAD from PaDADH-Y249F

pH titration of the extracted and purified hydroxylated FAD chromophore from PaDADH-Y249F was performed to establish the ionization state of the hydroxyl group from pH 6.0-8.0. HPLC purified samples of modified FAD at pH 1.0 and 7.0 showed distinct spectral properties and visible difference in colors suggesting that the hydroxyl group may ionize with a $pK_a \leq 7$ (**Figure 5.2A**). The pH titration (see Methods for details) showed evolution of absorbance in the long wavelength region between 500-800 nm with a peak around 585 nm. This absorbance increased between pH 6.0 to 8.0 and remained constant at pH > 8. The plot of absorbance at 585 nm as a function of pH indicates a pK_a of 7.1 (**Figure 5.6**), consistent with that published previously for the free 6-OH-FAD.⁹ pH titration of 6-OH-FAD bound to PaDADH was not possible, due to the instability of the enzyme at pH ≤ 6 . However, the spectrum of the enzyme fraction containing 6-OH-FAD alongside FAD at 6.5 still showed the presence of broad absorbance (data not shown) in the long wavelength region suggesting the perturbation of the pK_a to a lower value due to interaction with active site residues.

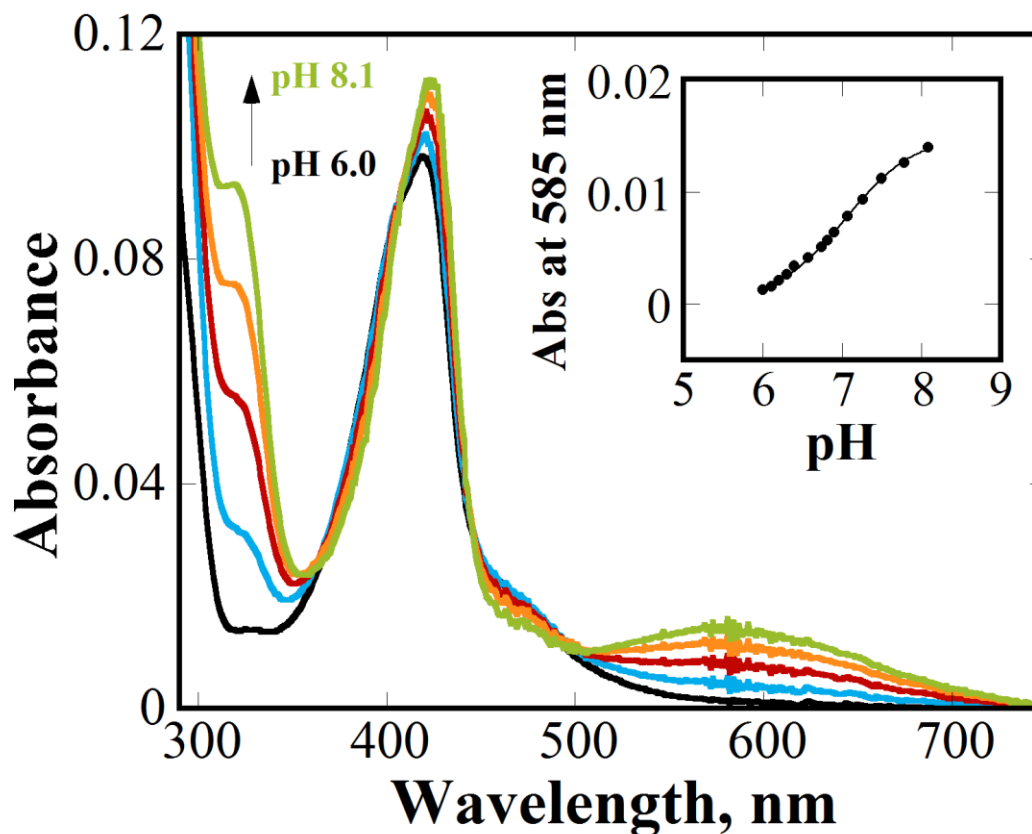


Figure 5.6 pH titration of 6-OH-FAD extracted from DADH-Y249F. Selected UV-visible absorbance spectra of the 6-OH FAD starting at pH 6.0 raised to 8.0 with the addition of increments of 0.5M potassium hydroxide resulting in the evolution of broad peak at the 500-800 nm region. Inset shows the plot of absorbance at 585 nm as a function of pH between 6-8 resulting in a pK_a of 7.05 ± 0.02 for the deprotonation of the hydroxyl group attached at the 6th position of the (iso)alloxazine moiety. A mixed buffer system of 20 mM sodium phosphate and sodium pyrophosphate with starting pH at 6.0 was used at 25 °C.

Biochemical Reactivity of Enzyme Bound 6-OH-FAD

Previous studies have shown that enzyme bound 6-OH-flavin is inactive with some exceptions.^{8, 9, 16-21, 23} Here, fraction of PaDADH-Y249F with FAD retained wild-type activity, which

was further investigated in the study addressing the role of Y249 in substrate binding and amine oxidation (Chapter 4). The reactivity of enzyme bound 6-OH-FAD in the current study was monitored by observing spectral changes in the long wavelength region between 580-800 nm that is unique to 6-OH-FAD on reaction with either D-arginine (native substrate) or D-leucine (slower substrate for catalysis). The fraction of PaDADH-Y249F with unmodified-FAD reacted instantly with either D-arginine or D-leucine as measured by the change in absorbance spectra around 446 nm regions, while no such observable changes were apparent in the 500-800 nm regions for the sample with 6-OH modified FAD (**Figure 5.7**). The absorbance in the long wavelength region was fully quenched in about one hour using D-arginine as substrate, while using the catalytically poor substrate, D-leucine, the absorbance of 6-OH-flavin in the long wavelength region did not change even after three hours of incubation (**Figure 5.7**). These observations suggest that enzyme bound FAD and 6-OH-FAD react at different time scales in PaDADH-Y249F irrespective of the substrate used.

Computational Analyses

In addition to the biochemical characterization, we also generated an *in silico* model of PaDADH-Y249F mutant in an effort to gain structural insights into this partial hydroxylation behavior (see Methods section for details). **Figure 5.8** shows optimized models of the wild-type PaDADH (**Figure 5.8a**) and the Y249F mutant (**Figure 5.8b**). These two models were used as starting structures to generate models of hydroxylated flavin at the C6 position (**Figures 5.8c** and **5.8d**, red arrow). Hence, the four optimized models of DADH were used to access DADH active site and FAD reactivity, in an effort to gain insight into the differential hydroxylation behavior observed experimentally.

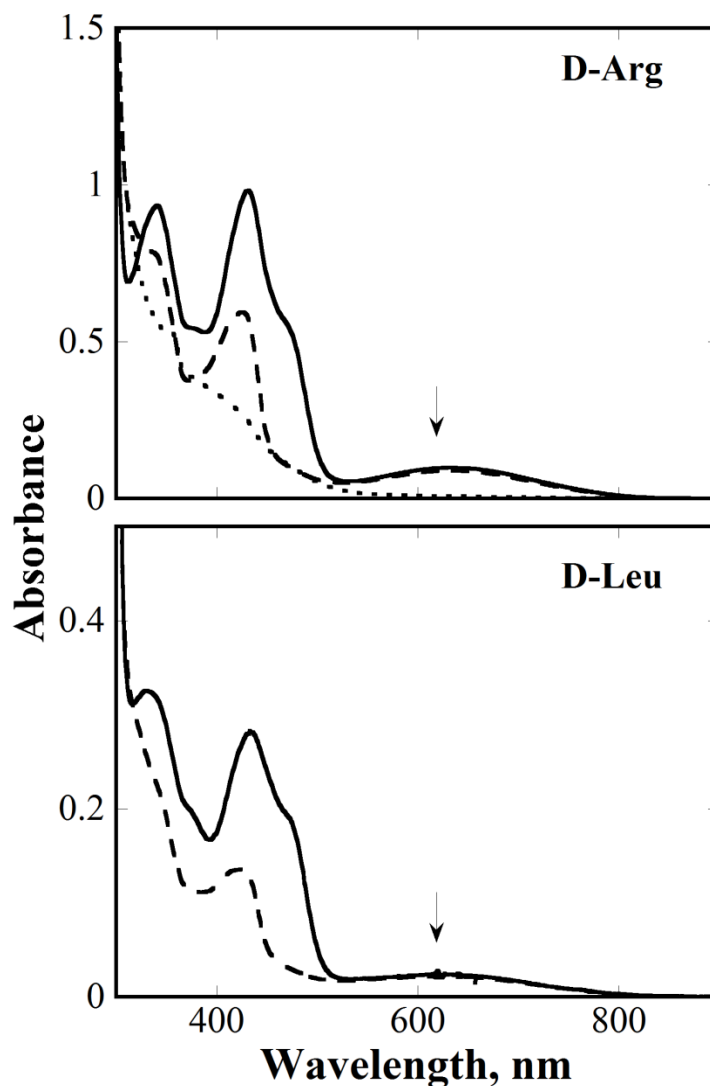


Figure 5.7 Biochemical reactivity of DADH-Y249F bound FAD and 6-OH-FAD. First panel shows the spectrum of enzyme bound FAD and 6-OH-FAD fraction before the addition of substrate in black solid curve, dashed spectrum represents seven minutes after reaction of $\sim 27 \mu\text{M}$ of 6-OH-FAD enzyme with 1 mM D-arginine, and dotted curve represents the spectrum after ~ 50 minutes of reaction with the substrate; the second panel shows the spectra of the reaction of enzyme bound FAD and 6-OH-FAD with a catalytically slower substrate, D-leucine. The black solid curve represents the spectrum of the enzyme ($\sim 6.7 \mu\text{M}$) before reaction with substrate while the dashed curve represents the spectrum of the enzyme 3 hours after reaction with 13 mM D-leucine

with 6-OH-FAD enzyme concentration at $\sim 6.2 \mu\text{M}$. The two reactions were carried out in 20 mM Tris-HCl at pH 8.7 and 25 °C.

We used site-map to characterize and subsequently visualize any changes introduced to DADH active site upon Y249 to phenylalanine mutation in addition to the hydroxylation of FAD at C6 position, see **Figure 5.9**. While these small perturbations did not alter the active site significantly, Y249F mutation results in the loss of a hydrogen bond donor and changes the local cavity near this residue (as expected). In the X-ray crystal structure, Y249 side chain forms a hydrogen bond with the carboxyl group of imino-arginine product. If one assumes that the substrate binds with a similar geometry, this could help orient the substrate in a reactive geometry. The hydroxylation of FAD at C6 position is effectively introducing a hydrogen bond donor and leads to the formation of a hydrogen bond donor region directly above the reactive N5 nitrogen, while the cavity about N5 region is characterized as having hydrogen bond donor character when FAD is not modified.

Subsequently, hydration sites were characterized for wild-type and Y249F DADH variants (in addition to the hydroxylated models) using WaterMap (see Methods section for details). Three similar hydration sites were identified in all four models that, when occupied by waters, could serve as the site of hydroxyl donor (**Figure 5.10**). In the wild-type DADH, hydration site # 1 (indicated using red arrow) has an overall energy of 5.4 kcal/mol, and this site is destabilized (by about 4.2 kcal/mol) in the Y249F mutant to a final energy of 9.6 kcal/mol. This ground state destabilization could help explain the differential hydroxylation of FAD in Y249F mutant relative to wild-type enzyme variant. Furthermore, the local electrophilicity index for N5 nitrogen decreased

about 5 percent in Y249F DADH with 6-hydroxyl-flavin, while this electrophilicity index remained constant for Y249F variant relative to wild-type DADH.

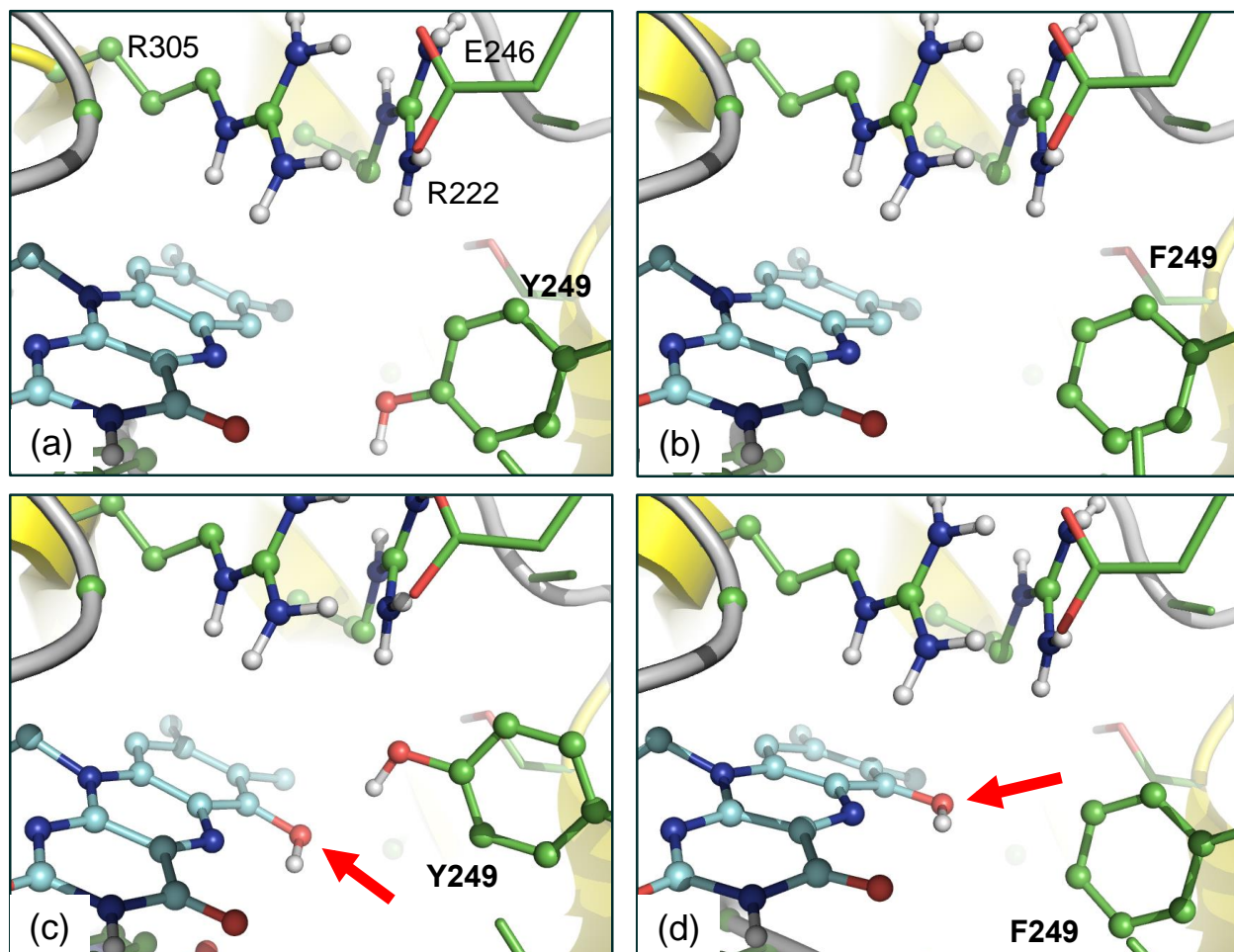


Figure 5.8 Illustration of DADH active sites of the optimized DADH models: (a) wild type, (b) Y249F, (c) wild type – 6-OH-FAD, and (d) Y249F – 6-OH-FAD. The hydroxylated C6 sites are pointed using red arrow. For simplicity only FAD (iso)alloxazine ring (cyan carbons), side chains of some active site residues (222, 246, 249, and 305) are illustrated.

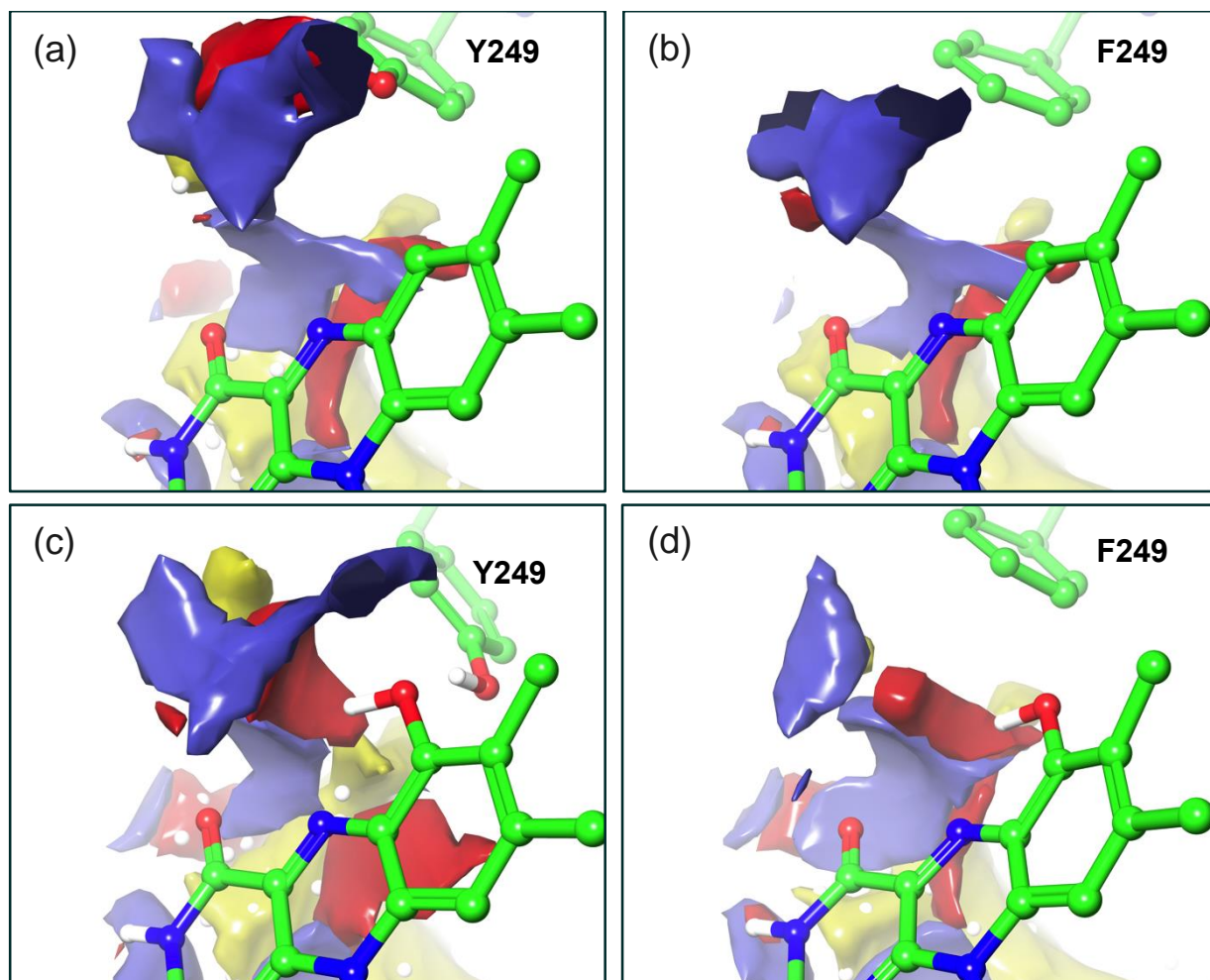


Figure 5.9 Illustration of the characterized active site cavities of the optimized DADH models: (a) wild type, (b) Y249F, (c) wild type – 6-OH-FAD, and (d) Y249F – 6-OH-FAD. The coloring scheme is such that H-bond donor regions are colored blue, while H-bond acceptor regions are colored red and hydrophobic regions are colored yellow.

5.5 Discussion

Several cases of flavoenzymes with naturally occurring modification to the flavin cofactors have been reported in the past. The reported modifications are usually at the 6th and 8th positions

of the (iso)alloxazine ring moiety and they include: 6 and 8 hydroxy flavins, and 8-amino riboflavins from a variety of prokaryotic and eukaryotic sources. 6-Hydroxy-flavins have in particular been detected in diverse flavoenzymes and were reported to be inactive. First instance of 6-hydroxy-flavin detection was reported four decades ago and yet much is not known about the physiological significance or different factors contributing to the differential reactivity of this cofactor compared to FAD. In the present study, we report the detection and characterization of 6-OH-FAD in a mutant variant of PaDADH using UV-visible

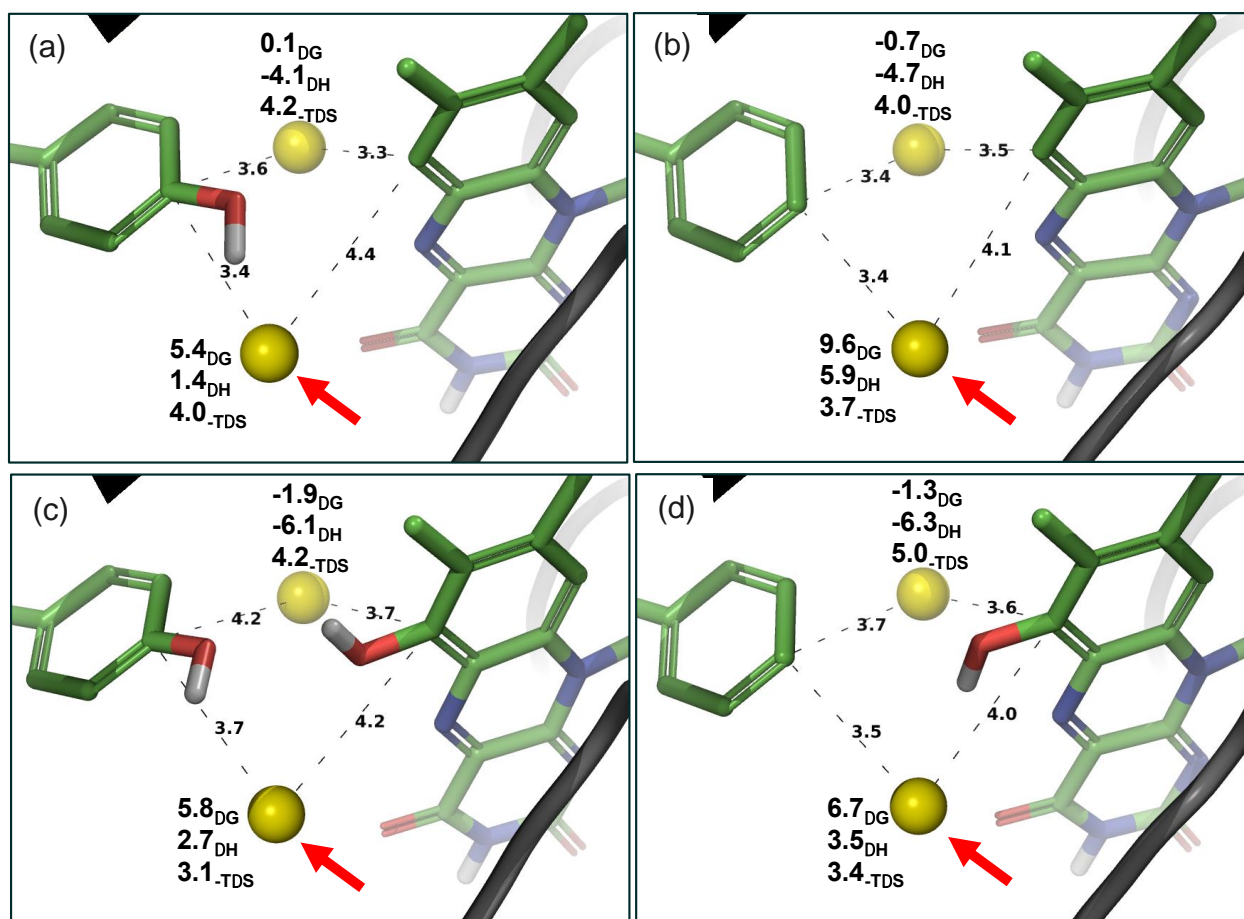


Figure 5.10 Thermodynamics of key hydration sites around C6 carbon for DADH variants: (a) wild type, (b) Y249F, (c) wild type – 6OH-FAD, and (d) Y249F – FAD-6OH. Hydration sites

are colored ranging from green (favorable) to red (unfavorable), which are computed which are computed relative to bulk solvent.

absorbance spectroscopy, ^1H and ^{13}C NMR, and mass spectrometry. Additionally, we used computational models to gain a structure-based understanding of the various factors responsible for the altered reactivity of native-FAD and 6-OH-FAD cofactors within PaDADH active site.

PaDADH-Y249 was mutated to phenylalanine to probe the role of Y249 in substrate binding. Purified PaDADH-Y249F mutant enzyme showed two major fractions following DEAE-sepharose fractionation, which differed in color and corresponding spectroscopic properties. The green fraction of PaDADH-Y249F enzyme, bound longer on the positively charged DEAE resin compared to the yellow enzyme, suggesting that the overall charge of the green enzyme as being more negative than the yellow enzyme. **Figure 5.1** shows that the yellow fraction has absorbance spectrum characteristic of wild-type PaDADH, which has unmodified FAD as its cofactor.¹⁴ The major difference between the yellow and green enzyme fractions of the mutant enzyme is the broad absorbance in the 580 to 800 nm region for the green fraction. Flavin cofactors are known to exist in yellow, orange or blue colors owing to their redox state in the active site of an enzyme and are also frequently involved in charge transfer transitions causing for transient increase in absorbance in the long wavelength regions without affecting the peaks in the 300 to 450 region.⁶ However, for the green fraction, the absorbance in the long wavelength region is stable and the observed spectroscopic properties are unusual for the species to be any of the known redox states of flavins. Literature survey indicated that addition of functional groups like $-\text{OH}$, $-\text{SH}$ or N_3 at certain (6th and/or 9th) sites on the (iso)alloxazine ring of flavin could result in the observed green coloration in DADH-Y249F fraction along with the observed stable long wavelength absorption with low

extinction coefficients.^{2-8, 41} Of these, hydroxylation at the 6th position of the (iso)alloxazine (**Scheme 5.2**) has been reported to occur naturally in some enzymes (**Table 5.1**).

¹H and ¹³C NMR analyses of FAD and modified FAD extracted from PaDADH-Y249F, and synthesized native-FAD and 6-OH-FAD are consistent with modification of (iso)alloxazine ring by –OH functional group at the 6th position in the modified FAD, extracted from PaDADH-Y249F (**Figure 5.3**). In addition, HSQC and TOCSY spectra allowed for the identification of the (iso)alloxazine 9th position (6.75 and 103 ppm, ¹H and ¹³C respectively) and differentiation of the 7 and 8 methyl positions (**Figure 5.4**) (2.41 and 2.18 ppm, respectively). The chemical shifts for the proton at the 9th position of the (iso)alloxazine ring of 6-OH-FAD has not been previously described and can be used as an alternative means for identification of the 6-OH modified FAD. Through NMR, we could determine that the modification was at the 6th and not the 9th position of the (iso)alloxazine ring in PaDADH-Y249F enzyme. Molecular weight determination through mass-spectrometry of the extracted modified FAD from PaDADH-Y249F agrees well with NMR analyses. An increase in molecular weight of 16 Da of the modified cofactor (**Figure 5.5**) suggests the addition of a hydroxyl group, but not a thiol or a N₃ functional group, which would result in a molecular weight increase of 32 and 42 respectively. Further evidence in favor of 6-OH-FAD as the modified cofactor in PaDADH-Y249F comes from pH titration of the enzyme free cofactor. A p*K*_a of 7.1 (**Figure 5.6**) was measured for the ionization of the hydroxyl group (**Scheme 5.2**), in good agreement with the published p*K*_a for free 6-OH-FAD. Also important to note is that the p*K*_a for –SH group at the 6th position is reported to be 5.9⁴ which is much lower than observed value for the modified cofactor from PaDADH-Y249F enzyme.

The fraction of PaDADH-Y249F enzyme with 6-OH-FAD as cofactor was enzymatically less active compared to FAD bound enzyme fraction. Results from **Figure 5.7** suggest that irrespective of the substrate, the reactivity of the two enzyme bound cofactors is on a completely different time-scale. This observation is in agreement with previous studies, where the 6-OH-FAD bound enzyme fractions were reported to be enzymatically slow in most cases (**Table 5.1**). Redox potential of free 6-OH-FAD is 57 mV more negative compared to FAD⁸ making 6-OH-FAD a poorer catalyst in comparison. However, it is yet to be demonstrated as to how the reactivity of 6-OH-FAD is affected in the context of an enzyme active site.

Structural analysis of PaDADH wild-type and *in-silico* Y249F mutant offered more insight regarding the different reactivity profiles observed for PaDADH-Y249F in complex with 6-OH-FAD and native-FAD. Hydroxylated FAD shows lowered reactivity compared with native FAD since the reactive N5 nitrogen is inaccessible to the substrate (see **Figure 5.11**). Here, the N5 of 6-OH-FAD can engage in an internal hydrogen bond with the OH group at the 6th position. Furthermore, hydroxylation of FAD at the 6th position changes the local environment around the N5 nitrogen: while this region indicates H bond-donating character in the wild-type and Y249F PaDADH (**Figure 5.9a, b**) this changes to predominantly H bond-accepting in Y249F enzyme with 6-OH-FAD (**Figure 5.9d**). In addition, hydroxylation of FAD at the 6th position renders the reactive N5 less accessible. Moreover, the local electrophilicity of N5 nitrogen in Y249F enzyme with 6-OH-FAD is slightly decreased making it less readily susceptible to nucleophilic attack by the substrate than the N5 of FAD bound enzyme. The factors highlighted from the computational analyses on PaDADH in combination with the differential redox potential of 6-OH-FAD cofactor may account for the lowered reactivity of most enzymes containing 6-OH-FAD. Characterization of hydration sites in the PaDADH-wild type and Y249F mutant suggested that the C6 site of FAD

may be more readily available for attack by a reactive water molecule thereby making it more likely for hydroxylation at this site in the mutant than in the wild-type.

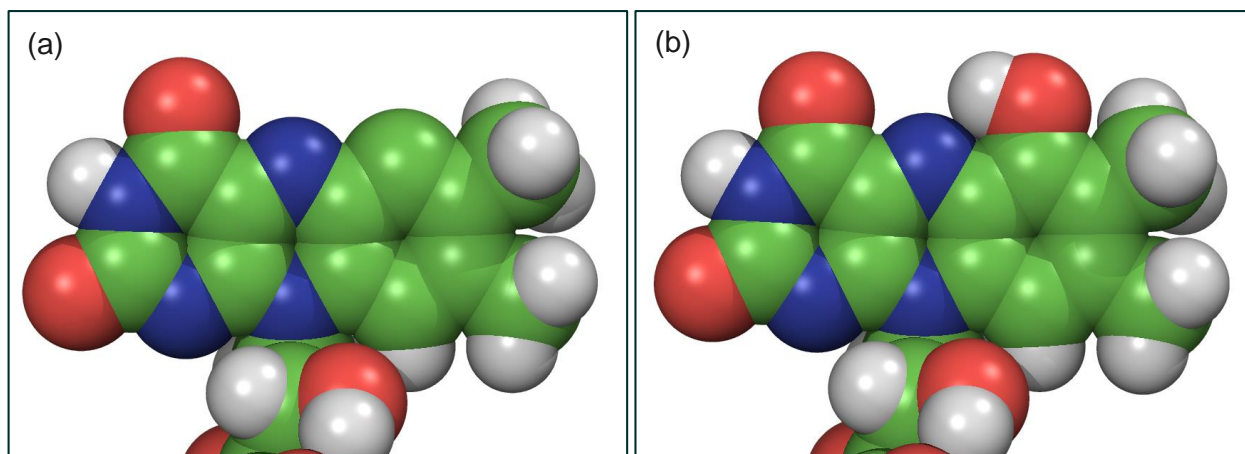


Figure 5.11 Van der Waals sphere representation of (a) unmodified flavin and (b) C6-hydroxylated flavin.

5.6 Conclusion

In conclusion, Y249F mutant of PaDADH results in two distinct enzyme populations, one in which cofactor FAD remains unmodified and the other population has 6-OH-FAD. We established this by biochemical characterization using UV-visible absorbance spectroscopy, NMR, mass spectrometry and pH titrations. By the use of ^1H and ^{13}C -NMR, a simple and easy approach of discriminating between 6- and 9-OH-flavin has originated through the course of this research. Furthermore, computational approaches for the first time allowed a molecular-level analysis of the hydroxylation of the flavin cofactor using PaDADH as the model enzyme. The poor reactivity of 6-OH-FAD bound PaDADH-Y249F as reported from biochemical studies is readily accommodated by observations from computational studies of the buried nature of N5 of 6-OH-FAD, its involve-

ment in an internal hydrogen bond with the hydroxyl group at C6 which may influence the substrate to bind in an unreactive mode and also decreased electrophilicity of N5 of the 6-OH-FAD relative to FAD. Taken together, we provide biochemical and structural characterization of green flavin detected in the mutant variant of PaDADH. The findings from this study as well as from previous reports raise the important questions on the commonality of this modification in nature, source of oxygen atom in the hydroxylation process, and biological significance if any. Future studies will be aimed at understanding the source of oxygen atom in the 6-hydroxy-flavin and the mechanism of hydroxylation which we hope will offer clues on the susceptibility of the flavin cofactor to such modifications and any effects such modifications may impose.

5.7 Acknowledgements

The authors would like to thank Dr. Siming Wang at the mass spectrometry facility, GSU, for carrying out mass spectrometry analysis, Dr. Bruce Palfey at the University of Michigan, Ann Arbor for the kind donation of synthesized 6-OH-FAD. The authors would also like to acknowledge schrödinger IT for providing computational resources.

5.8 References

1. Joosten, V., and van Berkel, W. J. H. (2007) Flavoenzymes, *Current Opinion in Chemical Biology* 11, 195-202.
2. Claiborne, A., Massey, V., Fitzpatrick, P. F., and Schopfer, L. M. (1982) 2-Thioflavins as active site probes of flavoproteins, *The Journal of biological chemistry* 257, 174-182.
3. Ghisla, S., and Massey, V. (1986) New flavins for old: artificial flavins as active site probes of flavoproteins, *The Biochemical journal* 239, 1-12.

4. Ghisla, S., Massey, V., and Yagi, K. (1986) Preparation and some properties of 6-substituted flavins as active site probes for flavin enzymes, *Biochemistry* 25, 3282-3289.
5. Massey, V., Claiborne, A., Biemann, M., and Ghisla, S. (1984) 4-Thioflavins as active site probes of flavoproteins. General properties, *The Journal of biological chemistry* 259, 9667-9678.
6. Massey, V., and Hemmerich, P. (1980) Active-site probes of flavoproteins, *Biochemical Society transactions* 8, 246-257.
7. Schöllnhammer, G., and Hemmerich, P. (1974) Nucleophilic Addition at the Photoexcited Flavin Cation: Synthesis and Properties of 6- and 9-Hydroxy-Flavocoenzyme Chromophores, *European Journal of Biochemistry* 44, 561-577.
8. Thorpe, C., and Massey, V. (1983) Flavin analogue studies of pig kidney general acyl-CoA dehydrogenase, *Biochemistry* 22, 2972-2978.
9. Mayhew, S. G., Whitfield, C. D., Ghisla, S., and Schuman-Jorns, M. (1974) Identification and properties of new flavins in electron-transferring flavoprotein from *Peptostreptococcus elsdenii* and pig-liver glycolate oxidase, *European journal of biochemistry / FEBS* 44, 579-591.
10. Fitzpatrick, P. F. (2010) Oxidation of amines by flavoproteins, *Arch Biochem Biophys* 493, 13-25.
11. Fu, G., Yuan, H., Li, C., Lu, C. D., Gadda, G., and Weber, I. T. (2010) Conformational changes and substrate recognition in *Pseudomonas aeruginosa* D-arginine dehydrogenase, *Biochemistry* 49, 8535-8545.

12. Li, C., and Lu, C. D. (2009) Arginine racemization by coupled catabolic and anabolic dehydrogenases, *Proceedings of the National Academy of Sciences of the United States of America* 106, 906-911.
13. Ball, J., Bui., Q., Gannavaram, S., Fu, G., Weber, I., Gadda, G.,. (2013) Mechanistic and Structural Investigation of D-arginine Dehydrogenase with Multiple Substrates.
14. Yuan, H., Fu, G., Brooks, P. T., Weber, I., and Gadda, G. (2010) Steady-state kinetic mechanism and reductive half-reaction of D-arginine dehydrogenase from *Pseudomonas aeruginosa*, *Biochemistry* 49, 9542-9550.
15. Yuan, H., Xin, Y., Hamelberg, D., and Gadda, G. (2011) Insights on the mechanism of amine oxidation catalyzed by D-arginine dehydrogenase through pH and kinetic isotope effects, *J Am Chem Soc* 133, 18957-18965.
16. Negri, A., Massey, V., and Williams, C. H., Jr. (1987) D-aspartate oxidase from beef kidney. Purification and properties, *The Journal of biological chemistry* 262, 10026-10034.
17. Tedeschi, G., Negri, A., Ceciliani, F., Ronchi, S., Vetere, A., D'Aniello, G., and D'Aniello, A. (1994) Properties of the flavoenzyme D-aspartate oxidase from *Octopus vulgaris*, *Biochimica et biophysica acta* 1207, 217-222.
18. Igarashi, K., Verhagen, M. F., Samejima, M., Schulein, M., Eriksson, K. E., and Nishino, T. (1999) Cellobiose dehydrogenase from the fungi *Phanerochaete chrysosporium* and *Humicola insolens*. A flavohemoprotein from *Humicola insolens* contains 6-hydroxy-FAD as the dominant active cofactor, *The Journal of biological chemistry* 274, 3338-3344.

19. Morpeth, F. F., and Jones, G. D. (1986) Resolution, purification and some properties of the multiple forms of cellobiose quinone dehydrogenase from the white-rot fungus *Sporotrichum pulverulentum*, *The Biochemical journal* 236, 221-226.
20. Mewies, M., Basran, J., Packman, L. C., Hille, R., and Scrutton, N. S. (1997) Involvement of a flavin iminoquinone methide in the formation of 6-hydroxyflavin mononucleotide in trimethylamine dehydrogenase: a rationale for the existence of 8 α -methyl and C6-linked covalent flavoproteins, *Biochemistry* 36, 7162-7168.
21. Huang, L., Scrutton, N. S., and Hille, R. (1996) Reaction of the C30A mutant of trimethylamine dehydrogenase with diethylmethylamine, *The Journal of biological chemistry* 271, 13401-13406.
22. Lu, X., Nikolic, D., Mitchell, D. J., van Breemen, R. B., Mersfelder, J. A., Hille, R., and Silverman, R. B. (2003) A mechanism for substrate-Induced formation of 6-hydroxyflavin mononucleotide catalyzed by C30A trimethylamine dehydrogenase, *Bioorganic & medicinal chemistry letters* 13, 4129-4132.
23. Marshall, K. R., Gong, M., Wodke, L., Lamb, J. H., Jones, D. J., Farmer, P. B., Scrutton, N. S., and Munro, A. W. (2005) The human apoptosis-inducing protein AMID is an oxidoreductase with a modified flavin cofactor and DNA binding activity, *The Journal of biological chemistry* 280, 30735-30740.
24. (2013) Prime version 3.2, Schrödinger, LLC, New York, NY.
25. (2013) Protein Preparation Wizard 2013-3; Epik version 2.4, , Schrödinger, LLC, New York, NY

26. Sastry, G. M., Inakollu, V. S., and Sherman, W. (2013) Boosting virtual screening enrichments with data fusion: Coalescing hits from 2D fingerprints, shape, and docking, *Journal of Chemical Information and Modeling*.
27. (2013) Impact version 5.9, Schrödinger, LLC, New York, NY.
28. Olsson, M. H., Søndergaard, C. R., Rostkowski, M., and Jensen, J. H. (2011) PROPKA3: consistent treatment of internal and surface residues in empirical pK_a predictions, *Journal of Chemical Theory and Computation* 7, 525-537.
29. (2013) BioLuminate, version 1.1, Schrödinger, LLC New York, NY.
30. Beard, H., Cholleti, A., Pearlman, D., Sherman, W., and Loving, K. A. (2013) Applying Physics-Based Scoring to Calculate Free Energies of Binding for Single Amino Acid Mutations in Protein-Protein Complexes, *PLOS ONE* 8, e82849.
31. (2013) Prime, version 3.4, Schrödinger, LLC, New York, NY.
32. Li, J., Abel, R., Zhu, K., Cao, Y., Zhao, S., and Friesner, R. A. (2011) The VSGB 2.0 model: a next generation energy model for high resolution protein structure modeling, *Proteins: Structure, Function, and Bioinformatics* 79, 2794-2812.
33. Ghosh, A., Rapp, C. S., and Friesner, R. A. (1998) Generalized Born model based on a surface integral formulation, *The Journal of Physical Chemistry B* 102, 10983-10990.
34. Yu, Z., Jacobson, M. P., and Friesner, R. A. (2006) What role do surfaces play in GB models? A new-generation of surface-generalized born model based on a novel gaussian surface for biomolecules, *Journal of computational chemistry* 27, 72-89.
35. Guvench, O., and MacKerell Jr, A. D. (2008) Comparison of protein force fields for molecular dynamics simulations, In *Molecular Modeling of Proteins*, pp 63-88, Springer.

36. Jorgensen, W. L., and Tirado-Rives, J. (1988) The OPLS [optimized potentials for liquid simulations] potential functions for proteins, energy minimizations for crystals of cyclic peptides and crambin, *Journal of the American Chemical Society* *110*, 1657-1666.
37. Kaminski, G. A., Friesner, R. A., Tirado-Rives, J., and Jorgensen, W. L. (2001) Evaluation and reparametrization of the OPLS-AA force field for proteins via comparison with accurate quantum chemical calculations on peptides, *The Journal of Physical Chemistry B* *105*, 6474-6487.
38. (2013) SiteMap, version 2.9, Schrödinger, LLC, New York, NY.
39. Young, T., Abel, R., Kim, B., Berne, B. J., and Friesner, R. A. (2007) Motifs for molecular recognition exploiting hydrophobic enclosure in protein–ligand binding, *Proceedings of the National Academy of Sciences* *104*, 808-813.
40. (2013) QSite, version 6.1, Schrödinger, LLC, New York, NY.
41. Entsch, B., Massey, V., and Claiborne, A. (1987) para-Hydroxybenzoate hydroxylase containing 6-hydroxy-FAD is an effective enzyme with modified reaction mechanisms, *The Journal of biological chemistry* *262*, 6060-6068.

6 RELATIVE TIMING OF HYDROGEN AND PROTON TRANSFERS IN THE REACTION OF FLAVIN OXIDATION CATALYZED BY CHOLINE OXIDASE

(This chapter has been published verbatim as, Gannavaram, S., and Gadda, G., *Biochemistry* 52(7): 1221-1226)

6.1 Abstract

The oxidation of the reduced flavin in choline oxidase was investigated with pH, solvent viscosity and KIEs in steady-state kinetics, and time-resolved absorbance spectroscopy of the oxidative half-reaction in a stopped-flow spectrophotometer. Both the effects of isotopic substitution on the KIEs and the multiple KIEs suggest a mechanism for flavin oxidation in which the H atom from the reduced flavin and a H⁺ from the solvent or a solvent exchangeable site are transferred in the same kinetic step. Stopped-flow kinetic data demonstrate flavin oxidation without stabilization of flavin-derived species. Solvent viscosity effects establish an isomerization of the reduced enzyme. A mechanism for flavin oxidation that satisfies the kinetic results is proposed.

6.2 Introduction

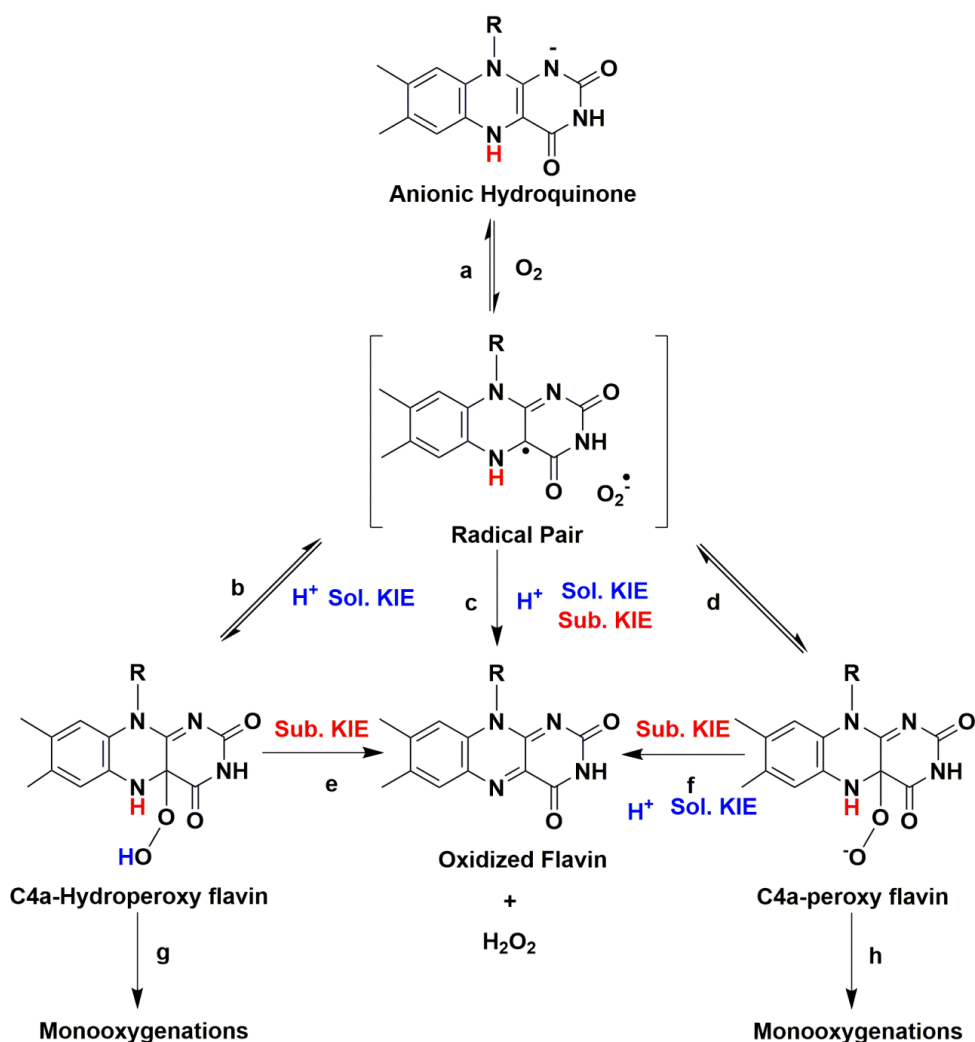
Flavin-dependent oxidases and monooxygenases react rapidly with dioxygen (O₂), with second-order rate constants of 10⁴ -10⁶ M⁻¹s⁻¹ (1, 2). The former yield H₂O₂, while the latter H₂O and a hydroxylated organic product (1, 2). Due to the diradical nature of the stable form of O₂ in the atmosphere, the direct transfer of an electron pair from the reduced flavin to O₂ is spin forbidden and cannot occur (3-5). Hence, O₂ reduction proceeds through two single electron transfers that generate a highly reactive flavosemiquinone/O₂^{-•} radical pair (**Scheme 6.1, step a**) (1-8). A

reaction intermediate with spectroscopic features similar to a flavosemiquinone was recently reported in the oxidative half-reaction of glycolate oxidase carried out in D₂O (9). Reduction of O₂ in monooxygenases typically reveals detectable C4a-hydroperoxy and -peroxy flavin intermediates in rapid kinetic studies (**Scheme 6.1: routes a-b-g and a-d-h**, respectively) (1, 10, 11). With the exception of pyranose 2-oxidase (12, 13) and a mutant form of NADH oxidase (14), those intermediates are not typically observed in oxidases, where rapid kinetics show monophasic oxidations of the reduced flavin (1, 2). Studies on glucose oxidase using ¹⁸O KIEs, enzyme reconstituted with flavin analogs, and temperature effects, support the notion that O₂ reduction occurs without formation of flavin intermediates (**Scheme 6.1: route a-c**) (15). Mutagenesis demonstrated that a positively charged histidine in glucose oxidase, H516, is the main site for O₂ activation through electrostatic catalysis (4, 16).

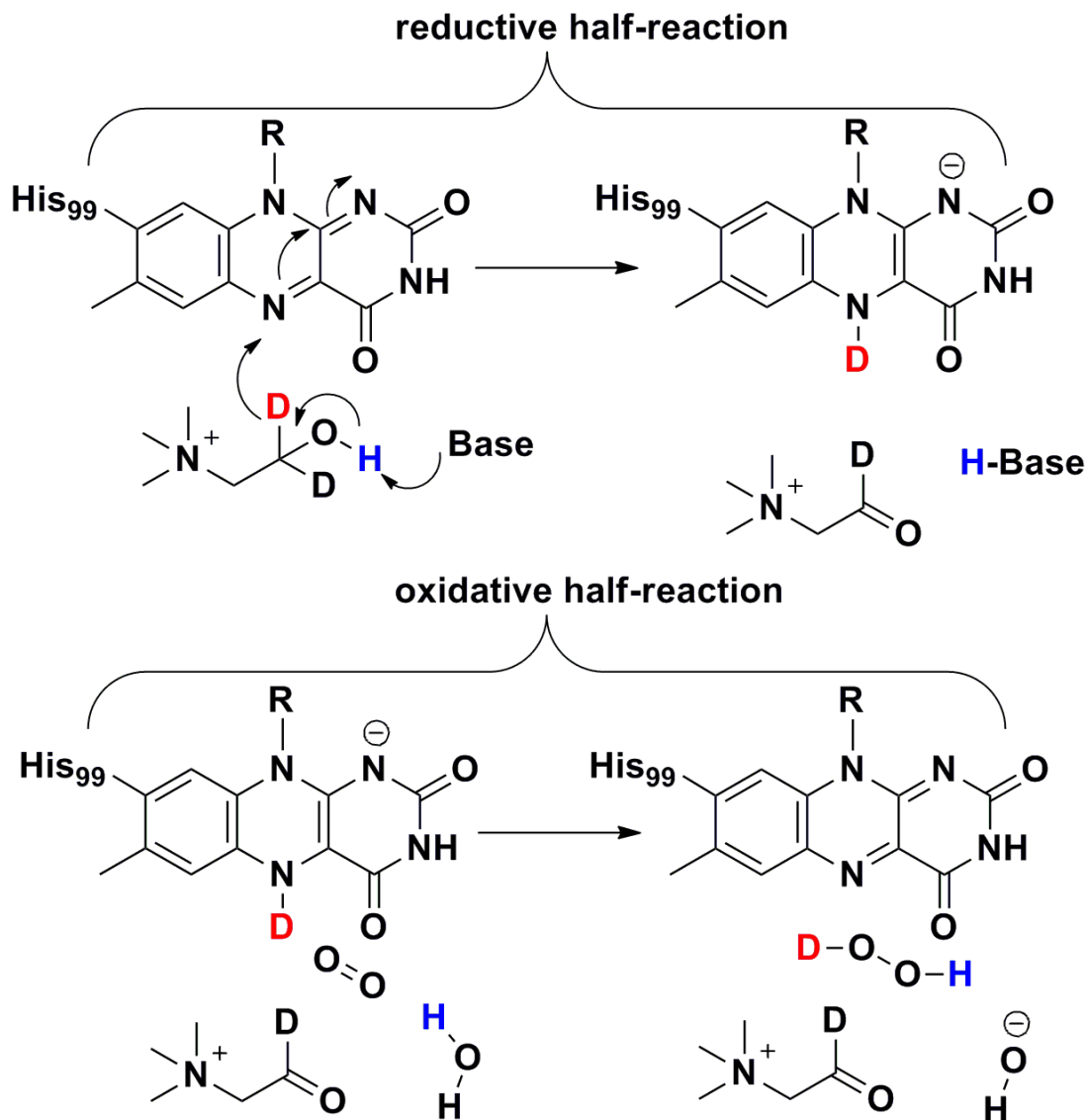
Irrespective of the mechanism, flavin oxidation by flavoprotein oxidases requires the transfer of one electron, a hydrogen (H) from the reduced flavin N5 atom (**Scheme 6.1**, red steps) and a proton (H⁺) from either the solvent or a solvent exchangeable site in the active site of the enzyme (**Scheme 6.1**, blue steps) (1). Studies on pyranose 2-oxidase using rapid kinetics, substrate and solvent KIEs have shown that the transfer of the flavin-bound H, which originates from the α -carbon of the substrate and is transferred as a hydride ion (H⁻) to the flavin N5 atom during substrate oxidation, is rate-determining for flavin oxidation (12). Flavin reduction in choline oxidase also occurs through the transfer of a H⁻ from the α -carbon of the substrate, but the flavin is oxidized with the organic product of the reaction still present in the active site, as seen in **Scheme 6.2**. Indeed, it is the positive charge harbored on the reaction product that activates O₂ for reaction with the flavin rather than a protein charge as in the case of glucose oxidase (17, 18). If the wash out of the H from the N5 atom of the reduced flavin is hampered in the presence of the reaction product,

the opportunity exists to use substrate deuterium KIEs to report on the H transfer from the reduced flavin in O₂ reduction. Solvent deuterium KIEs, instead, will directly report on the H⁺ transfer involving a solvent (exchangeable) site.

In this study, we have used pH, solvent and KIEs, along with time-resolved absorbance spectroscopy of the oxidative half-reaction, to investigate the relative timing of H and H⁺ transfers in the flavin oxidation reaction catalyzed by choline oxidase.



Scheme 6.1 Possible routes for flavin oxidation in flavoproteins.



Scheme 6.2 Reductive and oxidative half-reactions by choline oxidase with 1,2- $^{2}\text{H}_4$ -choline as substrate; note that the timing for the cleavages of the various bonds is not addressed here.

6.3 Experimental Procedures

Materials

Choline chloride was bought from ICN. 1,2- $^{2}\text{H}_4$ -Choline bromide (98%) and sodium deuterioxide were purchased from Isotec Inc. (Miamisburg, OH). Deuterium oxide (99.9%) and

deuterium chloride (99.5%) were obtained from Cambridge Isotope Co. (Andover, MA). Glycerol was from EMD. Recombinant choline oxidase from *Arthrobacter globiformis* strain ATCC 8010 was expressed from plasmid pET/*codAI* and purified to homogeneity based on a previous protocol (19). Completely oxidized enzyme was produced using a protocol described previously (20). The kinetic parameters reported in the current study have been normalized for flavin content per active site.

Kinetic Assays

The enzymatic activity was determined by measuring the rate of oxygen consumption polarographically using a computer-interfaced oxygen electrode from Hansatech. Determination of the steady-state kinetic parameters was carried out using the method of initial rates with concentrations of choline or 1,2-²H₄-choline fixed at 25 mM and oxygen within a range of 0.04 to 1.0 mM. As a starting step, the reaction mixture was equilibrated by bubbling in O₂/N₂ gas mixture for approximately 15 min at the desired concentration. Enzymatic assays were initiated with the addition of 5 μL of choline oxidase at a final concentration of 0.12 μM to a final reaction volume of 1000 μL. Enzymatic assays were performed using sodium pyrophosphate or sodium phosphate in either H₂O or 99.9% D₂O at pL 8.0, 9.0 and 7.0, respectively. For buffers containing D₂O, the pD values were adjusted by adding 0.4 to the pH value (21).

Solvent viscosity studies were carried out at pH 7.0, 8.0 and 9.0 using the procedure described above with glycerol as viscosigen. Based on relative viscosities at 20 °C available from Lide (22), the values at 25 °C were calculated.

Time-resolved absorbance spectroscopy in the double mixing mode was performed using an SF-61DX2 Hi-Tech KinetAsyst high performance stopped-flow spectrophotometer, thermostatted at 25 °C, and equipped with a photo diode-array detector. Choline oxidase was prepared fresh by gel filtration against 50 mM sodium phosphate, pD 7.0. The enzyme concentration before mixing it with the substrate was 94 μM . 1,2- $^{2}\text{H}_4$ -choline (130 μM) was prepared in 50 mM sodium phosphate, pD 7.0. The stopped-flow spectrophotometer was set up with glucose/glucose oxidase scrubbing system at pH 6.0 the day before and left over night. The buffer and substrate solutions contained in glass syringes were flushed with argon for approximately an hour before mounting on the stopped-flow spectrophotometer. The enzyme contained in a glass tonometer was subjected to 25 cycles of degassing by alternately flushing it with argon and applying vacuum. To ensure complete removal of traces of oxygen, glucose (2 mM) and glucose oxidase (0.5 μM) were present in the anaerobic enzyme, buffer and substrate solutions. Separately, glass syringes containing sodium phosphate buffer were saturated with 800, 540, 250, 140, 40 μM O_2 before mounting them onto the stopped-flow instrument. The aerobic syringes did not contain glucose/glucose oxidase. The first mixing in the stopped-flow spectrophotometer was between anaerobic enzyme and anaerobic substrate, thereby producing reduced enzyme; this sample was allowed to age in the instrument until complete reduction of the enzyme-bound flavin before being mixed with aerobic buffer at various concentrations of oxygen. Acquisition of the time-resolved absorbance spectra began 2.2 ms after the second mixing event.

Data Analysis

Data were fit using KaleidaGraph software (Synergy Software, Reading, PA). The steady-state kinetic parameters at a fixed (25 mM or 50 mM) choline or 1,2- $^{2}\text{H}_4$ -choline and varying

concentrations of O₂ were calculated using the Michaelis Menten equation. Solvent viscosity effects on $k_{\text{cat}}/K_{\text{ox}}$ (as a function of the concentration of O₂ as substrate) (Figure 1B) were fit to eq 1, in which $(k)_o$ and $(k)_\eta$ are the kinetic parameters in the absence and presence of glycerol as viscosigen, S is the degree of dependence on viscosity, and η_{rel} represents the relative viscosity.

Individual traces at 456 nm for each oxygen concentration (Figure 2B) were fit to eq 2 using the KinetAsyst 3 software (TgK-Scientific, Bradford-on-Avon, UK), where A is the value of absorbance at the selected wavelength, B is the amplitude of the change in absorbance, C is absorbance at infinite time and λ is the observed first-order rate constant for flavin oxidation. The time-resolved absorbance spectra were analyzed with the global-fitting analysis software SPECFIT/32, with the best fit of the data obtained to an A→B kinetic model.

$$\frac{(k)_o}{(k)_\eta} = S(\eta_{\text{rel}} - 1) + 1 \quad (1)$$

$$A = -Be^{-\lambda t} + C \quad (2)$$

6.4 Results and Discussion

Kinetics to determine flavin oxidation in choline oxidase-wild type

To probe flavin oxidation during turnover of the enzyme we used the $^{\text{app}}(k_{\text{cat}}/K_{\text{ox}})$ value determined at fixed, saturating concentration of choline. Enzyme saturation with choline was experimentally demonstrated upon comparing the $^{\text{app}}(k_{\text{cat}}/K_{\text{ox}})$ determined at pH 7.0 at two fixed concentrations of substrate. With 25 and 50 mM choline the $^{\text{app}}(k_{\text{cat}}/K_{\text{ox}})$ was essentially the same ($120,000 \pm 5000$ and $119,000 \pm 4000 \text{ M}^{-1}\text{s}^{-1}$, respectively). Similar results were obtained with 1,2-[²H₄]-choline ($87,000 \pm 4000$ and $87,000 \pm 5000 \text{ M}^{-1}\text{s}^{-1}$, respectively). These results agree well with published K_m values for choline (1.6 mM) and 1,2-[²H₄]-choline (2.5 mM) at pH 7.0, indicat-

ing that the enzyme is $\geq 90\%$ saturated with 25 mM substrate (23). Since previous kinetic investigations demonstrated a decrease in K_m with increasing pH (23), it is concluded that the true k_{cat}/K_{ox} value, which is required to draw mechanistic conclusions, is approximated well at pH ≥ 7.0 by the $^{app}(k_{cat}/K_{ox})$ determined at 25 mM substrate.

Solvent Effects

Previous studies showed that the k_{cat}/K_{ox} with choline or 1,2- $[^2H_4]$ -choline as substrate for choline oxidase is independent of pH between 6.0 and 10.0 (20, 24). In principle, substitution of H_2O with D_2O might yield solvent effects on k_{cat}/K_{ox} due to changes in the isotopic composition of solvent exchangeable sites participating in the reaction (i.e., isotope effects), increases in the relative viscosity of the solution (i.e., viscosity effects), perturbations of observed pK_a values (i.e., pH effects), or a combination of these effects (25-27). Mechanistic interpretation of solvent kinetic isotope effects requires to rule out pH effects and to dissect the contribution of relative viscosity to the measured effect. As illustrated in **Figure 1A**, the k_{cat}/K_{ox} with choline determined in D_2O was the same between pD 7.0 and 9.0, establishing lack of pD effects. The normalized k_{cat}/K_{ox} at various concentrations of glycerol as viscosigen increased with inverse hyperbolic pattern with increasing relative viscosity of the solvent (**Figure 1B**). While this pattern is consistent with an isomerization of the reduced enzyme in the oxidative half-reaction (28), it also establishes that solvent KIEs are not inflated due to increased solvent viscosity of D_2O ; indeed, they are slightly deflated. At 9% glycerol (22), with a relative viscosity equivalent to that of D_2O ($\eta = 1.25$) (25), the inverse viscosity effect was $\leq 8\%$ between pH 7.0 and 9.0. With these controls, solvent deuterium KIEs on k_{cat}/K_{ox} could be used to report on H^+ transfers involving solvent (exchangeable) sites, since there are no pH/D effects and negligible, inverse viscosity effects.

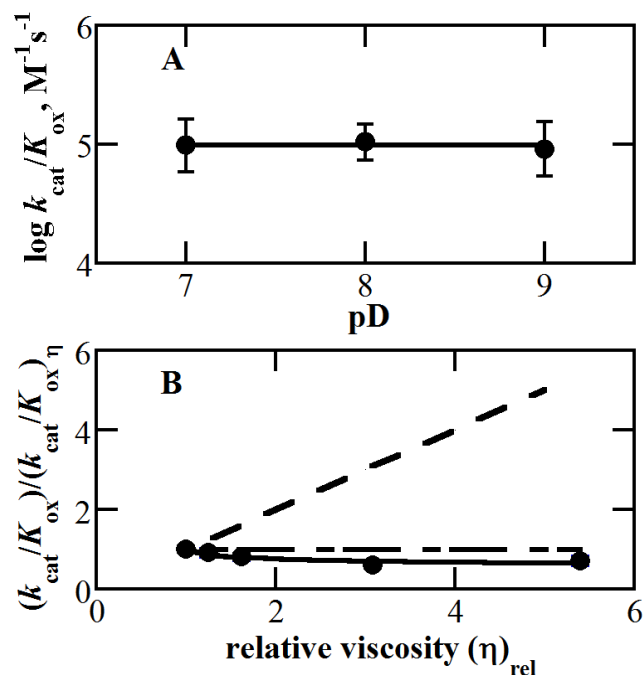


Figure 6.1 pD and viscosity contributions to solvent effects on $k_{\text{cat}}/K_{\text{ox}}$. Panel A: log of $k_{\text{cat}}/K_{\text{ox}}$ for choline in D₂O as a function of pD; Panel B: normalized $k_{\text{cat}}/K_{\text{ox}}$ for choline at varying concentrations of glycerol as viscosigen (0, 9, 18, 36 and 48%) as a function of relative viscosity at pH 8.0, with 25 mM choline and varying concentrations of O₂ from 0.04 to 1 mM.

Substrate Kinetic Isotope Effects

When choline is substituted with 1,2-[²H₄]-choline as substrate for choline oxidase, the enzyme-bound flavin acquires a D rather than H on the N5 atom (**Scheme 6.2**) (24). A normal substrate deuterium KIE is expected on $k_{\text{cat}}/K_{\text{ox}}$ in aqueous buffered solutions if the reaction of the reduced flavin with O₂ occurs prior to the potential wash out of the D from the reduced flavin N5 atom to the solvent. Alternatively, both the ${}^{\text{D}}(k_{\text{cat}}/K_{\text{ox}})_{\text{H}_2\text{O}}$ and ${}^{\text{D}}(k_{\text{cat}}/K_{\text{ox}})_{\text{D}_2\text{O}}$ should be equal to 1 if

the N5-D atom of the reduced flavin is rapidly exchanged with the solvent. As illustrated in **Table 6.1**, significant substrate deuterium KIEs were determined in aqueous and deuterated buffered solutions at pL 7.0 and 8.0, consistent with negligible wash out of the N5-H or -D from the reduced flavin during enzyme turnover. Thus, substrate KIEs could be used to report on the H transfer from the reduced flavin in O₂ reduction.

Table 6.1 Deuterium kinetic isotope effects on the second-order rate constant for flavin oxidation during steady-state turnover of choline oxidase.

KIE	pL 7.0 ^a	pL 8.0 ^b
^D (<i>k</i> _{cat} / <i>K</i> _{ox}) _{H2O}	1.4 ± 0.1	1.6 ± 0.1
^D (<i>k</i> _{cat} / <i>K</i> _{ox}) _{D2O}	1.7 ± 0.1	2.1 ± 0.1
^{D2O} (<i>k</i> _{cat} / <i>K</i> _{ox}) _H	1.2 ± 0.1	1.09 ± 0.05
^{D2O} (<i>k</i> _{cat} / <i>K</i> _{ox}) _D	1.5 ± 0.1	1.4 ± 0.1
^{D,D2O} (<i>k</i> _{cat} / <i>K</i> _{ox})	2.1 ± 0.4	2.2 ± 0.1
^D (<i>k</i> _{cat} / <i>K</i> _{ox}) _{H2O} × ^{D2O} (<i>k</i> _{cat} / <i>K</i> _{ox}) _H	1.7 ± 0.2	1.7 ± 0.1

Experimental conditions: 50 mM ^asodium phosphate or ^bsodium pyrophosphate in H₂O or D₂O, 25 °C at 25 mM of either choline (H) or 1,2-[²H₄]-choline (D) and varying concentrations of O₂ from 40 to 1000 μM.

Multiple Kinetic Isotope Effects

With the enzyme in turnover at pL 7.0 or 8.0, the ^{D2O}(*k*_{cat}/*K*_{ox})_H values were only slightly >1 (**Table 6.1**). However, they increased when 1,2-[²H₄]-choline was used as substrate instead of choline (^{D2O}(*k*_{cat}/*K*_{ox})_D > ^{D2O}(*k*_{cat}/*K*_{ox})_H in **Table 6.1**), indicating that although small, the solvent KIE was significant. This is consistent with the transfer of the H⁺ originating from the solvent, or a solvent exchangeable site, being manifested in the transition state for flavin oxidation catalyzed by the enzyme. At both pL values, the ^D(*k*_{cat}/*K*_{ox})_{H2O} values were significantly >1 (**Table 6.1**), and

they increased further upon substituting H₂O with D₂O (${}^D(k_{\text{cat}}/K_{\text{ox}})_{\text{D}_2\text{O}} > {}^D(k_{\text{cat}}/K_{\text{ox}})_{\text{H}_2\text{O}}$ in **Table 6.1**). These data are consistent with transfer of the H from the flavin N5 atom also being manifested in the transition state for flavin oxidation. Multiple deuterium KIEs were consequently determined at pL 7.0 or 8.0 to elucidate whether the H and H⁺ transfer reactions occurred in the same or in different kinetic steps. The ${}^{\text{D,D}_2\text{O}}(k_{\text{cat}}/K_{\text{ox}})$, which represents the effect of substituting choline in H₂O with 1,2-[²H₄]-choline in D₂O, was slightly larger than the product of the individual substrate and solvent KIEs (${}^{\text{D,D}_2\text{O}}(k_{\text{cat}}/K_{\text{ox}}) > {}^D(k_{\text{cat}}/K_{\text{ox}})_{\text{H}_2\text{O}} \times {}^{\text{D}_2\text{O}}(k_{\text{cat}}/K_{\text{ox}})_{\text{H}}$ in **Table 6.1**). These data rule out H and H⁺ transfers occurring on separate kinetic steps, for which multiple KIEs would be smaller than the product of the individual KIEs, and either substrate or solvent KIEs would have lower values when H₂O is substituted with D₂O or choline is substituted with 1,2-[²H₄]-choline, respectively (29, 30). Thus, a mechanism in which a C4a-hydroperoxy flavin is an intermediate in the oxidative pathway of reaction (**Scheme 6.1: route a-b-e**), i.e., for which H and H⁺ transfers would occur on separate kinetic steps, is ruled out.

Both the effects of isotopic substitution on the KIEs and the multiple KIEs are consistent with the H and H⁺ transfers from the flavin and the solvent (or a solvent exchangeable site) to O₂ occurring in the same kinetic step, in a synchronous (31) fashion. Furthermore, the enhancement of the measured individual KIE in the presence of the second isotopic substitution and of the multiple KIE with respect to the product of the individual KIEs are consistent with one step slowing down due to the effect of the isotopic substitution of the atom participating in the other bond cleavage, thereby making the isotope sensitive kinetic step of O₂ reduction more limiting in the oxidative half-reaction (29). Mechanisms for flavin oxidation that bypass formation of a C4a-hydroperoxy flavin (**Scheme 6.1: route a-c**) or go through an anionic C4a-peroxy flavin intermediate (**Scheme 6.1: route a-d-f**), i.e., in which H and H⁺ transfers occur in the same kinetic step, are

thus consistent with the observed KIEs on the $k_{\text{cat}}/K_{\text{ox}}$ values. In this regard, stabilization of an anionic C4a-peroxy flavin during oxidation of the flavin hydroquinone has been previously reported in cyclohexanone monooxygenase (11) and the oxygenase component of p-hydroxyphenylacetate 3-hydroxylase (32), where the enzyme-bound flavin species have pK_{a} s of 8.4 and >10.0 , respectively (11, 32). However, if an anionic C4a-peroxy flavin transiently forms in choline oxidase its pK_{a} would need to be significantly <6 , since no ionizable groups are seen in the pH profile of $k_{\text{cat}}/K_{\text{ox}}$ with choline (20).

Time-resolved absorbance spectroscopy of flavin oxidation

If an anionic C4a-peroxy flavin were an obligatory intermediate during the oxidation of the hydroquinone in choline oxidase (**Scheme 6.1, route a-d-f**), it would transiently accumulate during the oxidation of the reduced flavin, allowing for its spectrophotometric detection. Stabilization of a C4a-(hydro)peroxy flavin has been recently reported in pyranose 2-oxidase (12). In order to establish whether an anionic C4a-peroxy flavin is a reaction intermediate in the oxidative pathway, choline oxidase was mixed with a 1.4 molar excess of 1,2- $^{2}\text{H}_4$ -choline in a double-mixing stopped-flow spectrophotometer equipped with photodiode array detection, allowed to age until complete flavin reduction was achieved and then mixed with various concentrations of O_2 in deuterated buffered solution at pL 7.0 and 25 °C. Deuterated solvent and substrate, rather than choline and H_2O , were used in order to allow for a higher accumulation of the potential flavin intermediate in the oxidative half-reaction. Under these conditions, the oxidation of the enzyme-bound flavin proceeded without formation of any intermediate (Figure 2A-B). In agreement with the lack of observable intermediates, a global fitting analyses of the time-resolved absorbance spectra yielded best results with an A->B kinetic model (**Figure 6.2A, inset**). These results are not consistent with

the chemical mechanism in which an anionic C4a-peroxyflavin is a reaction intermediate (**Scheme 6.1, route a-d-f**). Recent kinetic and computational studies on the oxidation of aryl-alcohol oxidase showed lack of intermediates with the spectral properties of a C4a-intermediate, consistent with formation of such a species not being seen in that enzyme (33).

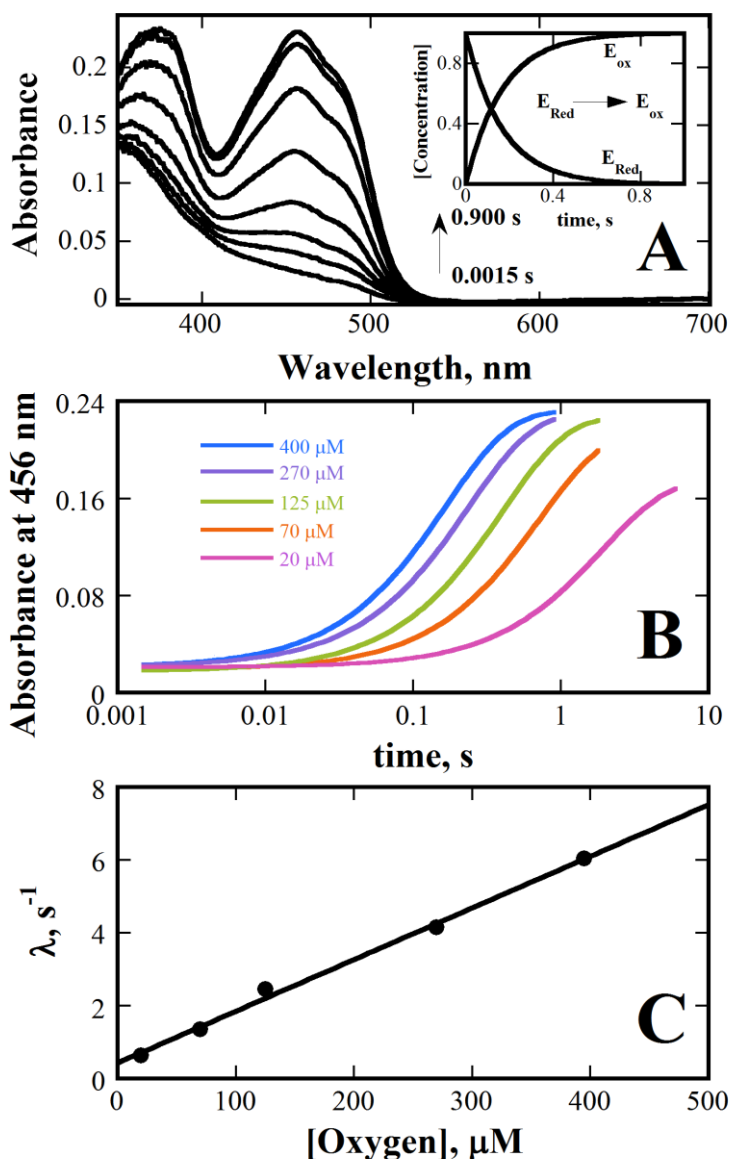


Figure 6.2 Time-resolved absorbance spectroscopy of the oxidation of reduced choline oxidase with O_2 . Anaerobic enzyme was pre-mixed with anaerobic 1,2- $^{2}\text{H}_4$ -choline (1.4 molar excess),

allowed to age until complete flavin reduction was achieved, and mixed with varying concentrations of O_2 in a double mixing stopped-flow spectrophotometer equipped with PDA detection. Conditions: enzyme (24 μ M after double mixing) in 50 mM sodium phosphate, pD 7.0 and 25 °C. All indicated times are after the end of flow, i.e., 2.2 ms. Panel A: selected time-resolved absorbance spectra upon mixing reduced enzyme with 0.4 mM O_2 ; inset: multivariate analysis of the time-resolved spectra to an A \rightarrow B kinetic model using SPECFIT/32, where E_{red} and E_{ox} are the reduced and oxidized enzymes, respectively. Panel B: traces at 456 nm at varying $[O_2]$. Panel C: plot of the observed λ values as a function of $[O_2]$, which were fit to a linear function yielding $y = 0.014x + 0.4$ ($R^2=0.996$).

The steady-state KIEs showed that the decay of the flavosemiquinone/ $O_2^{\cdot -}$ radical pair is at least partially rate limiting in the oxidative half-reaction. This suggests that a neutral flavosemiquinone intermediate should be observed when the reduced enzyme is reacted with O_2 (**Scheme 6.1: route a-c**). However, this is not the case (**Figure 6.2**). This apparent discrepancy can be explained with the effect of increasing solvent viscosity on the normalized k_{cat}/K_{ox} values (**Figure 6.1B**). Indeed, the inverse hyperbolic pattern to a limiting value of the normalized k_{cat}/K_{ox} with increasing glycerol concentration demonstrates that the solvent effect does not originate from diffusion of O_2 to the reactive site, for which linear dependencies with slopes between 0 and +1 are expected, but rather with a slow isomerization of the reduced enzyme (34). A slow isomerization of the reduced enzyme would mask subsequent kinetic events, i.e., formation and decay of the flavosemiquinone/ $O_2^{\cdot -}$ radical pair, resulting in lack of detection of the flavosemiquinone and decreased values for the KIEs.

In conclusion, pH, solvent viscosity and KIEs, as well as time-resolved absorbance spectroscopy of the oxidative half-reaction, have been used in this study to elucidate the relative timing of H and H⁺ transfers in the reaction of flavin oxidation catalyzed by choline oxidase. The results rule out a mechanism in which a C4a-hydroperoxy flavin forms in the oxidative pathway, for which H and H⁺ transfers are not synchronous, while time-resolved absorbance spectroscopy showed the lack of detection of an anionic C4a-peroxy flavin. In contrast, the results of the mechanistic investigation are consistent with a mechanism for O₂ reduction to H₂O₂ in which the H from the reduced flavin N5 atom and a H⁺ from either the solvent or a solvent exchangeable site in the active site of the enzyme are transferred in the same kinetic step without any flavin-derived transient intermediates (**route a-c in Scheme 6.1**). This study represents the first instance in which the synchronous timing of H and H⁺ transfers in the oxidation of a flavin was established in a flavoprotein oxidase. It complements previous studies on choline oxidase and other oxidases in which the mechanism for O₂ activation was probed with mechanistic tools (4, 16, 17, 35-38). This study provides also a framework for future studies on choline oxidase that will be aimed at the elucidation of the contribution of active site residues towards reduction of O₂.

6.5 References

1. Massey, V. (1994) Activation of molecular oxygen by flavins and flavoproteins, *J. Biol. Chem.* 269, 22459-22462.
2. Mattevi, A. (2006) To be or not to be an oxidase: challenging the oxygen reactivity of flavoenzymes, *Trends Biochem. Sci.* 31, 276-283.
3. Halliwell, B., and Gutteridge, J. M. (1984) Oxygen toxicity, oxygen radicals, transition metals and disease, *Biochem. J.* 219, 1-14.

4. Klinman, J. P. (2007) How do enzymes activate oxygen without inactivating themselves?, *Acc. Chem. Res.* *40*, 325-333.
5. Chaiyen, P., Fraaije, M. W., and Mattevi, A. (2012) The enigmatic reaction of flavins with oxygen, *Trends Biochem. Sci.* *37*, 373-380.
6. Eberlein, G., and Bruice, T. C. (1982) One and two electron reduction of oxygen by 1,5-dihydroflavins, *J. Am. Chem. Soc.* *104*, 1449-1452.
7. Ghisla, S., and Massey, V. (1989) Mechanisms of flavoprotein-catalyzed reactions, *Eur. J. Biochem.* *181*, 1-17.
8. Malmstrom, B. G. (1982) Enzymology of Oxygen, *Ann. Rev. Biochem.* *51*, 21-59.
9. Pennati, A., and Gadda, G. (2010) Stabilization of an Intermediate in the Oxidative Half Reaction of Human Liver Glycolate Oxidase, *Biochemistry*.
10. Palfey, B. A., and McDonald, C. A. (2010) Control of catalysis in flavin-dependent monooxygenases, *Arch. Biochem. Biophys.* *493*, 26-36.
11. Sheng, D., Ballou, D. P., and Massey, V. (2001) Mechanistic studies of cyclohexanone monooxygenase: chemical properties of intermediates involved in catalysis, *Biochemistry* *40*, 11156-11167.
12. Sucharitakul, J., Wongnate, T., and Chaiyen, P. (2011) Hydrogen peroxide elimination from C4a-hydroperoxyflavin in a flavoprotein oxidase occurs through a single proton transfer from flavin N5 to a peroxide leaving group, *J. Biol. Chem.* *286*, 16900-16909.
13. Thotsaporn, K., Chenprakhon, P., Sucharitakul, J., Mattevi, A., and Chaiyen, P. (2011) Stabilization of C4a-hydroperoxyflavin in a two-component flavin-dependent monooxygenase is achieved through interactions at flavin N5 and C4a atoms, *J. Biol. Chem.* *286*, 28170-28180.

14. Mallett, T. C., and Claiborne, A. (1998) Oxygen reactivity of an NADH oxidase C42S mutant: evidence for a C(4a)-peroxyflavin intermediate and a rate-limiting conformational change, *Biochemistry* 37, 8790-8802.
15. Roth, J. P., Wincek, R., Nodet, G., Edmondson, D. E., McIntire, W. S., and Klinman, J. P. (2004) Oxygen isotope effects on electron transfer to O₂ probed using chemically modified flavins bound to glucose oxidase, *J. Am. Chem. Soc.* 126, 15120-15131.
16. Roth, J. P., and Klinman, J. P. (2003) Catalysis of electron transfer during activation of O₂ by the flavoprotein glucose oxidase, *Proc. Natl. Acad. Sci. U. S. A.* 100, 62-67.
17. Gadda, G. (2012) Oxygen activation in flavoprotein oxidases: the importance of being positive, *Biochemistry* 51, 2662-2669.
18. Gadda, G., Fan, F., and Hoang, J. V. (2006) On the contribution of the positively charged headgroup of choline to substrate binding and catalysis in the reaction catalyzed by choline oxidase, *Arch. Biochem. Biophys.* 451, 182-187.
19. Fan, F., Ghanem, M., and Gadda, G. (2004) Cloning, sequence analysis, and purification of choline oxidase from *Arthrobacter globiformis*: a bacterial enzyme involved in osmotic stress tolerance, *Arch. Biochem. Biophys.* 421, 149-158.
20. Ghanem, M., Fan, F., Francis, K., and Gadda, G. (2003) Spectroscopic and kinetic properties of recombinant choline oxidase from *Arthrobacter globiformis*, *Biochemistry* 42, 15179-15188.
21. Schowen, K. B., Schowen, R.L. (1982) *In Meth. Enzymol.*, Vol. 87, Academic press, New York.
22. Lide, D. R. (2000) *Handbook of Chemistry and Physics*, 81 ed., CRC Press, Boca Raton, FL.

23. Fan, F., and Gadda, G. (2005) Oxygen- and temperature-dependent kinetic isotope effects in choline oxidase: correlating reversible hydride transfer with environmentally enhanced tunneling, *J. Am. Chem. Soc.* *127*, 17954-17961.
24. Fan, F., and Gadda, G. (2005) On the catalytic mechanism of choline oxidase, *J. Am. Chem. Soc.* *127*, 2067-2074.
25. Karsten, W. E., Lai, C.-J., and Cook, P. F. (1995) Inverse Solvent Isotope Effects in the NAD-Malic Enzyme Reaction Are the Result of the Viscosity Difference between D₂O and H₂O: Implications for Solvent Isotope Effect Studies, *J. Am. Chem. Soc.* *117*, 5914-5918.
26. Quinn, D. M. S., L. D. (1991) *In Enzyme Mechanism from Isotope Effects*, CRC press, Boca Raton, FL.
27. Schowen, K. B. S., R. L. (1982) *In Meth. Enzymol.*, Vol. 87, Academic Press, New York.
28. Ansari, A., Jones, C., Henry, E., Hofrichter, J., and Eaton, W. (1992) The role of solvent viscosity in the dynamics of protein conformational changes, *Science* *256*, 1796-1798.
29. Cleland, W. W. (1982) Use of isotope effects to elucidate enzyme mechanisms, *CRC Crit Rev Biochem* *13*, 385-428.
30. Edens, W. A., Urbauer, J. L., and Cleland, W. W. (1997) Determination of the Chemical Mechanism of Malic Enzyme by Isotope Effects[†], *Biochemistry* *36*, 1141-1147.
31. This study addresses the timing of H and H⁺ transfers, but not whether they are mechanistically coupled. Thus, synchronous is preferred to concerted because it defines events that occur at the same time, rather than events that are performed in cooperation.

32. Ruangchan, N., Tongsook, C., Sucharitakul, J., and Chaiyen, P. (2011) pH-dependent studies reveal an efficient hydroxylation mechanism of the oxygenase component of p-hydroxyphenylacetate 3-hydroxylase, *J. Biol. Chem.* *286*, 223-233.
33. Hernández-Ortega, A., Lucas, F., Ferreira, P., Medina, M., Guallar, V., and Martínez, A. T. (2012) Role of Active Site Histidines in the Two Half-Reactions of the Aryl-Alcohol Oxidase Catalytic Cycle, *Biochemistry* *51*, 6595-6608.
34. Yuan, H., Xin, Y., Hamelberg, D., and Gadda, G. (2011) Insights on the Mechanism of Amine Oxidation Catalyzed by d-Arginine Dehydrogenase Through pH and Kinetic Isotope Effects, *J. Am. Chem. Soc.* *133*, 18957-18965.
35. Bruckner, R. C., Winans, J., and Jorns, M. S. (2011) Pleiotropic impact of a single lysine mutation on biosynthesis of and catalysis by N-methyltryptophan oxidase, *Biochemistry* *50*, 4949-4962.
36. McDonald, C. A., Fagan, R. L., Collard, F., Monnier, V. M., and Palfey, B. A. (2011) Oxygen reactivity in flavoenzymes: context matters, *J. Am. Chem. Soc.* *133*, 16809-16811.
37. Roth, J. P. (2009) Oxygen Isotope Effects as Probes of Electron Transfer Mechanisms and Structures of Activated O₂, *Acc. Chem. Res.* *42*, 399-408.
38. Zhao, G., Bruckner, R. C., and Jorns, M. S. (2008) Identification of the oxygen activation site in monomeric sarcosine oxidase: role of Lys265 in catalysis, *Biochemistry* *47*, 9124-9135.

7 GENERAL DISCUSSION AND CONCLUSIONS

In general enzyme catalyzed biochemical reactions are a result of high specificity of an enzyme for a given substrate. This unique quality of enzymes sets apart biochemical reactions from regular chemical reactions which are usually prone to side reactions. Active-site residue(s) play important roles in affording such selectivity to enzymes. One aspect in this dissertation has dealt with dissecting the contribution of charges in substrate selectivity and specificity using FAD dependent PaDADH as a model. Efforts have also been made to understand the catalytic mechanism outlining substrate (amino acid) oxidation in PaDADH. Hydroxylation of FAD cofactor has been reported in a few flavin-dependent enzymes. However a consensus has not been reached in terms of the factors contributing to its formation and its relevance henceforth. Using a mutant variant of PaDADH, this dissertation attempts to contribute toward understanding a different aspect of flavin-dependent enzymes i.e. susceptibility of flavins to modifications (hydroxylation in particular) in enzyme active-sites thereby altering their reactivity. Another aspect of flavoenzyme chemistry that receives considerable attention is their reactivity with molecular oxygen; one part of this dissertation addresses the reactivity of reduced FAD with molecular oxygen using choline oxidase, a representative member of the Glucose-Methanol-Choline Superfamily.

As more structural and mechanistic data are becoming available for PaDADH, we can better understand the roles of different active-site residues in the context of the reaction catalyzed by PaDADH.¹⁻³ In chapter 3, one aspect of the reaction catalyzed by PaDADH that we expanded upon is the reactivity with cationic and zwitterionic D-amino acids. Previous structural studies on the enzyme suggested Glu87 to be an important residue in substrate binding.³ Based on the pH effects on k_{cat} and $k_{\text{cat}}/K_{\text{m}}$ for cationic D-Arg and D-Lys and zwitterionic D-Met and D-Leu, a group with

an apparent $pK_a \geq 7.9$ is seen in the binding of only the cationic substrates. Glu87 has emerged as the candidate that provides the point charge stabilization for tight binding, yielding k_{cat}/K_m values of $\geq 10^5 \text{ M}^{-1}\text{s}^{-1}$ observed for D-Arg and D-Lys³ over other D-amino acids in PaDADH. A group with a true pK_a of ~ 9.5 exemplifies general base catalysis with any of the four substrates tested; His48 or Tyr53 have emerged as likely candidates proposed to act as active site base by virtue of their placement in active site. D-Leu emerged as a non-sticky substrate for catalysis from lack of pH dependence of the substrate KIE generally accepted as lacking any external commitments (stickiness in other words) while D-Arg and D-Lys turned out to be sticky with a pK_a that is < 9.5 in either k_{cat} or k_{cat}/K_m . This study offered an understanding of the broad substrate specificity manifested by PaDADH at the level of active-site interactions. Notwithstanding, framework has been laid for unfolding the catalytic contribution of His48, Tyr53, Glu87 and Tyr249 lining the active site of PaDADH using site-directed mutagenesis in combination with other mechanistic probes.

Chapter 4 expounds the roles of Tyr53 and Tyr249 using site-directed mutagenesis as the mainstay in combination with several mechanistic and computational approaches to disclose their contribution in enzyme function and catalysis. Changes in pH of the buffer has no effect on the pK_a values of the groups involved in binding of the substrate (K_d) and chemical step (k_{red}) for Tyr53Phe and Tyr249Phe enzymes and hence neither is the proposed base to initiate catalysis for D-amino acid dehydrogenation by PaDADH. Deuterium isotope effects in combination with rapid-kinetics using a stopped-flow spectrophotometer that shed light on the isotope-sensitive NH and CH bonds were found to be rate determining for catalysis in the mutants as reported for the wild-type enzyme.¹ The timing of the NH and CH bond cleavages however underwent a small yet significant change from concerted asynchronous in wild-type¹ to concerted synchronous in the mutants as judged from the observations made using multiple deuterium kinetic isotope effects in this

study. Furthermore, time resolved absorbance spectroscopy showed no accumulation of any flavin-derived intermediates in the course of flavin reduction by the substrate (D-Leu) at 25 °C. Relative electrophilicity of the N5 and C4a sites of the flavin were determined using QM/MM methodologies and N5 atom emerged as the site where catalysis occurs on flavin due to lower electrophilicity in wild-type as well as *in silico* Tyr-249Phe and Tyr-53Phe mutants of PaDADH. Taken together, these results suggest that mutations of Tyr53 and Tyr249 to Phe do not affect the substrate binding cavity compared to the wild-type; N5 atom being the most electrophilic site and due to lack of any detectable flavin-based intermediates, the transfer of α -hydrogen has been proposed to take place as a hydride ion from the substrate (D-Leu) to N5 atom of flavin in PaDADH. The contributions made by this study are significant in the wake of lack of full understanding of amino acid dehydrogenation by flavoproteins.^{4, 5}

Chapter 5 focuses on the detection, isolation and characterization of novel 6-hydroxy-flavin⁶ from Tyr249Phe mutation of PaDADH. The 6-hydroxylation of flavin is only partial and not in stoichiometric amounts. The chromophores were separated through reversed-phase HPLC and characterized using UV-visible spectroscopy, ¹H and ¹³C NMR and mass spectrometry. Computational approaches such as QM/MM methodologies were sought to gain deeper understanding of the 6-OH-FAD formation within the context of PaDADH active site.

Choline oxidase catalyzes the oxygen-dependent conversion of choline to glycine betaine with a betaine aldehyde intermediate.⁷ The overall reaction involves the transfer of four e⁻ with 2e⁻ each from choline to FAD to produce betaine aldehyde and betaine aldehyde to FAD to produce glycine betaine.⁷⁻⁹ O₂ acts as the terminal electron acceptor from reduced FAD to regenerate it for further reaction and resulting in the production of H₂O₂. Flavin-dependent enzymes display a wide spectrum of reactivity toward O₂.¹⁰ While two classes of enzymes namely monooxygenases

and oxidases are characterized by rapid reaction rates with molecular O₂, others like dehydrogenases are known for their sluggish reactivity.¹⁰⁻¹⁴ While monooxygenases involve the formation of obligatory flavin-O₂ dependent intermediates (C4a-(hydro)peroxy intermediate),^{10, 12} it is attractive to extend the reaction mechanism to oxidases as well. However, to date, only pyranose-2 oxidase and a mutant of NADH oxidase from this class of enzymes have shown experimental evidence to involve a C4a-(hydro)peroxy intermediate in the course of reaction with O₂.¹⁵⁻¹⁷ Choline oxidase is a very well characterized member of the glucose-methanol-choline oxidoreductase family.^{7-9, 18-27} Previous studies on the enzyme relevant to oxygen reactivity showed that the positive charge that is required for stabilization of radicals and reactive oxygen species generated during the reaction of reduced flavin with O₂ is provided by the ligand and not an active site residue as has been initially proposed.^{9, 11, 23} Furthermore Val464 offers the hydrophobic patch required for oxygen to position and react at the C4a site of the flavin. Ser101 has also been found to be important for the oxidative half reaction. None of the studies however addressed the mechanism and involvement of any reaction intermediates in the reaction of reduced flavin with molecular oxygen. The overall reaction involves the transfer of a hydride-equivalent from reduced flavin and a solvent-exchangeable proton to O₂ to yield H₂O₂. Deuterium isotope effects showed that a H atom from the reduced flavin and a H⁺ from the solvent or solvent exchangeable site happen in the same kinetic step. Time resolved absorbance spectroscopy show no accumulation of flavin-derived species in the oxidation of flavin. Taken together, the results from this study allow us to eliminate oxidation of flavin involving stabilization of C4a-flavin intermediates in choline oxidase. With few exceptions, results from this study as well as others suggest that in oxidases lack of stabilization of reaction intermediates may be a key optimization strategy to diminish the potential leak of reactive oxygen species formed in the reaction pathway with O₂.

Work from this dissertation shed light on several fundamental questions associated with flavin chemistry using bacterial enzymes, D-arginine dehydrogenase and choline oxidase. While the mechanism of amino acid dehydrogenation has shown most likely to involve a hydride-ion transfer to flavin, it is only the second enzyme after D-amino acid oxidase with conclusive mechanistic data in favor of hydride transfer mechanism in either D/L- amino acid processing flavoenzymes. Furthermore, unexpectedly an active site mutation of the same enzyme resulted in the partial modification of flavin cofactor which raises important questions about the susceptibility of flavin cofactors in physiological set up to such unproductive modifications with a potential damaging outcome. One of the uniqueness of flavin chemistry is the reaction with O₂. While D-arginine dehydrogenase does not react with O₂, choline oxidase reacts rapidly and without stabilization of any detectable reaction intermediates in the process. The study also provided a first instance of synchronous transfer of H atom and H⁺ in the reaction of oxidation of flavin by a flavoprotein oxidase.

7.1 References

1. Yuan, H., Xin, Y., Hamelberg, D., and Gadda, G. (2011) Insights on the mechanism of amine oxidation catalyzed by D-arginine dehydrogenase through pH and kinetic isotope effects, *Journal of the American Chemical Society* 133, 18957-18965.
2. Yuan, H., Fu, G., Brooks, P. T., Weber, I., and Gadda, G. (2010) Steady-state kinetic mechanism and reductive half-reaction of D-arginine dehydrogenase from *Pseudomonas aeruginosa*, *Biochemistry* 49, 9542-9550.
3. Fu, G., Yuan, H., Li, C., Lu, C. D., Gadda, G., and Weber, I. T. (2010) Conformational changes and substrate recognition in *Pseudomonas aeruginosa* D-arginine dehydrogenase, *Biochemistry* 49, 8535-8545.

4. Fitzpatrick, P. F. (2010) Oxidation of amines by flavoproteins, *Archives of biochemistry and biophysics* 493, 13-25.
5. Fitzpatrick, P. F. (2001) Substrate dehydrogenation by flavoproteins, *Accounts of chemical research* 34, 299-307.
6. Ghisla, S., and Edmondson, D. E. (2001) Flavin Coenzymes, In *eLS*, John Wiley & Sons, Ltd.
7. Fan, F., and Gadda, G. (2005) On the catalytic mechanism of choline oxidase, *Journal of the American Chemical Society* 127, 2067-2074.
8. Fan, F., Ghanem, M., and Gadda, G. (2004) Cloning, sequence analysis, and purification of choline oxidase from *Arthrobacter globiformis*: a bacterial enzyme involved in osmotic stress tolerance, *Archives of biochemistry and biophysics* 421, 149-158.
9. Fan, F., Germann, M. W., and Gadda, G. (2006) Mechanistic studies of choline oxidase with betaine aldehyde and its isosteric analogue 3,3-dimethylbutyraldehyde, *Biochemistry* 45, 1979-1986.
10. Massey, V. (1994) Activation of molecular oxygen by flavins and flavoproteins, *The Journal of biological chemistry* 269, 22459-22462.
11. Gadda, G. (2012) Oxygen activation in flavoprotein oxidases: the importance of being positive, *Biochemistry* 51, 2662-2669.
12. Palfey, B. A., and McDonald, C. A. (2010) Control of catalysis in flavin-dependent monooxygenases, *Archives of biochemistry and biophysics* 493, 26-36.
13. Mattevi, A. (2006) To be or not to be an oxidase: challenging the oxygen reactivity of flavoenzymes, *Trends in biochemical sciences* 31, 276-283.

14. Chaiyen, P., Fraaije, M. W., and Mattevi, A. (2012) The enigmatic reaction of flavins with oxygen, *Trends in biochemical sciences* 37, 373-380.
15. Thotsaporn, K., Chenprakhon, P., Sucharitakul, J., Mattevi, A., and Chaiyen, P. (2011) Stabilization of C4a-hydroperoxyflavin in a two-component flavin-dependent monooxygenase is achieved through interactions at flavin N5 and C4a atoms, *The Journal of biological chemistry* 286, 28170-28180.
16. Sucharitakul, J., Wongnate, T., and Chaiyen, P. (2011) Hydrogen peroxide elimination from C4a-hydroperoxyflavin in a flavoprotein oxidase occurs through a single proton transfer from flavin N5 to a peroxide leaving group, *The Journal of biological chemistry* 286, 16900-16909.
17. Mallett, T. C., and Claiborne, A. (1998) Oxygen reactivity of an NADH oxidase C42S mutant: evidence for a C(4a)-peroxyflavin intermediate and a rate-limiting conformational change, *Biochemistry* 37, 8790-8802.
18. Yuan, H., and Gadda, G. (2011) Importance of a serine proximal to the C(4a) and N(5) flavin atoms for hydride transfer in choline oxidase, *Biochemistry* 50, 770-779.
19. Rungsriruriyachai, K., and Gadda, G. (2008) On the role of histidine 351 in the reaction of alcohol oxidation catalyzed by choline oxidase, *Biochemistry* 47, 6762-6769.
20. Quaye, O., Lountos, G. T., Fan, F., Orville, A. M., and Gadda, G. (2008) Role of Glu312 in binding and positioning of the substrate for the hydride transfer reaction in choline oxidase, *Biochemistry* 47, 243-256.
21. Quaye, O., Cowins, S., and Gadda, G. (2009) Contribution of flavin covalent linkage with histidine 99 to the reaction catalyzed by choline oxidase, *The Journal of biological chemistry* 284, 16990-16997.

22. Ghanem, M., and Gadda, G. (2005) On the catalytic role of the conserved active site residue His466 of choline oxidase, *Biochemistry* 44, 893-904.
23. Gadda, G., Fan, F., and Hoang, J. V. (2006) On the contribution of the positively charged headgroup of choline to substrate binding and catalysis in the reaction catalyzed by choline oxidase, *Archives of biochemistry and biophysics* 451, 182-187.
24. Finnegan, S., Yuan, H., Wang, Y. F., Orville, A. M., Weber, I. T., and Gadda, G. (2010) Structural and kinetic studies on the Ser101Ala variant of choline oxidase: catalysis by compromise, *Archives of biochemistry and biophysics* 501, 207-213.
25. Finnegan, S., Agniswamy, J., Weber, I. T., and Gadda, G. (2010) Role of valine 464 in the flavin oxidation reaction catalyzed by choline oxidase, *Biochemistry* 49, 2952-2961.
26. Fan, F., and Gadda, G. (2007) An internal equilibrium preorganizes the enzyme-substrate complex for hydride tunneling in choline oxidase, *Biochemistry* 46, 6402-6408.
27. Fan, F., and Gadda, G. (2005) Oxygen- and temperature-dependent kinetic isotope effects in choline oxidase: correlating reversible hydride transfer with environmentally enhanced tunneling, *Journal of the American Chemical Society* 127, 17954-17961.

Appendix

8 RESCUING OF THE HYDRIDE TRANSFER REACTION IN THE GLU312ASP VARIANT OF CHOLINE OXIDASE BY A SUBSTRATE ANALOGUE

(This chapter has been published verbatim in, Quaye,O., Nguyen,T., Gannavaram, S., Pennati,A., and Gadda,G., *Arch. Biochem. Biophys.* 499 (2010) 1-5)

8.1 Abstract

In the active site of choline oxidase, Glu312 participates in binding the trimethylammonium group of choline, thereby positioning the alcohol substrate properly for efficient hydride transfer to the enzyme-bound flavin. Previous studies have shown that substitution of Glu312 with aspartate results in a perturbed mechanism of hydride transfer, with a 260-fold decrease in the rate associated with the mutation. Here, the reaction of alcohol oxidation catalyzed by the Glu312Asp enzyme has been investigated with 3-hydroxypropyl-trimethylamine (3-HPTA), a choline analogue with an extra methylene, as substrate. The results of the kinetic investigation using steady state and rapid reaction approaches showed that the impaired ability of the Glu312Asp enzyme to catalyze a hydride transfer reaction can be effectively, but not completely, rescued in the presence of an extra methylene group on the substrate that compensates for the equivalent shortening of the side chain on residue 312. This observation is consistent with choline oxidase having evolved to optimally catalyze the oxidation of choline.

8.2 Introduction

Choline oxidase (E.C. 1.1.3.17; choline-oxygen 1-oxidoreductase) catalyzes the flavin-mediated, two-step oxidation of choline to glycine betaine with formation of betaine aldehyde as intermediate [1]. Both the oxidation of the alcohol substrate and the aldehyde intermediate require molecular oxygen to accept electrons from the reduced flavin [2, 3]. The reaction catalyzed by choline oxidase is of importance due to the trigger of glycine betaine accumulation in the cytoplasm of a number of plants and pathogenic bacteria in response to hyperosmotic and adverse temperature conditions to prevent dehydration and eventual cell death [4-11]. Thus, a better understanding of the reaction catalyzed by choline oxidase has potential for the development of therapeutic agents targeting the glycine betaine biosynthetic pathway for the management of microbial infections. Also, crops lacking the ability to cope with hyperosmotic environments and salt accumulation can be genetically engineered with choline oxidase to withstand adverse environmental conditions [7-11]. Finally, choline oxidase has been emerging as a model for deciphering the mechanism of alcohol oxidation catalyzed by flavin-dependent enzymes [1].

In *Arthrobacter globiformis* choline oxidase, the oxidation of choline involves a hydride transfer mechanism from the α -carbon of an activated, alkoxide species that is enzymatically produced by deprotonation of the substrate hydroxyl group, as suggested by substrate and solvent kinetic isotope effects [12]. In the wild-type enzyme, a highly preorganized enzyme-alkoxide complex allows for a quantum mechanical transfer of the hydride ion, as indicated by temperature effects on the reductive half-reaction [13]. In mutant enzymes where independent movement of the substrate α -carbon and the flavin N(5) atom is permitted, the hydride transfer reaction involves either sampling of the reactive configuration or an over-the-barrier transition state [14, 15].

The crystal structure of choline oxidase recently resolved to 1.86 Å revealed Glu312 as the only negatively charged residue in the active site of the enzyme [16]. This residue was shown to participate in substrate binding with the positively charged trimethylammonium group of choline, as indicated by the 500-fold increase in the K_d value for choline upon mutating Glu312 with glutamine [16]. The importance of spatial location of the negative charge for the correct positioning of the substrate in the active site of the enzyme was demonstrated in a choline oxidase variant in which Glu312 was replaced with aspartate. The Glu312Asp enzyme showed a 260-fold decrease in the rate constant for the hydride transfer reaction and did not transfer the hydride ion in a full quantum mechanical tunneling fashion [14, 16]. In the present study, the reaction of alcohol oxidation catalyzed by the Glu312Asp enzyme has been investigated with 3-hydroxypropyl-trimethylamine (3-HPTA), a choline analogue with an extra methylene, as substrate (**Figure 8.1**). The results of the kinetic investigation indicate that the reductive half-reaction can be effectively, but not completely, rescued upon introducing on the substrate the methylene that is missing from the side chain of residue 312.

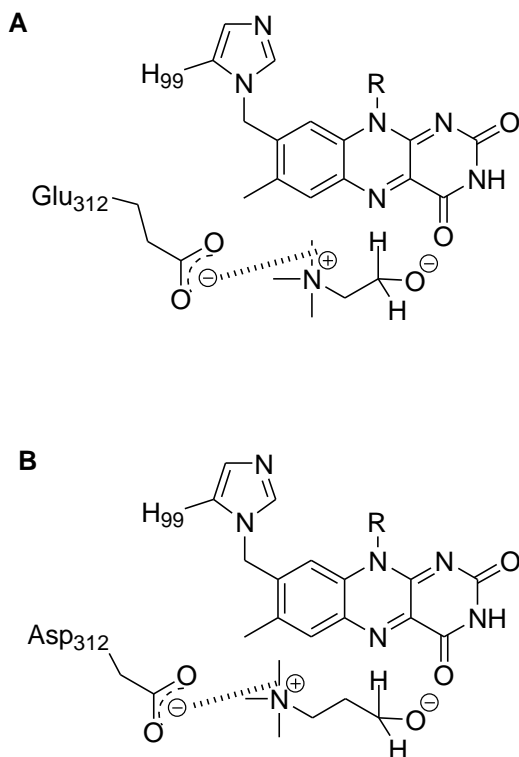


Figure 8.1 The interaction between the carboxylate on residue 312 of choline oxidase and the trimethylammonium moiety of the activated substrate. A, wild-type enzyme and choline; B, Glu312Asp enzyme and 3-HPTA.

8.3 Experimental Procedures

The Glu312Asp variant of choline oxidase was purified according to Quaye et al. [16]. Choline was from ICN Pharmaceutical Inc. (Irvine, CA); 3-HPTA was from Sigma-Aldrich (St. Louis, MO). All other reagents were of the highest purity commercially available.

The reductive half-reaction of the Glu312Asp enzyme with 3-HPTA as substrate was studied using a Hi-Tech SF-61KinetAsyst high performance stopped-flow spectrophotometer thermostated at 25 °C, in 50 mM sodium pyrophosphate, pH 10.0, under anaerobic conditions, as previously described [16]. The rate constants for flavin reduction were measured by monitoring the decrease in absorbance at 450 nm upon mixing the oxidized enzyme with the organic substrate.

Glucose and glucose oxidase at final concentrations of 0.5 μM and 5 mM, respectively, were added to the enzyme and substrate to scavenge traces of oxygen that may be present before mixing. Equal volumes of enzyme and 3-HPTA were anaerobically mixed in the stopped-flow spectrophotometer resulting in a reaction mixture with a final enzyme concentration of $\sim 10 \mu\text{M}$ and substrate concentrations of 0.1 to 15 mM, with each substrate concentration assayed in triplicate.

Steady state kinetics were measured by the method of initial rates in 50 mM sodium pyrophosphate by monitoring the rate of oxygen consumption with a computer-interfaced Oxy-32 oxygen monitoring system (Hansatech Instrument Inc.) at 25 °C, as described previously [12]. The measurements were carried out at varying concentrations of both 3-HPTA (0.1-10 mM) and oxygen (0.2-1 mM). The desired oxygen concentration for each assay was obtained upon blowing an appropriate O_2/N_2 gas mixture for a minimum of 10 min to equilibrate the reaction mixture. All assays were performed in 50 mM sodium pyrophosphate, with the exception of pH 7.0 where potassium phosphate was used.

Data were fit with KaleidaGraph (Synergy Software, Reading, PA), EnzFitter (Biosoft, Cambridge, UK), and the Hi-Tech Studio Software Suite (Hi-Tech Scientific, Bradford on Avon, U.K.) software. Stopped-flow traces were fit to eq 1, which describes a double-exponential process with $k_{\text{obs}1}$ and $k_{\text{obs}2}$ representing the observed rate constants for the fast and slow phases; t is time, A is the absorbance at 450 nm at any given time, B and C are the amplitudes of the total change in absorbance for the fast and slow phases, and D is the absorbance at infinite time. Pre-steady state kinetic parameters were determined by fitting the observed rate constants to eq 2, where $k_{\text{obs}1}$ is the observed rate constant for the reduction of the enzyme bound flavin, k_{red} is the limiting rate constant of flavin reduction at saturated substrate concentration and K_d is the dissociation constant for binding of the substrate to the enzyme.

$$A = Be^{-k_{obs}t} + Ce^{-k_{obs}t} + D \quad (1)$$

$$k_{obs} = \frac{k_{red}[3-HPTA]}{K_d + [3-HPTA]} \quad (2)$$

Steady state kinetic parameters were determined by fitting the initial rate data for pH 9.0 and 10.0 to eq 3, which describes a sequential steady state kinetic mechanism where $K_{[3-HPTA]} < K_b K_{ia}$. Initial rates determined in the pH range from 5.5 to 8.0 were fit to eq 4, which describes a sequential steady state kinetic mechanism. In eqs 3 and 4, e represents the concentration of enzyme, k_{cat} is the turnover number of the enzyme at saturating concentrations of 3-HPTA and oxygen, and K_{3-HPTA} and K_{O_2} represent the Michaelis constants for 3-HPTA and oxygen, respectively.

$$\frac{v}{e} = \frac{k_{cat}[3-HPTA][O_2]}{K_{O_2}[3-HPTA] + [3-HPTA][O_2] + K_{ia}K_{O_2}} \quad (3)$$

$$\frac{v}{e} = \frac{k_{cat}[3-HPTA][O_2]}{K_{3HPTA}[O_2] + K_{O_2}[3-HPTA] + [3-HPTA][O_2] + K_{ia}K_{O_2}} \quad (4)$$

The pH dependences of the steady state kinetic parameters were determined by fitting the initial rate data to eq 5, which describes a curve with a slope of + 1 and a plateau region at high pH, where C is the pH-independent value of the kinetic parameter that was measured (Y).

$$\log Y = \log \left[\frac{C}{1 + \frac{10^{-pH}}{10^{-pK_a}}} \right] \quad (5)$$

8.4 Results

The reductive half-reaction of the Glu312Asp variant of choline oxidase with 3-HPTA as substrate was investigated in a stopped-flow spectrophotometer at pH 10.0 and 25 °C. The choice of pH 10.0 stems from previous studies showing that at this pH the reaction catalyzed by the Glu312Asp enzyme is independent of pH [16]. As shown in **Figure 8.2A** the absorbance at 450 nm decreased in a double exponential fashion with a fast phase accounting for >95% of the total change. The observed rate constants for the slow phase ($k_{\text{obs}2}$) were independent of the concentration of 3-HPTA, with an average value of $\sim 0.1 \text{ s}^{-1}$. Such a value is significantly lower than the rate constant defining the overall turnover of the enzyme at saturating concentrations of 3-HPTA, with a value of 5 s^{-1} at pH 10.0. This is consistent with the slow phase of flavin reduction, which probably reflects the slow dissociation of the aldehyde product of the oxidation of choline from the reduced enzyme, not being part of the catalytic pathway of the enzyme. The observed rate constants for the fast phase ($k_{\text{obs}1}$) were hyperbolically dependent on the concentration of 3-HPTA (**Figure 8.2B**), allowing for the determination of the limiting rate constant for flavin reduction at saturating substrate concentration (k_{red}) and the macroscopic dissociation constant for substrate binding to the enzyme (K_{d}). As shown in Table 1, the k_{red} value with 3-HPTA was 20-times higher than the value determined with choline as substrate for the Glu312Asp enzyme [16]. In contrast, there were no differences in the K_{d} values with the two substrates with the Glu312Asp enzyme. The reductive half-reaction of the wild-type enzyme with 3-HPTA was also investigated at pH 10.0 and 25 °C. As illustrated in **Table 8.1**, the k_{red} and K_{d} values with 3-HPTA as substrate for the wild-type enzyme were 4- and 10-times larger than the corresponding parameters determined with the physiological substrate choline. The second-order rate constants for the capture of the

organic substrate onto enzyme complexes committed to flavin reduction (k_{red}/K_d) could be calculated from the k_{red} and K_d values determined in the stopped-flow spectrophotometer. As illustrated in **Table 8.1**, the k_{red}/K_d values increased 20-fold when choline was substituted with 3-HPTA as substrate for the Glu312Asp enzyme. A further 2-fold increase was seen upon substituting the Glu312Asp enzyme with the wild-type enzyme when 3-HPTA was used a substrate. Finally, another 2-fold increase was determined when 3-HPTA was substituted with choline as substrate for the wild-type enzyme.

The steady state kinetic parameters for the Glu312Asp enzyme with 3-HPTA were also investigated in the accessible pH range, by measuring initial rates of oxygen consumption at varying concentrations of 3-HPTA and oxygen. The $K_{3\text{-HPTA}}$ values could be determined only at $\text{pH} \leq 8.0$, where the kinetic data determined at varying concentrations of 3-HPTA and oxygen fit best to a sequential steady state kinetic mechanism (eq 4). In contrast, at $\text{pH} \geq 9.0$ the best fit of the data was obtained with eq 3, which describes a sequential mechanism where $K_{[3\text{-HPTA}]} < K_b K_{\text{ia}}$, as for the case previously reported for the wild-type enzyme with betaine aldehyde as substrate [3, 17, 18]. This allowed for a limited range of pH values for the pH profile of the $k_{\text{cat}}/K_{3\text{-HPTA}}$ value. As shown in Figure 3, the $k_{\text{cat}}/K_{3\text{-HPTA}}$ values increased with increasing pH to a limiting value, defining a $\text{p}K_a$ for an unprotonated group required for catalysis ≤ 7.0 . This value was significantly lower than the value of 7.5 determined for either wild-type choline oxidase or the Glu312Asp enzyme with choline [13, 16]. The pH profile for the k_{cat} value showed the presence of an ill-defined $\text{p}K_a \leq 6.0$, which was significantly lower than the value of 7.3 reported with choline as substrate for the wild-type enzyme (**Figure 8.3**) {Fan, 2005 #9}. Finally, the pH profile for the $k_{\text{cat}}/K_{\text{oxygen}}$ values with 3-HPTA and the Glu312Asp enzyme were pH-independent ≥ 7.0 , slightly decreasing at lower pH values (**Figure 8.3**). In all cases, the pH-independent values of the kinetic parameters with 3-HPTA

as substrate for the Glu312Asp enzyme were about one order of magnitude lower than the corresponding values determined with choline as substrate for the wild-type enzyme (**Figure 8.3**).

Table 8.1 Reductive Half-Reaction with Choline and 3-HPTA as Substrate for Choline Oxidase Wild-type and Glu312Asp Variant.

Enzyme	Substrate	k_{red} (s^{-1})	K_{d} (mM)	$k_{\text{red}}/K_{\text{d}}^{\text{a}}$ ($\text{M}^{-1}\text{s}^{-1}$)
Glu312Asp	Choline	0.36 ± 0.01	~0.1	~3,600
Glu312Asp	3-HPTA	7.5 ± 0.1	~0.1	~75,000
Wild-type	3-HPTA	400 ± 8	2.8 ± 0.2	144,000
Wild-type	Choline	93 ± 1	0.29 ± 0.01	320,000

^a Calculated from the k_{red} and K_{d} values.

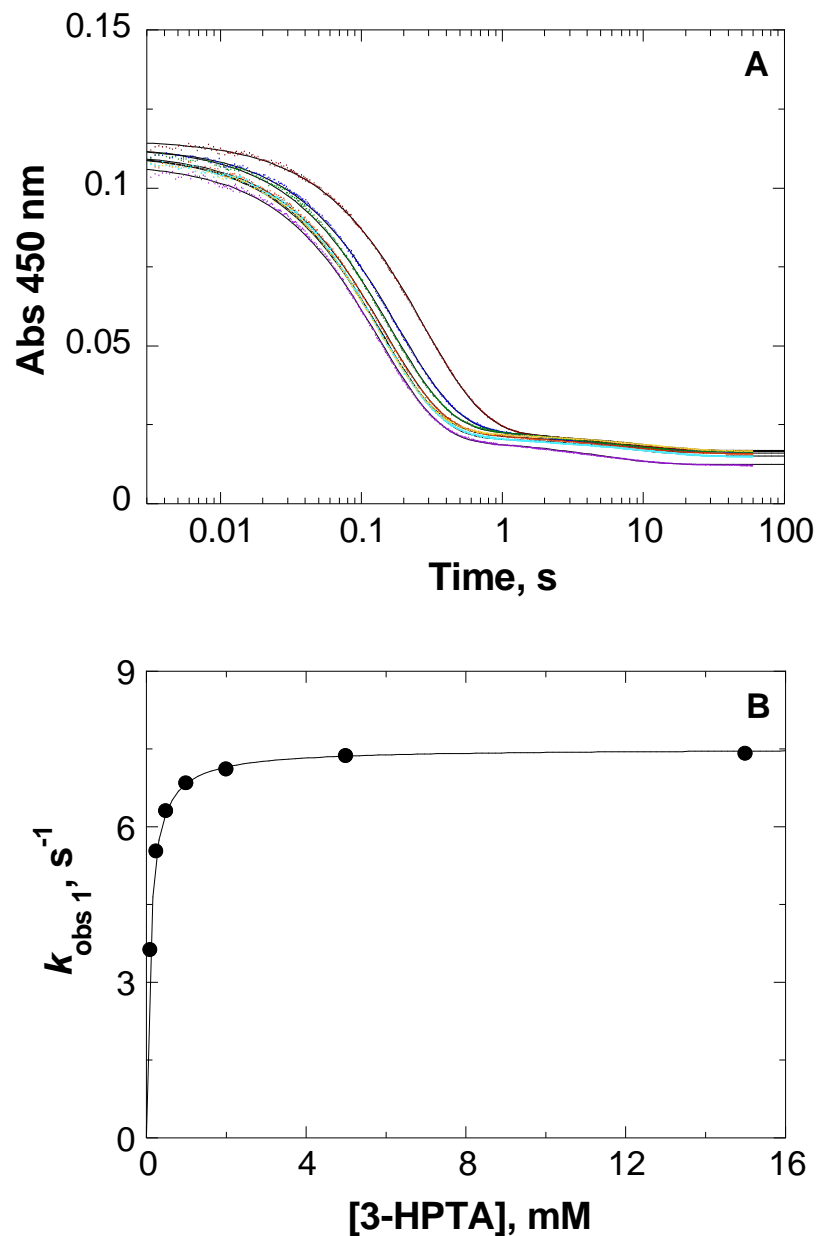


Figure 8.2 Reductive half-reaction of the Glu312Asp enzyme with 3-HPTA Stopped-flow traces were obtained at 450 nm upon mixing anaerobically the enzyme and substrate under pseudo first-order conditions at pH 10.0 and 25 °C. Panel A, traces obtained with, 0.01, 0.25, 0.5, 0.1, 0.2, 0.5 15 mM 3-HPTA; the time indicated is after the end of flow, i.e., 2.2 ms; the solid curves represent the fit of the data to eq 1. Panel B, dependence of the k_{obs1} values on [3-HPTA]; the solid curve represents the fit of the data to eq 2

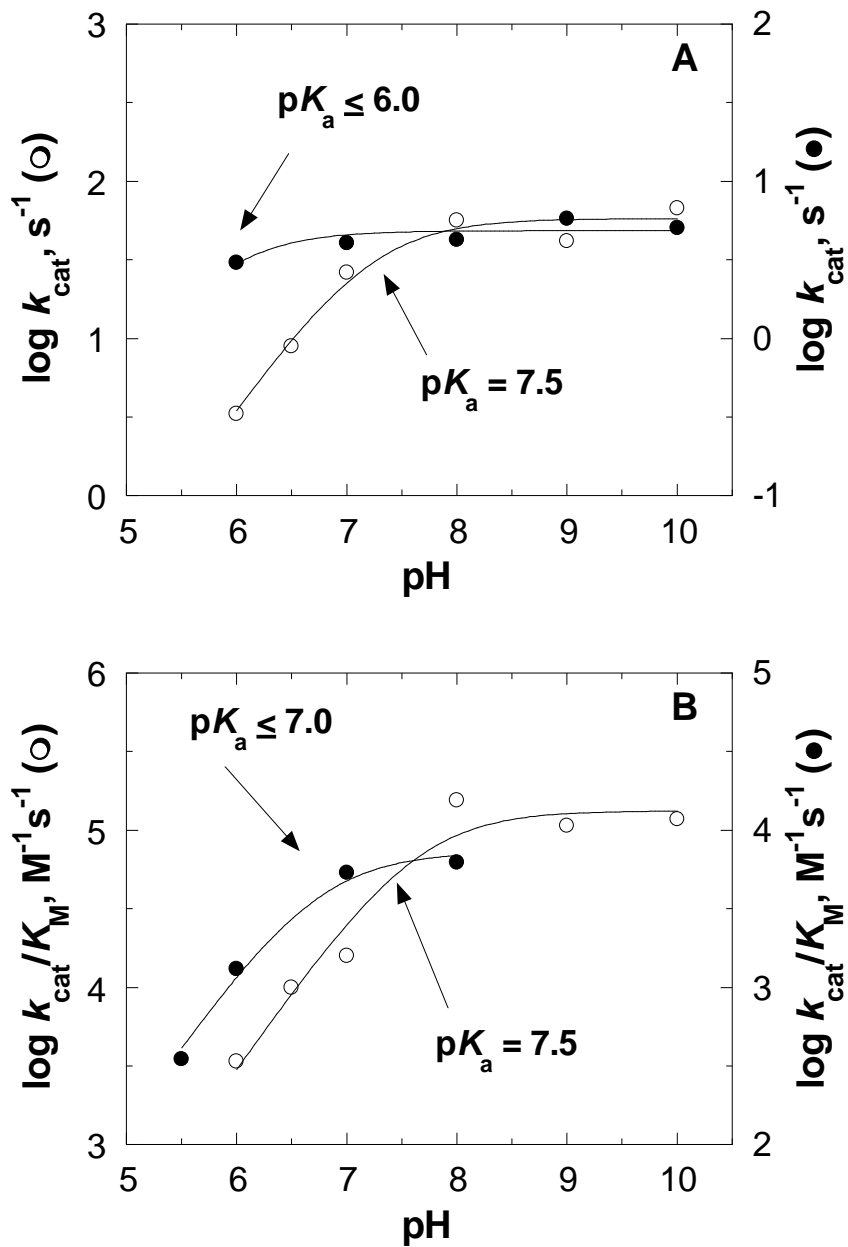


Figure 8.3 pH-dependence of the steady-state kinetic parameters for wild-type choline oxidase (empty circles) with choline and Glu312Asp enzyme (solid circles) with 3-HPTA as substrate. The curves were obtained by fitting the data to eq 5.

8.5 Discussion

A recent study established that the conservative replacement of Glu312 with aspartate perturbs the mechanism of hydride transfer in the reaction catalyzed by choline oxidase, therefore underscoring the importance of substrate positioning in the active site of an enzyme for efficient catalysis [14]. In the wild-type enzyme, the hydride ion tunnels within a highly preorganized enzyme-substrate complex at a rate of 93 s^{-1} with minimal assistance from the environment [13, 19]. In the Glu312Asp enzyme the same reaction occurs at a rate of 0.36 s^{-1} through either environmentally coupled tunneling within an enzyme-substrate complex that is not preorganized or without tunneling [14]. In the present study, we have used a substrate analogue with an extra $-\text{CH}_2-$ group as compared to choline to establish whether the missing methylene resulting from the Glu312 \rightarrow Asp substitution can be harbored on the substrate for an effective hydride transfer reaction from the α -carbon of the alcohol substrate to the flavin.

The impaired ability of the choline oxidase variant containing Asp312 to catalyze a hydride transfer reaction can be effectively, but not completely, compensated by increasing the length of the substrate. Evidence supporting this conclusion comes from the stopped-flow data on the reductive half-reactions catalyzed by the mutant and wild-type forms of choline oxidase with 3-HPTA or choline. The k_{red} value in the Glu312Asp enzyme was sped up by 20-fold upon substituting choline with its longer analog 3-HPTA (**Table 8.1**). Instead, a 4-fold increase in the k_{red} value was observed in the wild-type form of the enzyme upon similar substrate substitution. While the increased rate constant for flavin reduction with the wild-type enzyme and 3-HPTA as compared to choline was not investigated further in this study, one can assume similar effects of substrate substitution in the wild-type and Glu312Asp enzymes. Consequently, the lengthening of the substrate by one $-\text{CH}_2-$ group contributes a 5-fold increase in the rate of flavin reduction that

partially compensates for the geometrically equivalent shortening of the side chain on residue 312 (**Figure 8.1**).

The second-order rate constants for the capture of the substrate on the enzyme ($k_{\text{red}}/K_{\text{d}}$) establish that while 3-HPTA is a better substrate than choline with the Glu312Asp enzyme, the opposite holds true for the wild-type enzyme. Indeed, the $k_{\text{red}}/K_{\text{d}}$ value increased 20-fold upon substituting choline with 3-HPTA as substrate for the Glu312Asp enzyme (**Table 8.1**). Such an increase accounts for a stabilization of 2 kcal/mol of the extra substrate methylene group in the enzyme complexes that are committed to flavin reduction. In contrast, the $k_{\text{red}}/K_{\text{d}}$ value decreased by 2-fold when a similar substrate substitution was carried out with the wild-type enzyme, thereby indicating that in the wild-type enzyme the extra methylene group of the substrate destabilizes by 0.4 kcal/mol enzyme-substrate complexes committed to catalysis.

Flavin oxidation by molecular oxygen is significantly impaired in the Glu312Asp enzyme upon using 3-HPTA instead of choline. Indeed, the $k_{\text{cat}}/K_{\text{oxygen}}$ value is almost an order of magnitude lower when the reduced Glu312Asp enzyme that reacts with oxygen is in complex with the product of the oxidation of 3-HPTA rather than choline. This result is unexpected given that with choline as substrate for the Glu312Asp enzyme there is no significant change of the $k_{\text{cat}}/K_{\text{oxygen}}$ value with respect to the wild-type [16]. However, it is probable that the spatial location, geometry, or relative orientation of the catalytic groups that participate in flavin oxidation, as well as the accessibility of oxygen to the reactive center, may have been altered in the Glu312Asp enzyme reacting with 3-HPTA as compared to choline, since these are all features that have been proposed to affect the reactivity of flavoprotein oxidases with oxygen [20].

The overall turnover of the Glu312Asp enzyme at saturating concentrations of 3-HPTA and oxygen is predominantly controlled by the hydride transfer reaction that results in the reduction

the enzyme-bound flavin. Evidence in support of this conclusion comes from the comparable values for k_{red} and k_{cat} (i.e., with values of 7.5 s^{-1} and 5 s^{-1} at pH 10.0, respectively) for the oxidation of the substrate analogue by the Glu312Asp enzyme. Similarly, previous results demonstrated that the reaction of hydride transfer of choline oxidation is rate limiting for the overall turnover of the wild-type and the Glu312Asp enzymes with choline as substrate [12, 16].

Comparison of the pH profiles for the $k_{\text{cat}}/K_{\text{choline}}$ and k_{cat} values of the Glu312Asp enzyme with 3-HPTA and of the wild-type enzyme with choline indicates that with the former there are significant perturbations of the $\text{p}K_{\text{a}}$ values to lower values (**Figure 8.3**). Previous inhibition and kinetic isotope effect studies have firmly established that the $\text{p}K_{\text{a}}$ value of 7.5 seen in the $k_{\text{cat}}/K_{\text{choline}}$ pH profile of choline oxidase with choline is an intrinsic value [1, 3, 19]. This $\text{p}K_{\text{a}}$ value was assigned to a group in the active site of the enzyme that was proposed to abstract the hydroxyl proton of the alcohol substrate and initiate catalysis [1, 23]. For a base-catalyzed chemical step of the type proposed in choline oxidase [1, 23], the outward perturbation of the $\text{p}K_{\text{a}}$ values seen with 3-HPTA and the Glu312Asp enzyme is indicative of the presence of a forward commitment to catalysis of the enzyme-substrate complex [3]. The alternate possibility of Glu312Asp having a $\text{p}K_{\text{a}}$ for the active site base that is significantly different from 7.5 can be immediately ruled out based on recent results showing that the same enzyme displays a $\text{p}K_{\text{a}}$ identical to the wild-type enzyme when choline is used as substrate [19]. It is likely that the interaction of the extra methylene group of 3-HPTA in the active site of the enzyme makes the dissociation of the substrate from the enzyme-substrate complex significantly slower than in the case of choline, thereby resulting in a significant forward commitment to catalysis.

In summary, the results of the kinetic investigation with 3-HPTA as substrate for the Glu312Asp enzyme have indicated that while the reductive half-reaction catalyzed by the enzyme

is partially rescued by the substrate analogue, the oxidative half-reaction is not. This study demonstrates that the impaired ability to catalyze a hydride transfer reaction in the Glu312Asp variant of choline oxidase can be effectively compensated by lengthening the chain of the substrate. However, such compensation is not sufficient to provide a full recovery of the hydride transfer reaction, underscoring the importance of substrate positioning in the active site of an enzyme for efficient catalysis.

8.6 Acknowledgements

The authors thank Kevin Francis for critically reading the manuscript.

8.7 References

- [1] G. Gadda, *Biochemistry* 47 (2008) 13745-13753.
- [2] S. Ikuta, S. Imamura, H. Misaki, Y. Horiuti, *J Biochem* 82 (1977) 1741-1749.
- [3] G. Gadda, *Biochim Biophys Acta* 1646 (2003) 112-118.
- [4] M. Ghoul, T. Bernard, M. Cormier, *Appl Environ Microbiol* 56 (1990) 551-554.
- [5] R.M. Kappes, B. Kempf, E. Bremer, *J Bacteriol* 178 (1996) 5071-5079.
- [6] R. Garcia-Esteva, D. Canovas, F. Iglesias-Guerra, A. Ventosa, L.N. Csonka, J.J. Nieto, C. Vargas, *Syst Appl Microbiol* 29 (2006) 626-633.
- [7] P. Sharmila, M.L. Phanindra, F. Anwar, K. Singh, S. Gupta, P. Pardha Saradhi, *Plant Physiol Biochem* 47 (2009) 391-396.
- [8] H. Kathuria, J. Giri, K.N. Nataraja, N. Murata, M. Udayakumar, A.K. Tyagi, *Plant Biotechnol J* 7 (2009) 512-526.

- [9] E.J. Park, Z. Jeknic, M.T. Pino, N. Murata, T.H. Chen, *Plant Cell Environ* 30 (2007) 994-1005.
- [10] E.J. Park, Z. Jeknic, A. Sakamoto, J. DeNoma, R. Yuwansiri, N. Murata, T.H. Chen, *Plant J* 40 (2004) 474-487.
- [11] A. Mohanty, H. Kathuria, A. Ferjani, A. Sakamoto, P. Mohanty, N. Murata, A.K. Tyagi, *Theor Appl Genet* 106 (2002) 51-57.
- [12] F. Fan, G. Gadda, *J Am Chem Soc* 127 (2005) 2067-2074.
- [13] F. Fan, G. Gadda, *J Am Chem Soc* 127 (2005) 17954-17961.
- [14] O. Quaye, G. Gadda, *Arch Biochem Biophys* 489 (2009) 10-14.
- [15] O. Quaye, S. Cowins, G. Gadda, *J Biol Chem* 284 (2009) 16990-16997.
- [16] O. Quaye, G.T. Lountos, F. Fan, A.M. Orville, G. Gadda, *Biochemistry* 47 (2008) 243-256.
- [17] M. Ghanem, F. Fan, K. Francis, G. Gadda, *Biochemistry* 42 (2003) 15179-15188.
- [18] F. Fan, M.W. Germann, G. Gadda, *Biochemistry* 45 (2006) 1979-1986.
- [19] F. Fan, G. Gadda, *Biochemistry* 46 (2007) 6402-6408.
- [20] A. Mattevi, *Trends Biochem Sci* 31 (2006) 276-283.
- [21] F. Fan, G. Gadda, *Biochemistry* 46 (2007) 6402-6408.
- [22] A. Mattevi, *Trends Biochem Sci* 31 (2006) 276-283.
- [23] M. Ghanem, G. Gadda, *Biochemistry* 44 (2005) 893-904.